(A) Photoregulation of DNA Functions by Cyclic Azobenzene-tethered Oligonucleotides

(B) Site-specific Fluorescent Labeling of DNA using Inverse Electron Demand Diels-Alder Reaction between *trans*-Cyclooctene Derivatives and BODIPY-Tetrazine Adducts

Fatma Mohamed Eljabu

Department of Chemistry

Submitted to the Department of Chemistry

in partial fulfillment of the requirements for the degree of

Master of Science

Faculty of Mathematics and Science, Brock University

St. Catharines, Ontario

November, 2015

Abstract

(A) Most azobenzene-based photoswitches require UV light for photoisomerization, which limit their applications in biological systems due to possible photodamage. Cyclic azobenzene derivatives, on the other hand, can undergo *cis*-*trans* isomerization when exposed to visible light. A shortened synthetic scheme was developed for the preparation of a building block containing cyclic azobenzene and D-threoninol (cAB-Thr). *trans*-Cyclic azobenzene was found to thermally isomerize back to the *cis*-form in a temperature-dependent manner. cAB-Thr was transformed into the corresponding phosphoramidite and subsequently incorporated into oligonucleotides by solid phase synthesis. Melting temperature measurement suggested that incorporation of *cis*-cAB into oligonucleotides destabilizes DNA duplexes, these findings corroborate with circular dichroism measurement. Finally, Fluorescent Energy Resonance Transfer experiments indicated that *trans*-cAB can be accommodated in DNA duplexes.

(B) Inverse Electron Demand Diels-Alder reactions (IEDDA) between *trans*-olefins and tetrazines provide a powerful alternative to existing ligation chemistries due to its fast reaction rate, bioorthogonality and mutual orthogonality with other click reactions. In this project, an attempt was pursued to synthesize *trans*-cyclooctene building blocks for oligonucleotide labeling by reacting with BODIPY-tetrazine. *Rel*-(1*R*-4*E*-p*R*)-cyclooct-4-enol and *rel*-(1*R*,8*S*,9*S*,4*E*)-Bicyclo[6.1.0]non-4-ene-9-ylmethanol were synthesized and then transformed into the corresponding propargyl ether. Subsequent Sonogashira reactions between these propargylated compounds with DMT-protected 5-iododeoxyuridine failed to give the desired products. Finally a methodology was pursued for the synthesis of BODIPY-tetrazine conjugates that will be used in future IEDDA reactions with *trans*-cyclooctene modified oligonucleotides.

Acknowledgments

First, I must express my gratitude to my advisor, Prof. Tony Yan, for everything he has done to make this thesis possible. I appreciate his support and advice throughout my graduate program. In addition, I thank my committee members, Prof. Jeffery Atkinson and Prof. Feng Li for their advice and insight over the past two years. I would like also to thank Prof. Christopher Wilds, Concordia University, Quebec, Canada for accepting to be my external examiner.

I would like to thank Nader Elajaili for being the most loving and supportive husband in the world. Your encouragement has meant the world to me, and I am sure I would not be where I am today if I had not had you to inspire me. I appreciate your patience and unwavering love and support. My acknowledgment also goes to my family, mother, father and siblings for their constant love and encouragement.

Furthermore, I would like to express my appreciation to my fellow labmates, especially, Ravi Yalagala, Dhruval Joshi and Viola Yang for their help and support. Also I thank Razvan Simionescu for his assistance in collecting data for NMR spectroscopy and Prof. Richard Pon for helping with the DNA synthesis.

Lastly, I would like to thank the Ministry of Higher Education in Libya for giving me this opportunity to continue my study, and the Natural Sciences and Engineering Research Council of Canada for funding this work.

Table of contents

List of Tables

List of Figures

List of Schemes

List of Abbreviations

BODIPY	borondipyrromethene difluoride
b. p.	boiling point
$CDCl_3$	deuterated chloroform
DNA	deoxyribonucleic acid
DFT	density functional theory
d	doublet
dd	doublet of doublet
ddd	doublet of doublet of doublet
ESI	electrospray ionization
FRET	Förster resonance energy transfer
g	gram
h	hour
Hz	Hertz
kcal	kilocalories
$MgSO_4$	magnesium sulphate
m	multiplet
M	molar concentration
mg	milligram
ml	millilitre
m*M*	millimolar
min	minute

mol	moles
m-	meta
NMR	nuclear magnetic resonance
NOE	nuclear overhauser effect
nm	noanometer
n-	non-bonding
o-	ortho
p-	para
q	quartet
R_f	retention factor
s	second
TLC	thin layer chromatography
t	triplet
UV-Vis	ultraviolet-visible
Å	Angstrom
π	pi bonding
π*	pi anti-bonding
°C	degrees in Celsius
α	alpha
γ	gamma
λ	lambda

CHAPTER 1: Regulation of nucleic acids functions by photoresponsive molecules

1.1 Introduction to nucleic acids

Nucleic acids are macromolecules made up of a linear array of monomers called nucleotides, each composed of a pentose sugar, a nucleobase (purine and pyrimidine) and a phosphate diester group. The purine bases, adenine (Ade) and guanine (Gua) as well as the pyrimidine bases, cytosine (Cyt) and thymine (Thy) can exist in different chemical isomeric forms (tautomers); however, the equilibrium favors the keto and amino forms (Figure 1-1) by a ratio of about 10^4 to 1. Two types of nucleic acids exist in nature, deoxyribonucleic acid (DNA) and ribonucleic acid (RNA).

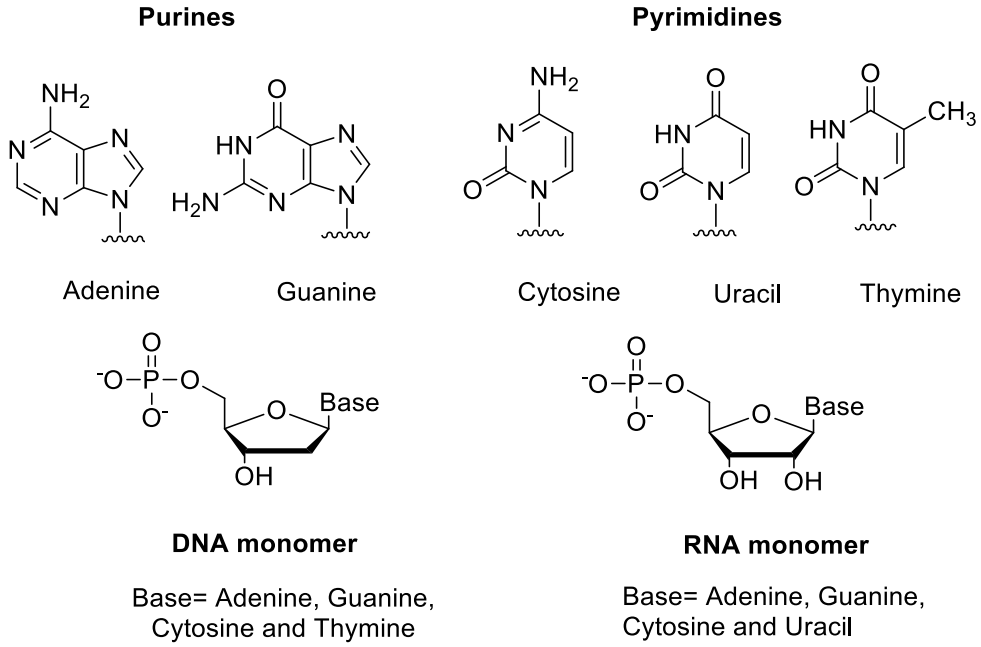

Figure 1-1. Structures of the favored tautomers of purine and pyrimidine bases, sugar units and phosphate groups in nucleic acids.

The sugar units in DNA are D-2-deoxyriboses, and they are linked to one another by the phosphodiester bridges. Specifically, the 3'-hydroxyl group of the sugar moiety of one nucleotide is esterified to a phosphate group, which in turn is joined to the 5'-hydroxyl group of the adjacent nucleoside, essentially forming the backbone of the nucleic acids. The nucleobases are joined from a ring nitrogen to C-1' of the pentose sugar.[1]

The covalent structure of RNA differs from that of DNA in two respects. First, the sugar units are D-riboses which have extra hydroxyl group at 2' position as compared with D-2-deoxyribose found in DNA. Second, thymidine (Thy) is replaced with uracil (Ura) (Figure 1-2).[2]

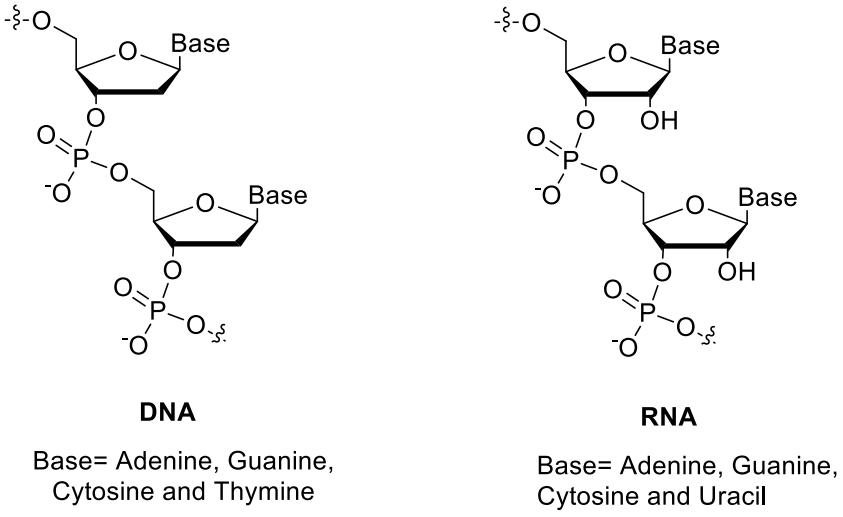

Figure 1-2. Backbones of DNA and RNA.[2]

In living organisms, most RNAs are single-stranded while most DNA molecules are double stranded. The two strands of DNA are antiparallel to each other; one strand runs in a 5'-3' direction whereas the other runs in a 3'-5' direction. Each strand serves as a template in DNA replication .[1] The nucleobases in the two separate anti-parallel DNA strands form specific hydrogen bonds in such a way that a helical structure is formed. In the model of DNA double helix first described by Watson and Crick in 1953, guanine forms three sets of hydrogen bonds with cytosine and adenine

forms two sets of hydrogen bonds with thymine.[3] The stacking of base pairs contributes to the stability of DNA helix by the hydrophobic effect and dipole interactions (Figure 1-3).[4, 5]

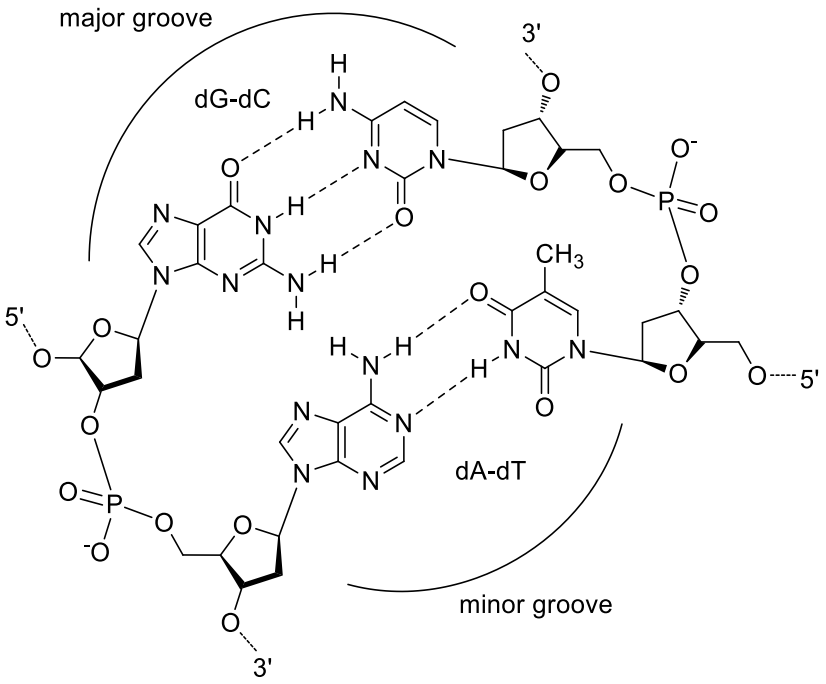

Figure 1-3. Watson-Crick base pairs found in the usual double stranded DNA.[4]

Because the glycosidic bonds of a base pair are not diametrically opposite to each other, two grooves arise, major and minor grooves. In B-DNA, the major groove is wider (12 versus 6 Å) and deeper (8.5 versus 7.5 Å) than the minor groove (Figure 1-3).[4, 5]

X-Ray diffraction analyses of single crystals of DNA revealed that DNA exhibits three different conformations A- , B- and Z-forms, of which B-DNA is the most common. In this form, the double helix is right-handed with a mean twist angle of 36°, giving 10 nucleotides per helical turn. The stacked base pairs form a central core surrounded by the phosphate backbone.[1]The center of the helix is a relatively chemically inert space for storing the genetic information.[3]

DNA and RNA are responsible for the storage and flow of genetic information in biological systems.[6] DNA sequence information is converted to RNA in a process called transcription. Then the sequence encoded in the RNA molecule is decoded and converted to an amino acid sequence

in a process called translation (Figure 1-4). In addition, nucleic acids have been found to possess various functions and applications, such as RNA interference (RNAi) and antisense oligonucleotides, riboswitches, DNAzymes, aptamers, molecular diagnostics such as nucleic acid microarrays, and as building blocks for nanoscale material. Therefore, study of these biological processes, will provide insight into biochemical functions of nucleic acids. Moreover, identifying and examining the nature of DNA-protein interactions is a crucial prerequisite to understand the molecular basis of fundamental processes such as DNA replication, packaging, and DNA damage and repair.[7]

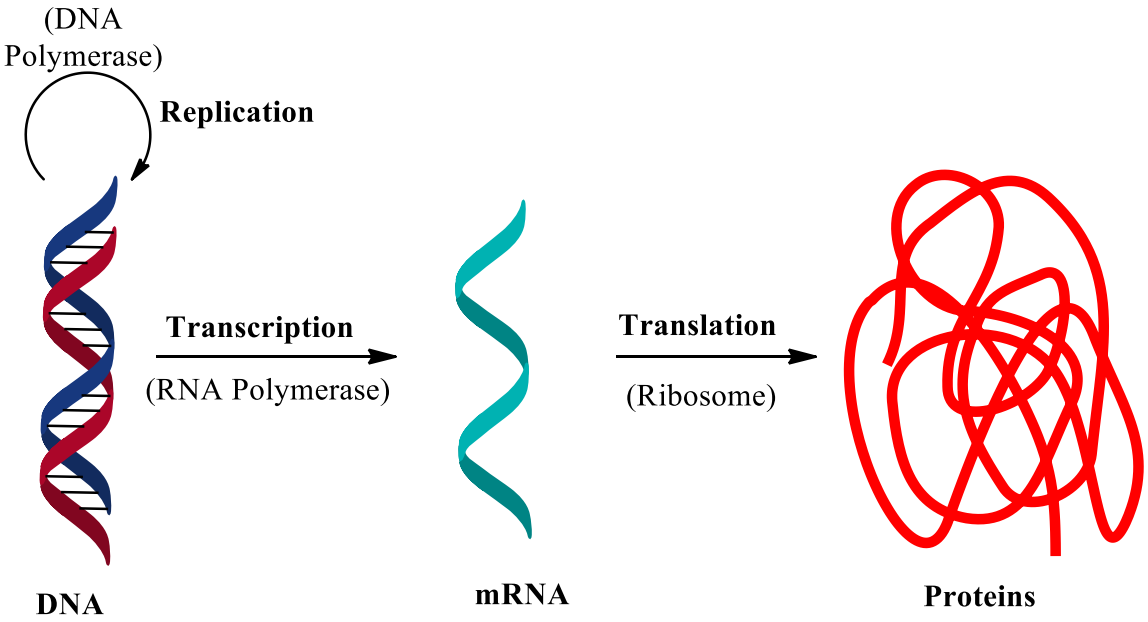

Figure 1-4. A diagram of the central dogma showing the information flow from DNA to RNA to proteins.

1.2 Functional regulation of biomolecules

Recently, much attention has been focused on the artificial control of gene expression to study cellular processes as an important tool to investigate the details of cellular signaling and differentiation as well as disease progression.[8]

Regulation of nucleic acid information flows has been achieved by different techniques such as small molecules, antigene and antisense oligonucleotides, and RNA interference (RNAi). Despite their efficiency, these techniques do not provide precise control of dosages and sites of action.[9]

One strategy to achieve spatiotemporal control or to enhance the selectivity in regulating a particular cellular function is to subject the system to the control of either internal or external stimuli. [10] In this respect, spatial and temporal control of cellular processes using light could provide unparalleled opportunities to study biological processes such as organism development and disease progression.[11]

Light provides excellent potential as external trigger signal as: i) it is generally noninvasive at a range of wavelengths, ii) it is orthogonal toward most elements of living systems,[12] iii) it is easy to control irradiation time and local excitation without the need for direct contact to the material, and iv) controlling of excitation wavelength can be accomplished through the design of photo-responsive molecules.[10, 13]

One example of naturally occurring light-dependent processes occurs in the plant, where light influences plant development at various levels of gene expression. In the nuclear-cytosolic compartment this regulation takes place primarily at the transcriptional level. However, the photo-regulation of chloroplast genes has been observed mainly at the level of translation.[14] Another example of light-dependent processes involves phototropins, a class of light-activated kinases. In this cascade**,** light initiates signaling in these proteins by generating a covalent protein–flavin mononucleotide (FMN) adduct within sensory Per-ARNT-Sim (PAS) domains.[15]

Two strategies for the introduction of light-sensitivity into biomolecules have been investigated. The first one is usually referred to as “caging” and involves the modification of a

biologically active substance with a photolabile "protecting" group to make it temporarily inactive. The second strategy involves functionalization with bistable molecular photoswitches, so that these molecules can be reversibly switched between an active and an inactive state.[9, 12]

1.3 Irreversible photoregulation of nucleic acid properties by caged molecules

Photolabile caged compounds are biologically inert precursors of active molecules, which upon exposure to light release the active species at its site of action.[16] Photolysis of caged molecules represents a convenient approach to achieve spatiotemporal control of biomolecules with light as an external trigger. The concept behind the caging technique is that the biomolecule of interest can be made biologically inert (or caged) by chemically modifying its structure with a photoremovable protecting group (PPG). Illumination gives rise to active species, allowing spatiotemporal control of the targeted process.[17]

The criteria for the design of a good PPG depend on the application. Ideally, caged compounds should be soluble and stable in the targeted media, and they must be biologically inert before photolysis. The uncaging, or photodeprotection, step should occur with high quantum yield and at wavelengths well above 300 nm to avoid damaging the biological entity. It is also important that the rate of photodeprotection is faster than the process being studied, and the by-products accompanying the released bioactive reagent should be nontoxic and biocompatible.[9, 18]

Before the term "caging" was coined, Martinek and coworkers performed a series of studies in 1971 on peptidase α-chymotrypsin (CT).[19] The reaction between CT **1** and *cis*-cinnamoyl imidazole **2** resulted in the formation of *cis*-acylated product **3** (Scheme 1-1). As a result, α-chymotrypsin was temporarily deactivated. Only upon isomerization to the *trans*-adduct **5** was the cinnamoyl group cleaved, regenerating the active CT enzyme **1** which can then cleave the substrate

tyrosine ester to tyrosine to be converted by tyrosinase into the pigment melanine. As such, *cis*-cinnamoylated CT could be called "caged".[19]

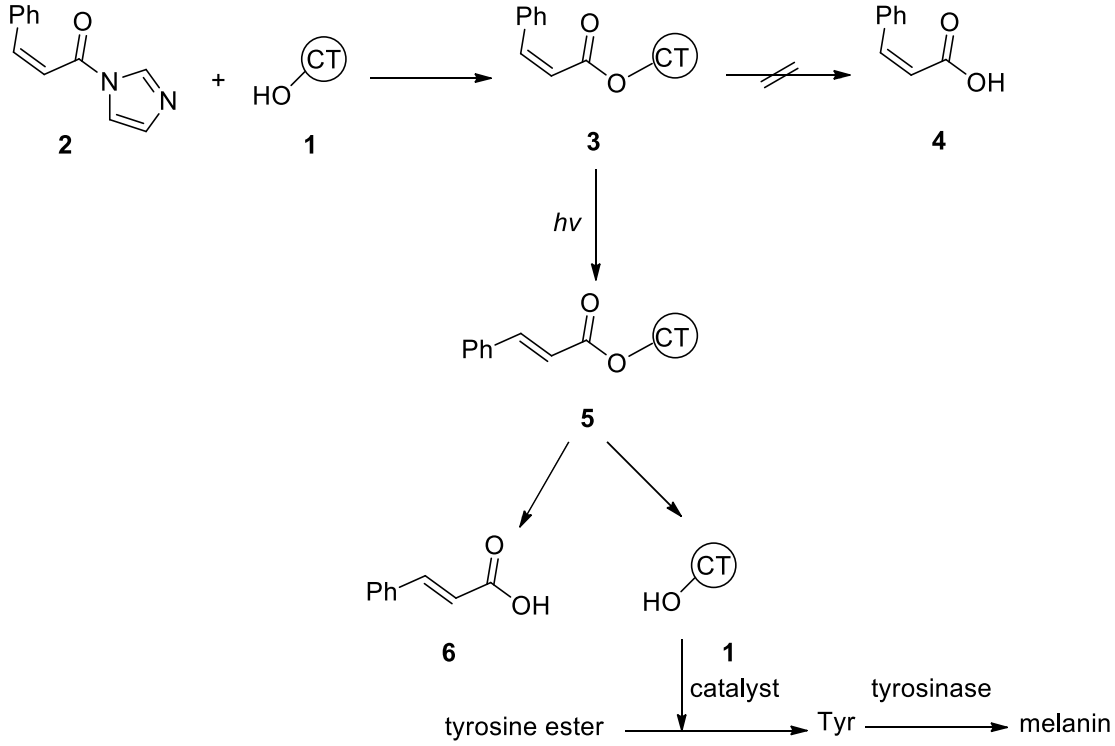

Scheme 1-1. Photoregulation of peptidase α-chymotrypsin.[9]

In 1978 Koplan *et al.* synthesized a photolabile precursor of adenosine triphosphate ATP **7** (Scheme 1-2), and introduced the term "caged" for the first time to describe these compounds. The γ-phosphate of ATP was masked with a photoremovable *o*-nitrobenzyl group. Upon irradiation at 350 nm, the caged ATP photolyzes to release ATP **8** and a nitrosoketone **9**.[20] This work paved the way for introducing the photorelease approach as a useful technique to study the mechanism of a wide range of ATP-dependent processes, including the ion-transporting ATPases, muscle contraction and time-resolved structural studies of the sarcoplasmic reticulum Ca^{2+} pump.[21]

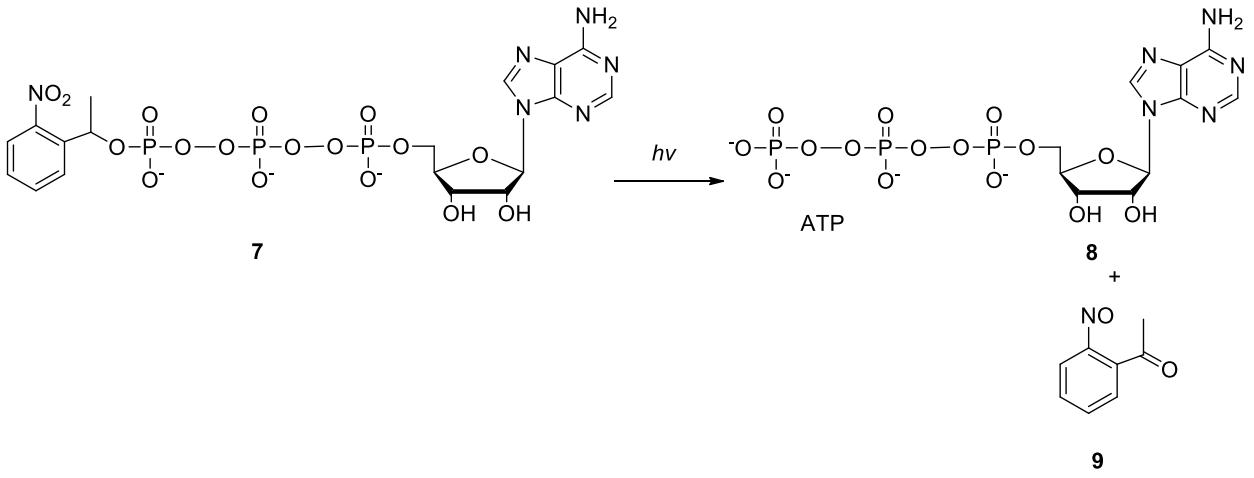

Scheme 1-2. Overall photolysis reaction of caged ATP **7**.[9]

Figure 1-5 shows the most commonly used caging groups for the photoregulation of nucleic acids and gene expression such as *o*-nitrobenzyl (ONB) and its derivative nitrophenylethyl (R = Me, NPE) **10**,[22] 2-(2-nitrophenyl) propyl (NPP) **11**,[23] nitrodibenzofurane chromophore **12**,[24] coumarin based group [7-(dimethylamino) coumarin-4-yl] methyl (DMACM) **13**,[25] 8-bromo-7-hydroxyquinoline (BHQ) **14**,[26] and ketoprofen derivative **15**.[27]

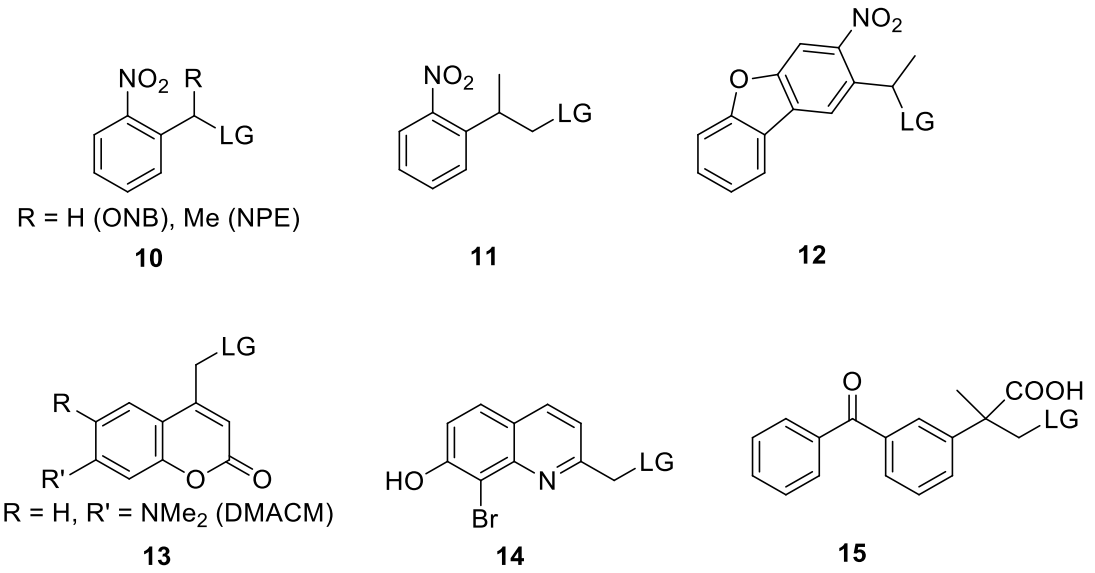

Figure 1-5. The most commonly used caging groups.[9]

1.4 Photoregulation of DNA hybridization using caged molecules

DNA hybridization is a process where two complementary strands join together to form duplex DNA. Nucleic acid hybridization is responsible for the fundamental roles that these important molecules play in the biological system. It is also fundamental in many molecular biology techniques such as polymerase chain reaction (PCR) and detection of specific DNA sequences *via* hybridization. As such, regulation of nucleic acid hybridization using external light stimuli provides spatiotemporal control of processes where nucleic acid hybridization is critical.

In 2003, Saito *et al.* demonstrates a light-based technique using a photocleavable cage compound to transiently block DNA hybridization.[28] They developed caged molecular beacons, which are oligonucleotide hybridization probes, to regulate the hybridization of single-stranded DNA with its complementary sequence. In this study, molecular beacon is modified with a naphthalene quencher at the 5′-end and a photolabile pHP (4-hydroxyphenacyl ester) group to which biotin is linked at the 3′-end. In the absence of complementary DNA sequence, the photoreaction was inefficient because the molecular beacon containing the photoactive group was in the closed form **16**, *i.e*. a stem and loop structure, whereas irradiation of the open form **17** led to hybridization with the complementary strand, effectively moving the naphthalene quencher away to allow the cleavage of photolabile group releasing the biotin residue **18** (Scheme 1-3).[28]

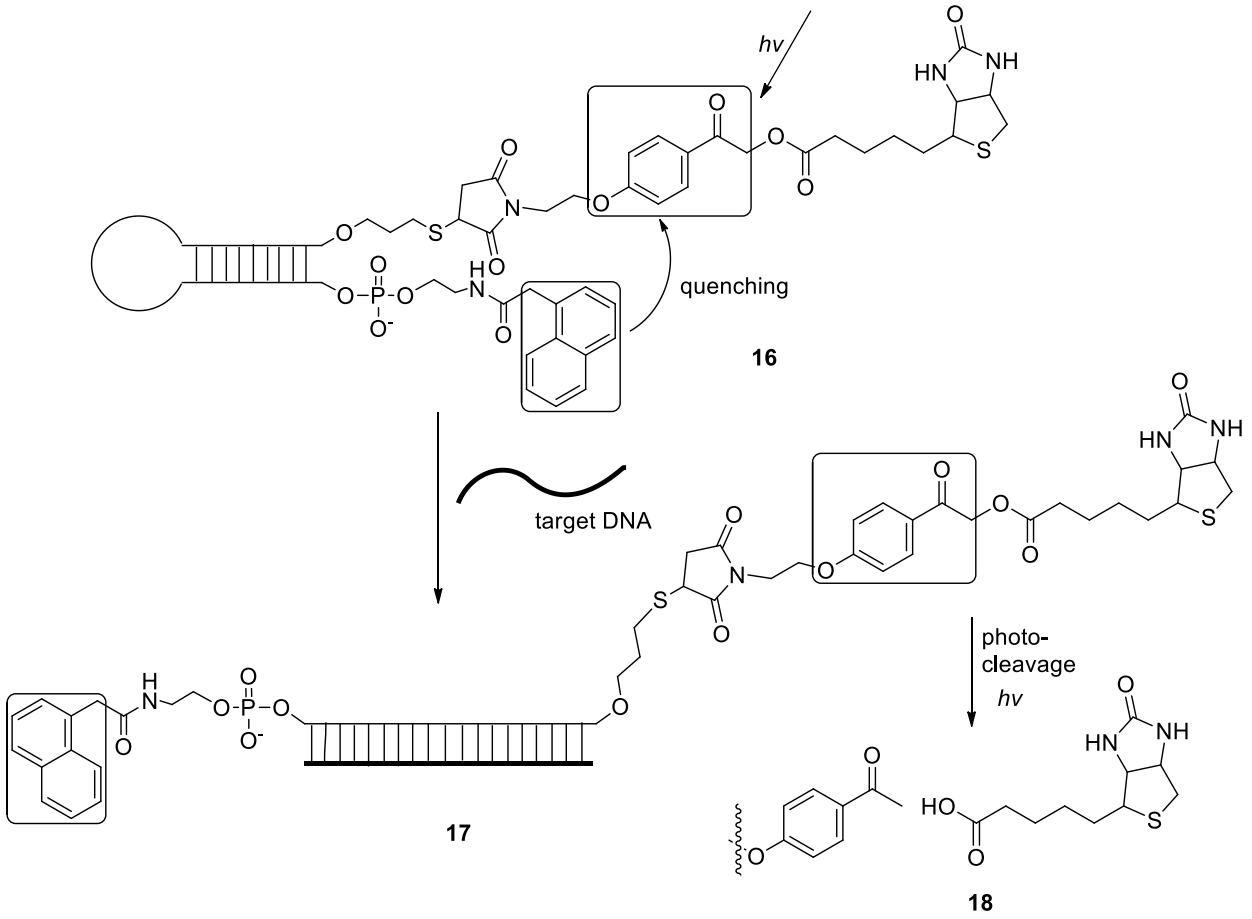

Scheme 1-3. Photoregulation of molecular beacon hybridization using pHP photolabile group.[28]

In 2005 Bilal Ghosn *et al.* explored the use of 1-(4,5-dimethoxy-2-nitropheny1)ethyl ester (DMNPE) of the phosphate backbone to regulate DNA hybridization.[29] In this experiment, the photolabile (DMNPE) group was attached to the DNA phosphate backbone as shown in **19** (Scheme 1-4). Hybridization assay was then performed with complementary molecular beacon **20** which does not show fluorescence until hybridized to a complementary DNA. It was found that DMNPE-caged DNA does not hybridize with the molecular beacon until it is photoactivated with 365 nm light to cleave the DMNPE group. Fluorescent experiment results and gel shift assays confirmed that up to 80% the hybridization of modified DNA was achieved after irradiation with light when an average of 14–16 DMNPE groups were incorporated in the DNA **19**.[29]

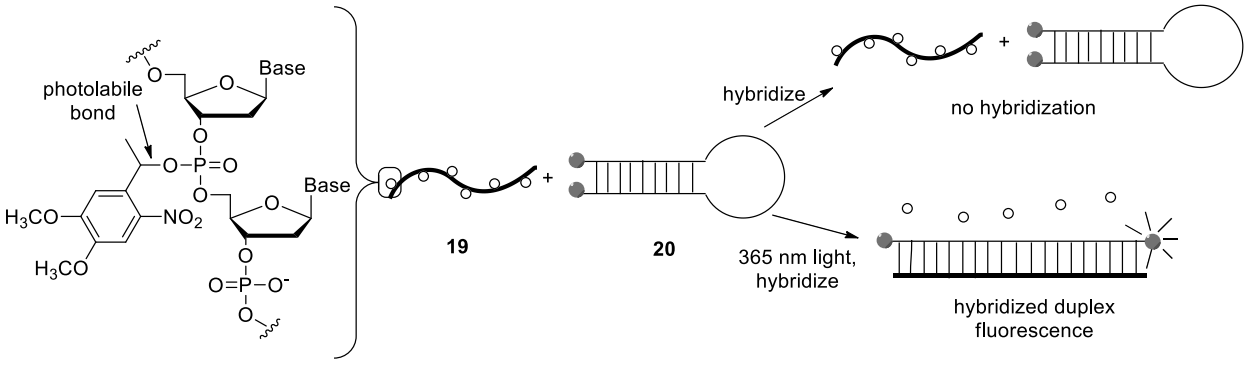

Scheme 1-4. Hybridization assay of caged DNA and complementary molecular beacon.[29]

1.5 Photoregulation of DNA transcription and gene expression using caged molecules

Haselton and co-workers were the first to study the possibility of light activated transcription with modified nucleic acids.[30] They developed caged plasmid DNAs which encode for luciferase or GFP expression. The DMNPE-caging groups were introduced to the phosphate backbone in an unselective manner using 1-(4,5-dimethoxy-2-nitrophenyl)ethyl ester as a reagent (as in **21**, Figure 1-6). The purified photocaged plasmids were then introduced to rat skin cells or HeLa cells. The GFP expression in both cells was temporarily blocked until exposed to 355 nm light which induces the GFP expression in a dose-dependent manner.[30]

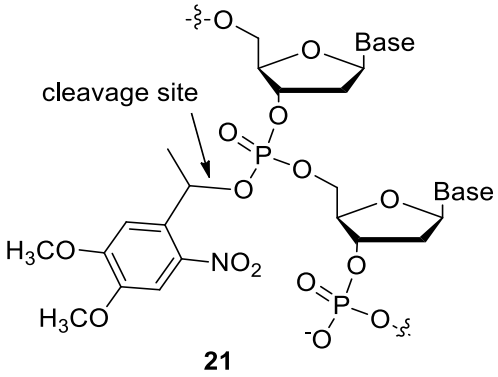

Figure 1-6. DMNPE caging group on the phosphate backbone of DNA.[30]

A similar approach was employed by Okamoto *et al*. to design caged GFP-mRNA.[31]Thus, the mRNA was caged with a coumarin-derivative group Bhc (6-bromo-7-hydroxycoumarin-4-

ylmethyl) using **22** as reagent (Figure 1-7),[32] similar to the previous study. The caged mRNA was then introduced to zebrafish embryos through injection at the one-cell stage. While only 4% GFP expression was seen with the caged mRNA, indicating very efficient blocking, up to 18% (4.5-fold enhancement) and 23% (6-fold enhancement) GFP expression were seen after 10 s and 20 s irradiation with 350-365 nm light, respectively.[31]

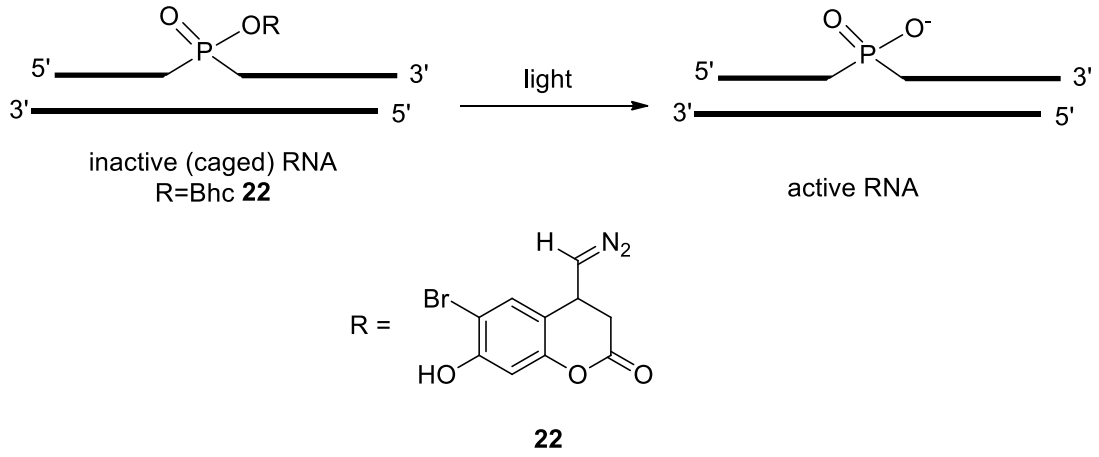

Figure 1-7. A structure of Bhc caging group precurser and its applications for caging RNA.[32]

Light regulation can also be accomplished by installation of a caging group on a nucleoside phosphoramidite followed by introduction of "caged" nucleosides into nucleic acid sequences by solid phase synthesis.[32] The caging group can effectively block the interaction or basepairing properties with its complementary sequence.[33] In this regard, Heckel and co-workers reported the synthesis of caged thymidine phosphoramidites and their usage for controlling DNA transcription by light.[6] In this work, thymidine was modified at the *O*4-position with a photolabile *o*-nitrophenyl-isopropyl (NPP) group (as in **23** in Figure 1-8).[34] The chemical modification introduced on thymidine was recognised as a mismatch by the T7 RNA polymerase, preventing the transcription of the duplex DNA. After irradiation, the same amount of transcription product was formed as in the control reaction with the uncaged sequence [6] (Figure 1-8).

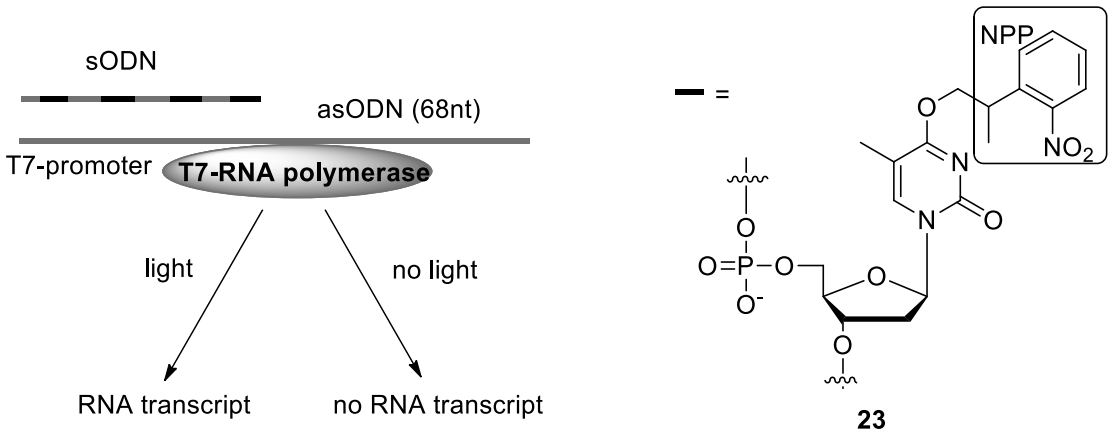

Figure 1-8. Strategy of controlling RNA transcription with a sense oligodeoxynucleotide (sODN) primer that contains one or more caged thymidine nucleobases; where asODN is antisense oligodeoxynucleotide.[34]

Thermal denaturation experiments were performed in order to investigate the effect of NPP caged thymidine on the duplex stability. It was found that introduction of just one caged nucleotide leads to a significant reduction (by up to 5°C) in the melting temperature (T_m). While with three caged nucleotides the T_m decreased by 21.5°C. After irradiation with 366 nm for 30 min, the T_m of caged DNA was restored to the same as the unmodified oligomer (Table 1-1).[6]

Table 1-1. T_m before and after (in parenthesis) irradiation of caged NPP-T25 (error ca. 0.7°C). T_m of unmodified T25 is 53.8 (54.0)°C.[6] X = NPP-dT.

Sequence	5'-T_8TTTTXTTTTT$_8$–3'	5'-T_8TTTXXXTTTT$_8$-3'	5'-T_8XTTTXTTTXT$_8$-3'
T_m (°C)	48.5 (54.0)	44.5 (52.7)	32.3 (53.2)

Figure 1-9 shows examples of caged nucleosides with different caging groups used for light responsive regulation of DNA and RNA, which include: NPOM-dT **24**, NPP-dC **25**, NPE-dA **26**,[33] NPE-G **27**, NPE-U **28**[35] and NPE-A **29**.[35, 36]

Morpholino oligonucleotides (MOs) are synthetic DNA analogues in which the sugar phosphate backbone is replaced with morpholino moieties. Caged MOs have been found useful for the regulation of gene function in both cell culture and living embryos. Dieters *et al*.[38] reported

the synthesis of morpholino oligomers caged with a photolabile 6-nitropiperonyloxymethyl (NPOM) caging group **30** (Figure 1-10). In this study, the authors demonstrated that a caged MO that targets enhanced green fluorescent protein (EGFP) inhibits EGFP expression only after exposure to UV light of 365 nm in both transfected cells and living zebrafish and xenopus frog embryos.[38]

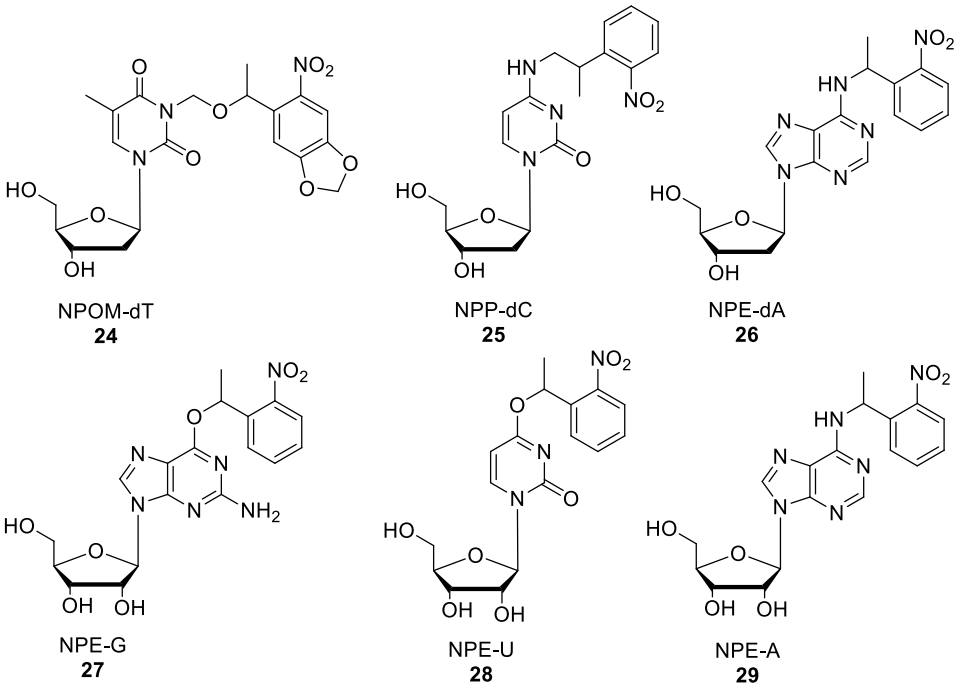

Figure 1-9. Examples of caged nucleosides with different caging groups for the nucleobases.[33, 35, 36]

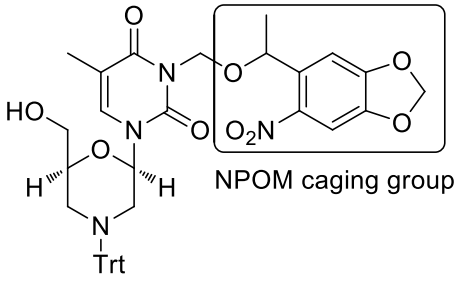

Morpholino	Sequence
EGFP-MO^0	ACAGCTCCTCGCCCTTGCTCACCAT
EGFP-MO^4	ACAGCT*CCT*CGCCCT*TGCT*CACCAT

T* denotes caged monomer, Trt is triphenylmethyl

Figure 1-10. Caged morpholino monomer **30**, and morpholino oligomers containing the caged monomer.[37]

Caging groups are synthetically malleable and accessible, offering a wide range of structures for designed applications. As a result they offer excellent spatial and temporal control for the substrate release. However, photolysis of these compounds forms potentially toxic by-products such as *o*-nitrosobenzaldehyde, limiting their applications in the photoregulation of biological systems.[12] Further, bidirectional regulation is not possible with the caging approach.

1.6 Reversible photoregulation of nucleic acids by photoswithches

Photoswitches are a class of compounds that undergo reversible photochemistry in that they can be shifted between at least two different states or forms.[13, 38, 39] These two forms differ in their absorption spectra and other physical properties, such as their redox potential, fluorescent intensity, acid/base strength, dielectric constant, dipolar moment, and molecular shape.[13]

A variety of synthetic organic molecules have been investigated for reversible photocontrol of biomolecules (Table 1-2). These molecules either switch upon irradiation between the *cis* and *trans* isomers, such as azobenzenes, stilbenes, and hemithioindigos, or interconvert between closed and open forms, such as spiropyrans, diarylethenes, and fulgides.[12]

In terms of thermal stability of the photogenerated isomer, photoswitches can be classified in two categories: P-type (photochemically reversible type), which do not isomerize back to the initial isomer even at elevated temperatures, e.g. fulgides and diarylethenes, and T-type (thermally reversible type), where the photogenerated isomer can reverse back to original state by either heating or irradiation with light, e.g. azobenzenes, stilbenes and spiropyranes.[13]

Table 1-2. Selected molecular structures of photoswitches introduced into biomolecules.[12]

Photoswitches	Isomerization	λ_1/λ_2
Stilbenes	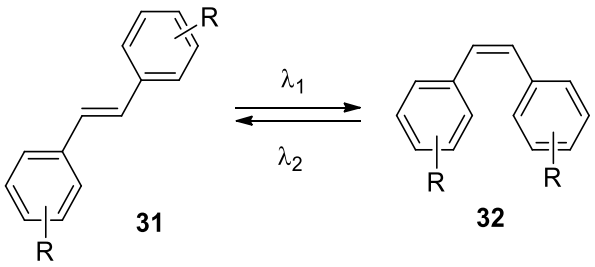	UV/vis
Hemithioindigos	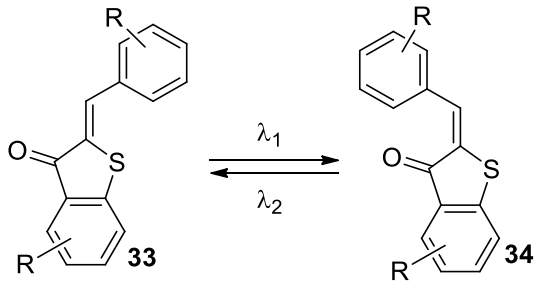	UV/vis (ΔT)
Spiropyrans	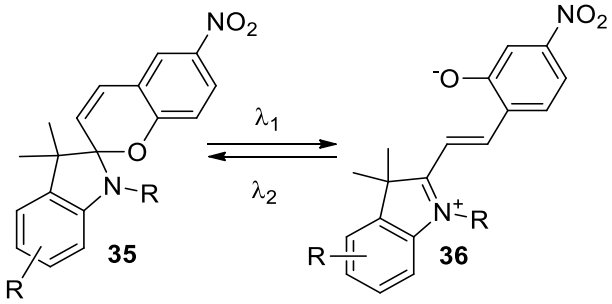	UV/vis (ΔT) or vis/UV
Diarylethenes	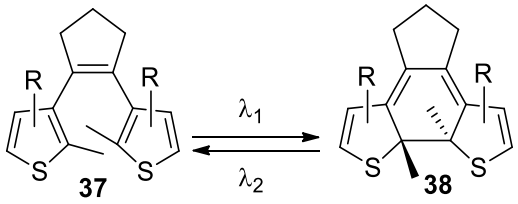	UV/vis
Thiophenefulgides	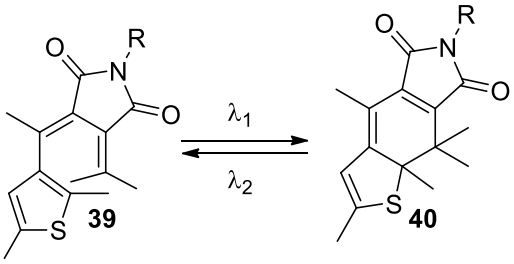	UV/vis
Azobenzenes	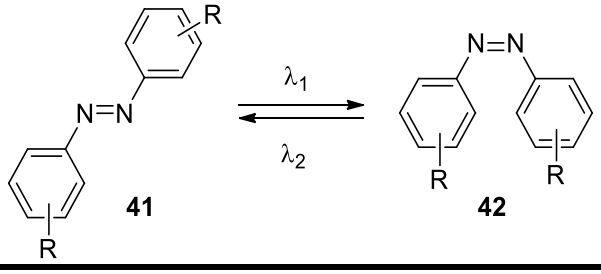	UV/vis (ΔT)

1.6.1 Stilbenes

The stilbenes system **31**, **32** (Table 1-2) which is an example of the general class of diarylethene chromophore, undergoes an analogous *trans-cis* isomerization.[40] Thermal isomerization is negligible at room temperature because the barrier of the thermal *cis-trans* reisomerization is 41−46 kcal/mol. Letsinger and Wu were the first to incorporate a photoswitchable unit into nucleic acid structure in the form of stilbene as a backbone linker of two DNA oligonucleotides.[12] In this study, stilbene dicarboxamide bridge was used to introduce photoreversibility to the hairpin structure **43** (Figure 1-11). The *cis* form of the stilbene unit was found to destabilize hairpin structure, because its geometry is too short a linker to properly stack with the underlying helix. For instance, in the strand T_6-[ST]-A_6, a shift of 10°C in T_m was observed for the *trans* (59°C) and *cis* (49°C) isomers in the presence of 100 m*M* NaCl.[41]

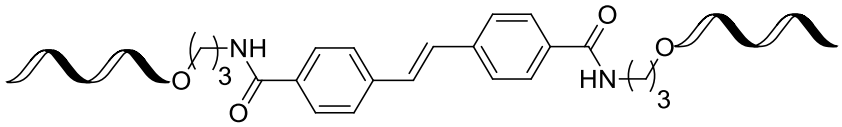

43

Figure 1-11. Stilbene derivatives for photoreversible regulation of hairpin structure. [12]

A major drawback of stilbenes is their tendency to undergo irreversible cyclization and oxidation in the *cis* form.[42]

1.6.2 Spiropyrans

In these photochromic compounds **35**, the C_{spiro}−O bond undergoes heterolytic cleavage upon exposure to UV light (360−370 nm),[43] resulting in the formation of a zwitterionic conjugated system, known as the merocyanine form, or the open-form **36** (Table 1-2).[12, 44] The isomerization process is accompanied by a very large change in polarity which is reflected by changes in hydrophilicity/hydrophobicity. The back isomerization can be achieved both thermally and photochemically with visible (>460 nm) light.[12]

The importance of these molecules for the photoregulation of nucleic acids can be attributed to the assumption that the ring-closed non-planar spiropyran form **35** is unable to insert into the base stack whereas the open and planar merocyanine form could potentially intercalate. This assumption was supported experimentally by Wagenknecht and Beyer's study.[45] In this study, the spirobenzopyran was incorporated as an internal modification into DNA sequences by two different synthetic strategies: incorporation of spiropyran phosphoramidite to DNA by solid phase synthesis and post-synthetic 'click'-type ligation which gives products such as **44** (Figure 1-12).[45]

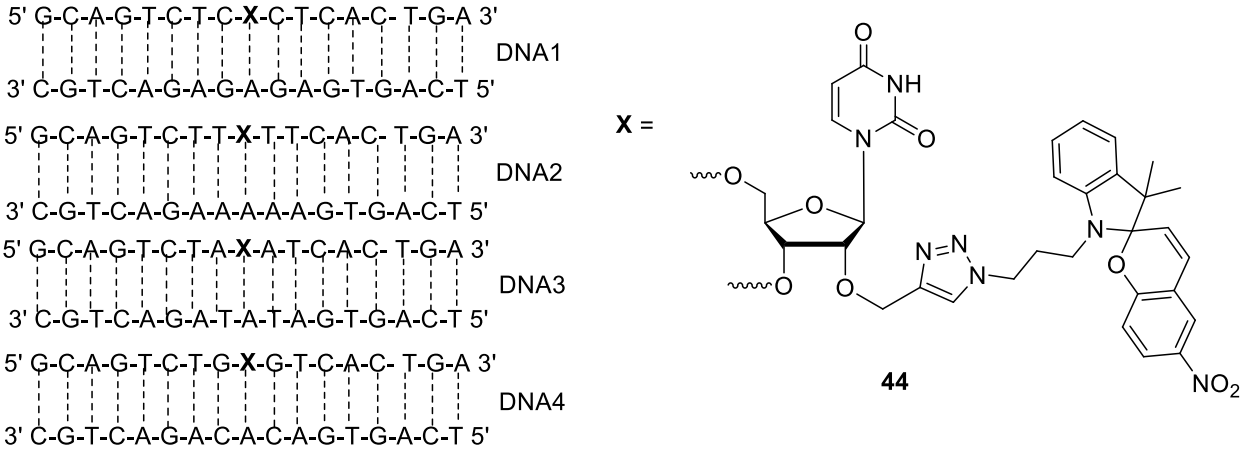

Figure 1-12. Spiropyran-modified DNA duplexes.[45]

The T_ms of those spiropyran-modified duplexes were measured (Table 1-3). The duplexes showed a significant destabilization compared with the T_ms of their corresponding unmodified duplexes, *i.e.* X = T in Figure 1-12.

Table 1-3. T_ms of spiropyran-modified DNA duplexes in comparison to the corresponding unmodified duplexes.[45]

Duplex	T_m (°C)	T_m' (°C)	ΔT_m
DNA1	47.9	66.0	–18.1
DNA2	50.0	62.5	–12.5
DNA3	48.0	61.0	–13.0
DNA4	47.8	68.0	–20.2

Surprisingly, ring opening of the spiropyran-modified DNA duplexes with UV light could not be achieved although the same irradiation conditions have been used for switching spiropyran derivatives without DNA. The explanation for this observation was that the DNA nucleobases might quench the triplet state of the spiropyran by energy or electron transfer processes thereby inhibiting the photoswitching process.[45]

1.6.3 Diarylethene

The first examples of these thermally irreversible molecules **37** (Table 1-2) were reported in the late 1960s.[46] The thermal stability of diarylethene can be attributed to the low aromatic stabilization energies of the heterocyclic aryl groups on both sides of the alkene moiety.[47] Diarylethene photoswitches show very high fatigue resistance, as they can undergo reversible photoisomerization for more than 10^4 times.[48]

Cahova and coworkers reported the synthesis of nucleoside-based diarylethene photoswitches in which one of the two aryl moieties of diarylethene was replaced by a nucleoside, namely 2-[2-methyl-5-phenylthien-3-yl]cyclopent-1-ene for the photoregulation of DNA functions.[49] Upon irradiation with light, these compounds **45** were found to undergo a highly efficient, reversible, rearrangement to give products such as **46** (Scheme 1-5).

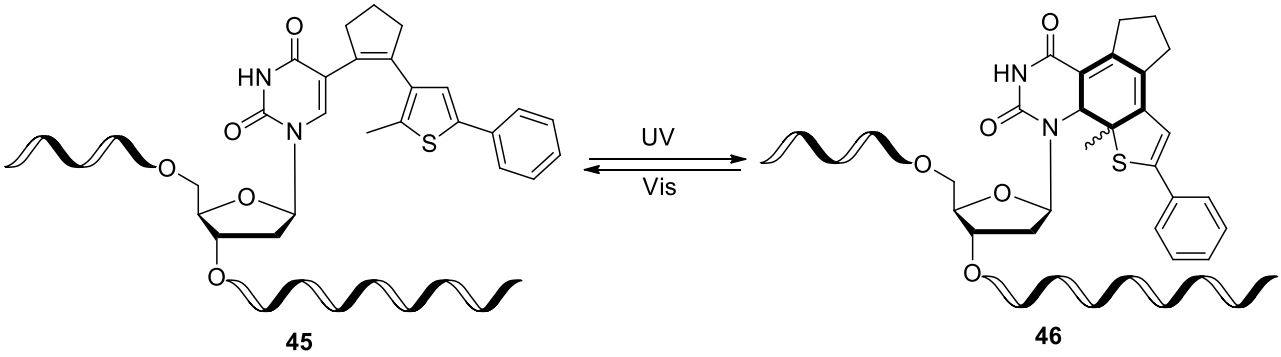

Scheme 1-5. New photoswitchable DNA where a pyrimidine nucleotide is part of the photoswitch.[49]

The influence of this diarylethene photoswitch on DNA transcription was investigated. Generally, promoters incorporating photoswitchable diarylethene gave higher amounts of product in their closed-ring forms than the opened-ring forms.[49]

1.6.4 Azobenzenes

Azobenzenes form one of the largest and most commonly used organic chromophores for optical switching applications.[50] These photoswitches exist in two isomeric states, *trans* and *cis*, with the former being ~10 kcal/mol more stable than the latter.[51] The *trans*-isomer **41** (Scheme 1-6) is virtually planar with nearly zero dipole moment; however, this polarity is considerably changed upon isomerization to the *cis*-form **42** (Scheme 1-6), which has a dipole moment of ~3 D. The distance between the two carbon atoms in the 4- and 4'-positions are 9.0 and 5.5 Å for the *trans*- and *cis*- isomers, respectively.[52] The reverse, *cis* to *trans* isomerization occurs thermally or can be achieved by irradiation with visible light (>460 nm).[12] The photoisomerization of azobenzene occurs with moderate quantum yields, where $\phi_{Z\text{-}E}$ = 53 % and $\phi_{E\text{-}Z}$ = 24 %.[53]

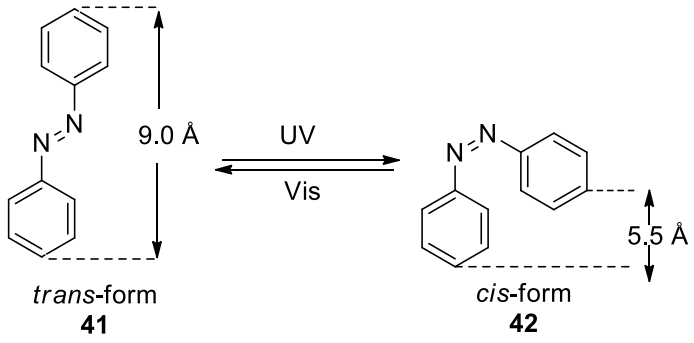

Scheme 1-6. Structural changes during the photoisomerization of azobenzene.[52]

The UV/vis spectrum of unsubstituted *trans*-azobenzene shows two absorption maxima. The *trans*-azobenzene isomer displays a strong absorption band at 318 nm resulting from $\pi \rightarrow \pi^*$ transition and another weak absorption band at 432 nm indicative of the forbidden symmetry $n \rightarrow \pi^*$ transition. The *cis*-azobenzene isomer shows a strong $n \rightarrow \pi^*$ band at 440 nm and a weak

π→π* band at 260 nm. The absorption spectra of the two isomers of azobenzene are distinct but partially overlap, especially in the visible region.[54, 55]

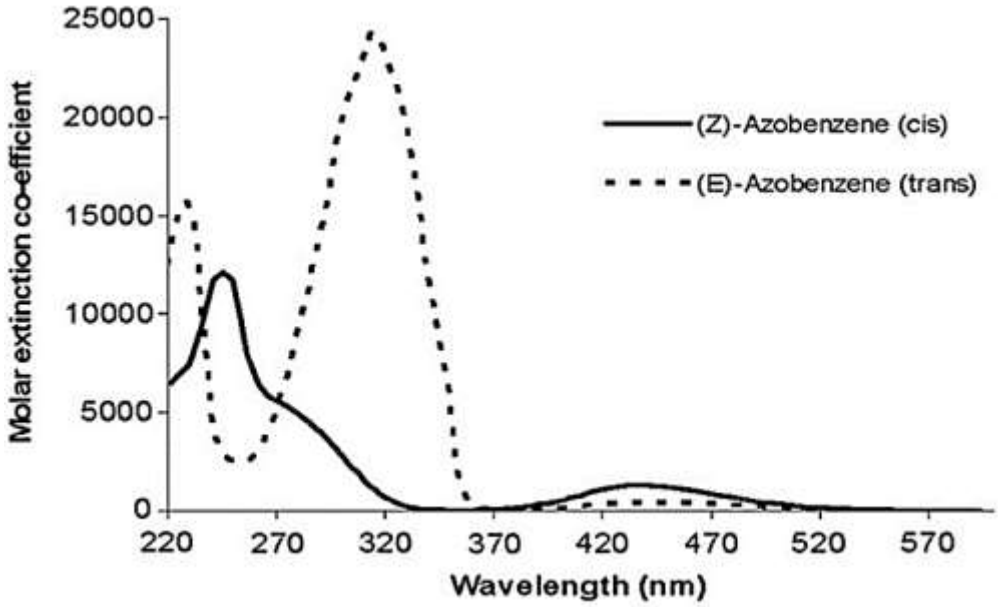

Figure 1-13. UV/Vis absorption spectra of azobenzene isomers **41** and **42** (solid line: *cis*-isomer; dash line: *trans*-isomer).[55] (Reproduced with permission from Zimmerman, G.; L. Y.; Paik, U. J. *J. Am. Chem. Soc.* **1958**, *80*, 3528-3531).

The mechanism of photoisomerization of azobenzene has attracted much attention for many years and has given rise to controversy. For the process, two different mechanisms have been proposed. In the inversion mechanism, the nonbonding electron pair of each nitrogen atom may undergo an n→π* electronic transition with inversion at the nitrogen atom, while the rotation mechanism involves a simple rotation around the N=N double bond (Figure 1-14).[16, 56]

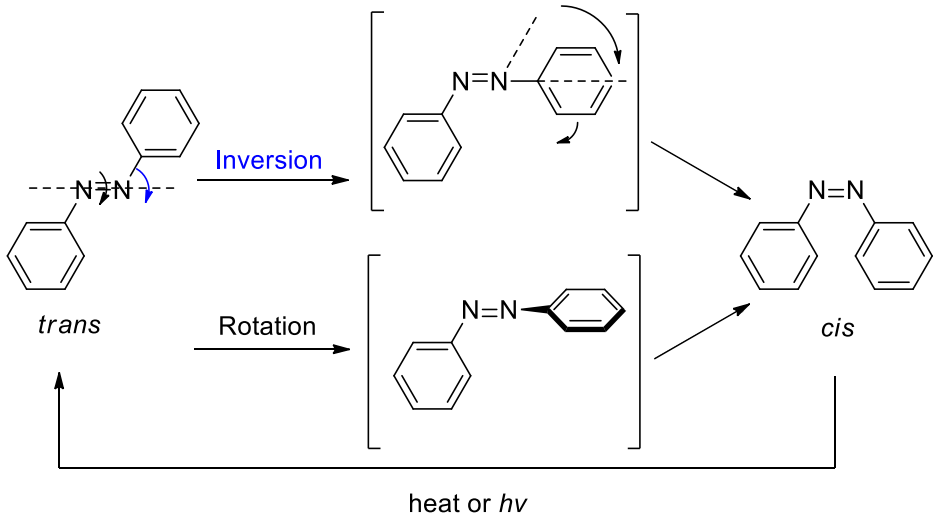

Figure 1-14. Photoisomerization pathways from *trans*-to *cis*- azobenzene and vice versa.[57]

Azobenzenes are easy to synthesize in general. They possess relatively high photostationary states, which is defined as the equilibrium composition during irradiation, and they isomerize with fast photoisomerization kinetics, with low rate of photobleaching.[58] Due to these features, azobenzenes have become the most widely used photoswitches in biological applications.

1.6.4.1 Photoregulation of DNA functions by azobenzenes

The incorporation of switches as nucleoside surrogates remains the gold standard in photoswitchable nucleic acids.[56] Komiyama, Asanuma, and co-workers were the pioneers in this approach by using a phosphoramidite-functionalized switch as nucleoside surrogate.[59] In their study, up to 10 azobenzene units were introduced into the DNA sequence through a D-threoninol linker (as shown in Figure 1-15) in order to photoregulate the formation and dissociation of DNA duplex. Azobenzene intercalates between the neighboring pairing bases in the *trans*-form which stabilizes the duplex formation due to its planarity. Following irradiation, the non-planar *cis*-form destabilizes the duplex, presumably due to diminished ability to intercalate (Figure 1-15).[10]

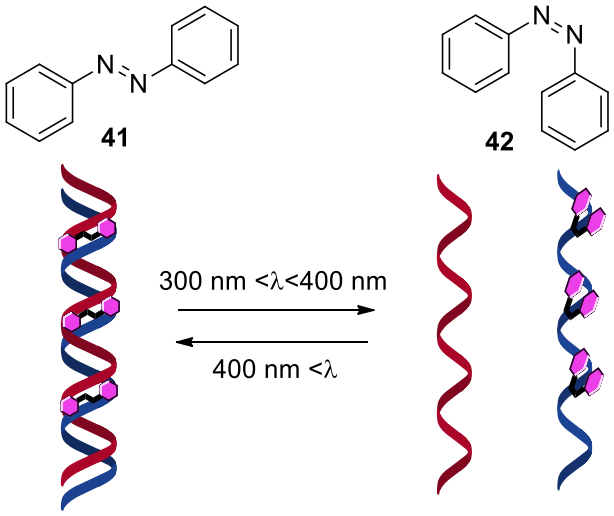

Figure 1-15. The photoregulation of DNA hybridization through incorporating azobenzene residues into oligonucleotides.[10]

Hybridization affinity was compared by measuring the T_m of unmodified and modified DNA sequences.[59] It was found that when azobenzenes took the *trans*- form, introduction of multiple azobenzenes did not interfere with the duplex formation compared with their unmodified complexes; however, the T_m uniformly decreases with the number of azobenzenes when they exist in the *cis*-form. For instance, T_m of Azo-9 which is a 20-mer with nine azobenzenes was 63.5°C for the *trans*-form, which is even higher than that of natural Azo-0 (61.5°C). In contrast, change of T_m by 31.5°C was observed upon *trans-cis* isomerization.[59]

The extent of hybridization was further investigated using a FRET (Fluorescence Resonance Electron Transfer) assay. Thus, fluorescein (FAM) and a fluorescent quencher (Dabsyl) were attached to the 5'-end of the unmodified oligomer and the 3'-end of the azobenzene-modified oligomers, respectively. When azobenzenes adopt the *trans*-form, the modified and complementary strands anneal, thus the fluorescence from the FAM is quenched by the Dabsyl. However, fluorescence is restored to varying degrees when azobenzenes exist in the *cis*-form (Figure 1-16).[10]

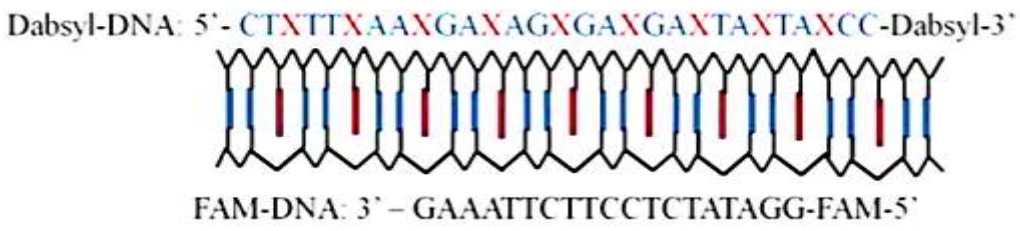

Figure 1-16. Oligonucleotide sequence with a FRET pair used in the incorporation of multiple azobenzene moieties (X= Azobenzene units).[10] (Reproduced with permission from Asanuma, H.; Liang, X.; Nishioka, H.; Matsunaga, D.; Liu, M.; Komiyama, M., *Nat. Protoc.* **2007,** *2*, 203-212).

Komiyama, Asanuma, and co-workers also introduced azobenzenes into specific T7 promoter regions for the photoregulation of the transcriptional activity of T7-RNA polymerase (Figure 1-17a).[10, 60] Two azobenzene units were incorporated between the -3 and -4 sites (unwinding region loop) and between the -9 and -10 sites (loop-binding region) in the non-template strand of the T7 promoter, while keeping the template strand intact (Figure 1-17b). Under UV irradiation, which leads to the formation of *cis*-azobenzene, the rate of transcription with T7 RNA polymerase RNAP was 10-times faster than that under visible light (*trans*-azobenzene) as determined by gel electrophoresis (Figure 1-17c).[10, 60]

a)

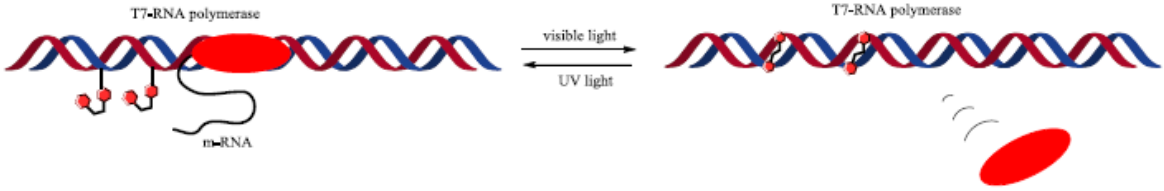

b)

T7 promoter region

	-17	-11	-7	-4	-1	
Non-template	5' – ATAATACGAXCTCACTXATAGGGAGGAAGATAGAGCA					– 3'
template	3' – TATTATGCT	GAGTGA	TATCCCTCCTTCTATCTCGT			- 5'

c)

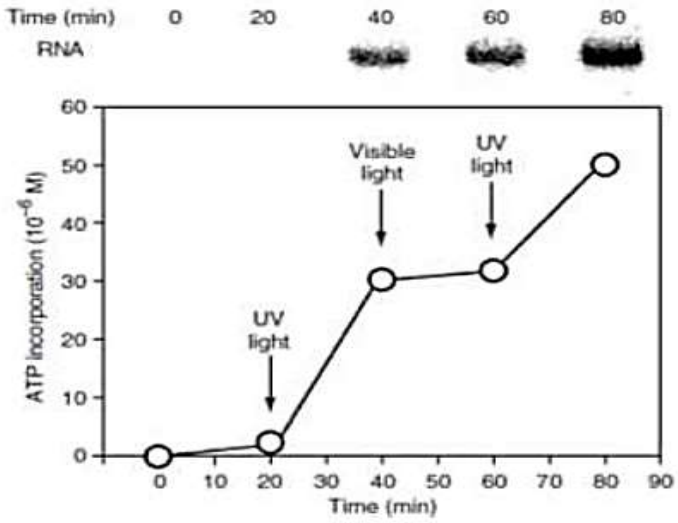

Figure 1-17. a) Photoregulation of transcription by T7-RNA polymerase using azobenzene tethered DNA, b) sequence design of the photoresponsive T7 promoter, and c) photoswitching of transcription by T7-RNA polymerase as determined by gel electrophoresis (X : azobenzene units).[10] (Reproduced with permission from Asanuma, H.; Liang, X.; Nishioka, H.; Matsunaga, D.; Liu, M.; Komiyama, M., *Nat. Protoc.* **2007,** *2*, 203-212).

The application of azobenzene as photoswitch in the regulation of nucleic acid functions is limited by a number of drawbacks. Due to the obvious overlap in the absorption spectra of the two azobenzene isomers, complete isomerization is not possible. Further, irradiation by light in the UV region may lead to DNA damage. The isomerization of azobenzene in both directions (*trans*→*cis* and *cis*→*trans*) is associated with relatively low quantum yields.[55, 61]

1.6.5 Cyclic azobenzenes

Cyclic, or "bridged", azobenzene (cAB), was first prepared quite some time ago,[62] but attracted little attention until very recently, when its potential as a molecular photoswitch was discovered by Siewertsen *et al.* who showed that the photochromic properties of cAB is much more favourable for photoswitching compared to plain azobenzene (AB).[63]

Compared with AB, the n→π* transition of *trans*-cAB isomer **48** (Scheme 1-7) is red-shifted, but the n→π* transition of the *cis*-isomer **47** is also significantly blue-shifted, indicating a large separation of n-π* bands of the two isomers.[63, 38]

The *cis*-isomer of cAB is switched to the *trans*-isomer with purple light (370-400 nm) with an efficiency >90%, and the latter can be transformed back to the *cis*-isomer in virtually quantitative efficiency with green light (480-550nm) (Scheme 1-7).[63] Moreover, due to the ring strain, the *cis*-, but not *trans*-, isomer is the thermodynamically stable form at room temperature by 6-7 kcal/mol,[63] which makes cAB photoswitch a useful turn-on system for biological applications.

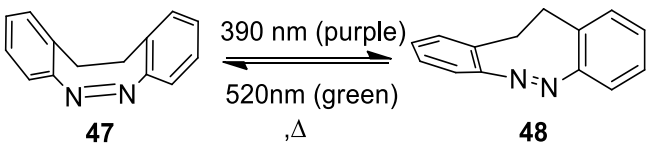

Scheme 1-7. Photoisomerization of cyclic azobenzene.[63]

Figure 1-18 shows the UV/vis spectra of unmodified cyclic azobenzene. The *cis*-isomer exhibits a characteristic absorption band at 404 nm due to its n→π* transition. This band disappears upon irradiation with the purple light and a more intense absorption band at 490 nm was observed with quantum yields of 72±4% and 50±10% for the forward and backward directions, respectively.[55, 64]

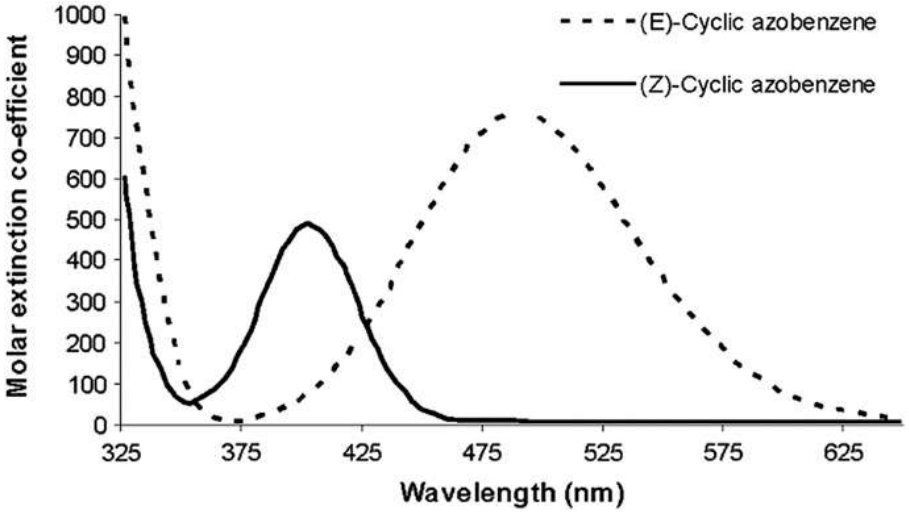

Figure 1-18. UV/vis absorption spectra of cyclic azobenzene **47** and **48**. Solid line: (*cis* or *Z*)-isomer; dash line: (*trans* or *E*)-isomer.[55] (Reproduced with permission from Zimmerman, G.; L. Y.; Paik, U. J. *J. Am. Chem. Soc.* **1958**, *80*, 3528-3531)

In 2012, Yan *et al.* reported the synthesis of cyclic azobenzene analogue **49** (Figure 1-19) through the transformation of 2,2'-dinitrodibenzyl. Upon exposure to purple light, as much as 70% of *cis*-cAB analogue **49** can be isomerized into the corresponding *trans*-cAB, compared with up to 90% isomerization for the unmodified cAB.[55]

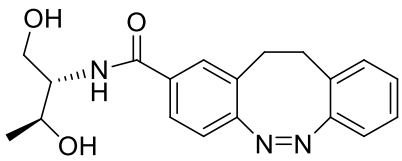

49

Figure 1-19. Structure of cAB-threoninol.[55]

Like linear azobenzene, the photoisomerization property of cyclic azobenzene can also be exploited to regulate nucleic acid functions such as hybridization, transcription, and gene expression by light.

1.7 Objectives of this project

The goal of this project is to first develop a shorter route to synthesize cAB phosphoramidite by modifications of the previously reported procedures.[55] cAB will then be incorporated into DNA sequences by solid phase synthesis with different numbers of cAB units and at different positions in the DNA sequence in order to investigate the effect of these modifications on DNA hybridization. Impact of cAB on the hybridization affinity of DNA sequences will be investigated by measuring the T_ms of these modified and unmodified sequences. It is hypothesized that *cis*-cAB will destabilize the DNA duplex to give lower T_m values, while *trans*-cAB can be accommodated by DNA duplex.

The impact of cAB on the hybridization of DNA will also be explored by FRET experiment. In this respect, FAM and the Black Hole Quencher will be incorporated to the 5'- and 3'- of the complementary strand and modified DNA sequence respectively. As fluorescent quenching by FRET is only possible when the FRET pair is in close proximity, these experiments will provide more direct evidence for hybridization.

CHAPTER 2: Site-specific labeling of DNA using Inverse Electron Demand Diels-Alder reaction of *trans*-cyclooctene derivatives and BODIPY-tetrazine adduct.

2.1 Inverse Electron Demand Diels-Alder reaction (IEDDA)

The Diels-Alder (DA) reaction is arguably the most used pericyclic reactions.[65] It involves a [4+2] cycloaddition between a conjugated diene and a substituted alkene, commonly termed the dienophile, to form a substituted cyclohexene system. According to frontier orbital theory, Diels–Alder reactions can be divided into three subclasses, normal, neutral, and inverse electron demand (Figure 2-1).[66]

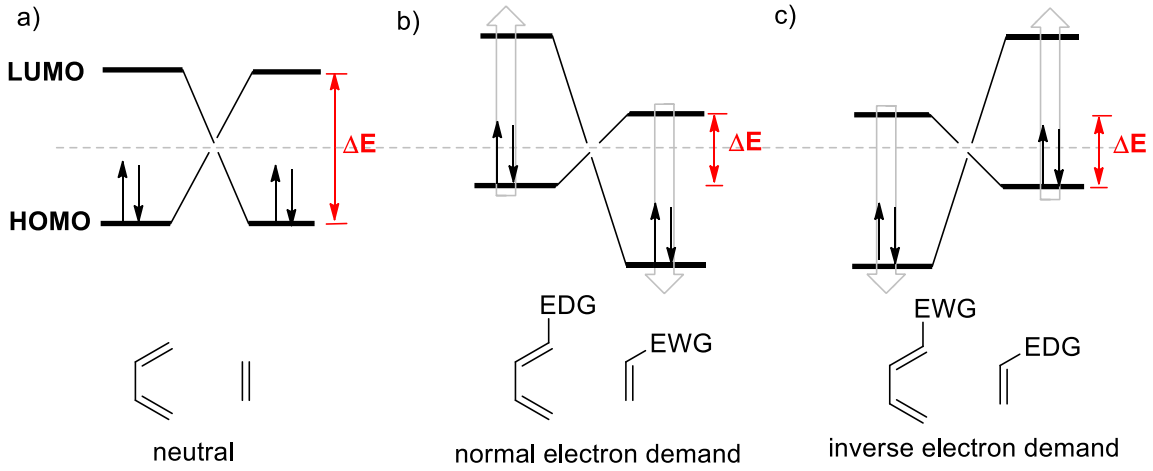

Figure 2-1. Frontier orbital model of (a) neutral, (b) normal electron demand and (c) inverse electron demand Diels–Alder additions (EDG = electron-donating group, EWG = electron-withdrawing group).[66]

Electron-withdrawing groups (EWG) lower the energy of both the HOMO and LUMO on a cycloaddend, whilst electron-donating groups (EDG) have the opposite effect. Therefore, normal Diels–Alder additions feature electron-rich dienes and electron-poor dienophiles. As a result, these reactants show a reduced $HOMO_{diene}$–$LUMO_{dienophile}$ separation, compared with the

$HOMO_{dienophile}$–$LUMO_{diene}$ separation which dominates the reactivity (Figure 2-1b).[65-67] In IEDDA, dienes are electron-poor while dienophiles are more electron-rich which makes the $LUMO_{diene}$ and $HOMO_{dienophile}$ closer in energy than the $HOMO_{diene}$ and $LUMO_{dienophile}$. Thus, the $LUMO_{diene}$ and $HOMO_{dienophile}$ are the frontier orbitals that interact the most strongly (Figure 2-1c).[68] As for neutral Diels–Alder additions, ΔE between the HOMO and LUMO of both reactants is similar (Figure 2-1a).[66]

Recently, there has been tremendous interest in the use of the click reaction for biological labeling. The typical click reaction (Huisgen cycloaddition) involves copper (I)-catalysts, which are cytotoxic, for coupling of an azide and terminal alkyne to generate a stable triazole.[69] The requirement for copper salt in this reaction was circumvented by the work demonstrated by Bertozzi and co-workers where ring-strained cyclooctyne derivatives react with organic acids in the absence of a catalyst.[70, 71] In this regard, the cycloaddition reaction between azides and ring-strained cyclooctynes has been employed for imaging of cells[70] and zebra fish embryos.[72] The applications of this copper-free click chemistry are somewhat limited by the poor water solubility of the cyclooctynes and the difficulty in synthesizing the cyclooctynes in large quantities.[73]

2.2 IEDDA between 1,2,4,5-tetrazines and olefins as a potential click reaction

The presence of nitrogen in the aza-dienes framework such as 1,2,4,5-terazines (*s*-tetrazine) lower both the HOMO and LUMO energy, making tetrazines ideal substrates for IEDDA reactions.[65] Additionally, introduction of electron-withdrawing substituents at 3- and 6-positions of tetrazine further lower its LUMO, thus accelerating IEDDA, while electron donating substituents have a negative effect on reaction rates. Furthermore, dienophiles with electron-rich substituents and with a high degree of ring strain are preferred, since the latter can facilitate IEDDA

reactions by reducing the activation energy, caused by a raised $HOMO_{dienophile}$ and reduction of the distortion energy.[66]

Scheme 2-1 shows the mechanism of IEDDA. Tetrazine **50** reacts with a suitable dienophile **51** to form a highly strained bicyclic adduct **52** which is then rapidly converted to the corresponding 4,5-dihydropyridazine **53** upon release of a molecule of dinitrogen.[74] 1,3-Prototropic isomerisation, followed by oxidation, leads to the formation of the pyridazine product **55**.[75]

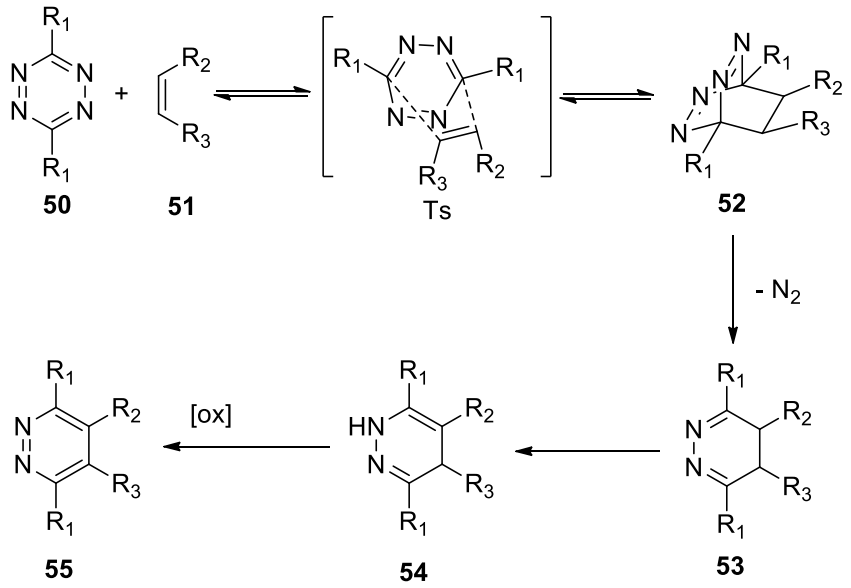

Scheme 2-1. IEDDA reaction scheme.[66]

In 1990, Sauer and coworkers described the reaction kinetics of electron-deficient tetrazines with a number of dienophiles and quantitatively demonstrated that strained alkenes such as *trans*-cyclooctenes are seven orders of magnitude more reactive than *cis*-cyclooctenes toward these tetrazines.[76] Eight years later, Schuster *et al.*[77] demonstrated that un-substituted tetrazine can react very rapidly with alkenes and alkynes. It was then until 2008 when IEDDA was demonstrated as a potential click chemistry scheme by two independent groups. Fox *et al.* described the bioorthogonal cycloaddition reaction between *s*-tetrazine and *trans*-cyclooctene derivatives. The

reactions tolerate a broad range of functionality and proceed in high yields in organic solvents, water, cell media, or cell lysate. The second-order rate constant for the reaction between 3,6-di-(2-pyridyl)-*s*-tetrazine **57** and *trans*-cyclooctene **56** at 25 °C is 2000 (± 400) M^{-1} s^{-1} in 9:1 methanol/water (Scheme 2-2). This fast reactivity has been employed in protein labeling at low concentration[78]

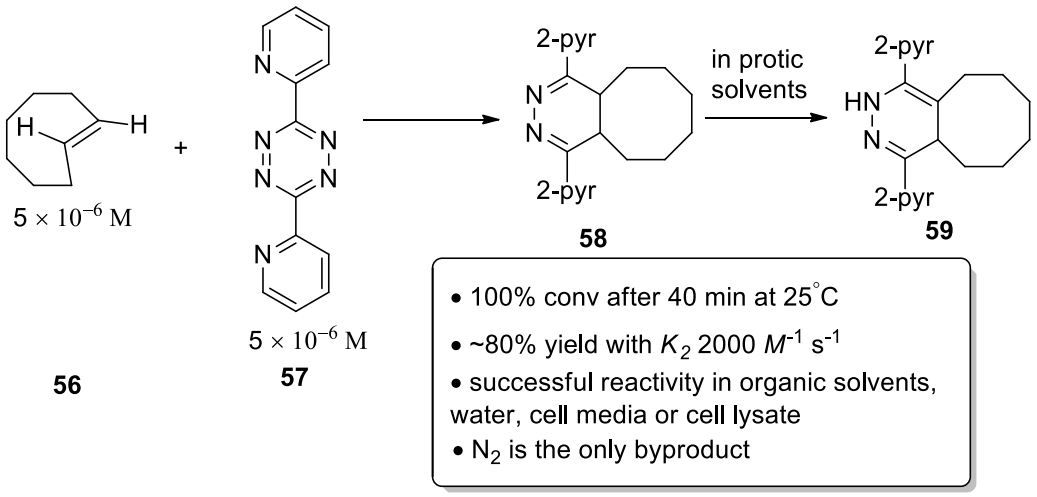

Scheme 2-2. Fast reactions between 3,6-di-(2-pyridyl)-*s*-tetrazine and *trans*-cyclooctene at sub micromolar concentrations.[78]

The second study by Hilderbrand *et al*. applied the bioorthogonal tetrazine cycloadditions to live cell labeling. They found that benzylamine-modified tetrazine **60** reacts irreversibly with the strained dienophile norbornene **61** in aqueous buffer and fetal bovine serum (stain buffer) with second-order rate constants of 1.9 and 1.6 M^{-1} s^{-1} respectively, forming dihydropyrazine products and dinitrogen (Scheme 2-3).

This chemistry was subsequently used for targeting Her2/neu receptors in live human breast cancer cells with a monoclonal antibody modified with a norbornene ("pretargeted antibody"). Tetrazines conjugated to fluorophore selectively and rapidly label this pretargeted antibody in the

presence of serum, suggesting that this chemistry is a useful strategy for *in vivo* pretargeted imaging.[73]

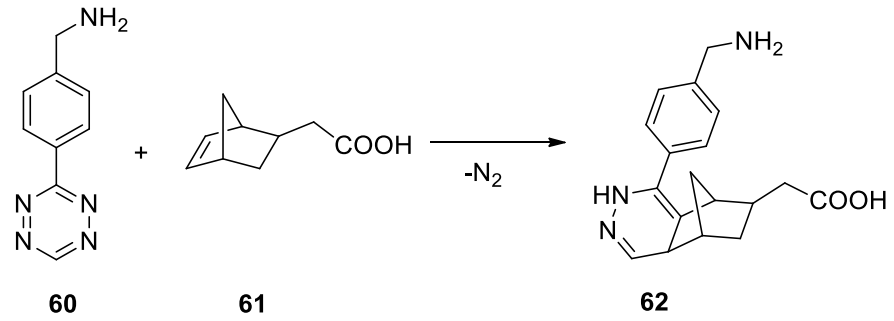

Scheme 2-3. Click reaction between benzylamine-modified tetrazine and strained dienophile norbornene.[73]

IEDDA makes a powerful alternative to existing ligation chemistries due to its high reaction rate, bioorthogonality and mutual orthogonality with other click reactions. In addition, IEDDA cycloaddition of olefins with tetrazines results in irreversible coupling in contrast to many Diels-Alder reactions, giving dihydropyridazine with releasing of dinitrogen.[73] As a result, IEDDA has found various applications in labeling nucleic acids, glycans, peptides and proteins, intracellular imaging of small molecules, and *in vivo* imaging as well as modification of cells with nanomaterials for clinical diagnostics.[79]

2.3 IEDDA features

2.3.1 Rapid kinetics

IEDDA reaction kinetics can be tuned by selecting appropriate dienes and dienophiles. For example, IEDDA reaction between norbornene **63** (Figure 2-2) and tetrazine proceeds with an impressive rate of ~ 1–10 $M^{-1}s^{-1}$,[80] which is considerably faster than other click reactions including CuAAC (Cu-catalyzed azide alkyne cycloaddition)[81] and SPAAC (strain promoted azide alkyne cycloaddition)[82] as shown in Table 2-1.[66] Replacement of the initially used norbornenes by more reactive *trans*-cyclooctenes **64** speeds up the reaction to 2000 $M^{-1}s^{-1}$.[73] Further chemical

modification, for example, enhancement of ring strain of **64** by a condensed cyclopropanyl ring to form *trans*-bicyclo[6.1.0]nonene **65** resulted in the fastest IEDDA example with k_2 of up to 380,000 $M^{-1}s^{-1}$(Table 2-1).[83] Furthermore, the use of cyclopropene derivative **66** as a precursor for IEDDA click reaction gave a rate constant of 7 ± 1 $M^{-1}s^{-1}$ in water/DMSO at 20°C. Although this rate constant is comparable to previous bioorthogonal click reactions including IEDDA with norborene, it is much slower than the reaction of other strained alkenes with tetrazine, such as *trans*-cyclooctene and its derivatives.[84]

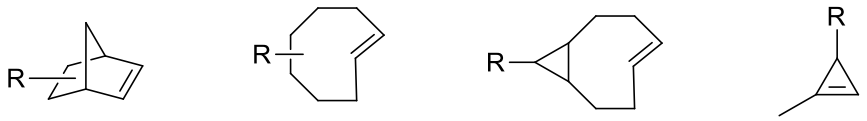

63 **64** **65** **66**

Figure 2-2. Examples of IEDDA dienophiles.[66, 84]

Table 2-1. Typical reaction rates for popular bioorthogonal click reactions.[66]

Reaction	Reactants	Rate [$M^{-1}s^{-1}$]
CuAAC	Terminal alkyne+azide	10^{-2}-10^{-4}
Staudinger–Bertozzi ligation	Azide + phosphine	2.2×10^{-3}[b]
SPAAC	BARAC[a] + azide	1[b]
IEDDA	**63** + tetrazine	1-10[c]
IEDDA	**65** + tetrazine	3.8×10^{5}[d]

[a] Biarylazacyclooctynone. [b] measured in CD_3CN. [c] In H_2O-MeOH (95 : 5), 21°C. [d] H_2O-dioxane (90 : 10), 25 °C.

Very recently, 1,2,4-triazines have been described as a new class of bioorthogonal reagent for IEDDA.[85] These scaffolds are stable in biological media, in contrast to tetrazines which are prone to hydrolysis and side reactions with endogenous thiols. The stability of 1,2,4-triazines can be attributed to the high energetics of 1,4-adduct formation and subsequent N_2 release transition state. As an example, the activation energy for the reactions between methanethiol and 6-phenyl-1,2,4-triazine **67** and 3-phenyl-1,2,4,5-tetrazine **68** are ~31.5 kcal/mol and 28.6 kcal/mol, respectively.

In terms of reactivity, however, 1,2,4-triazines are less reactive than 1,2,4,5-tetrazines with activation free energy of 29.3 versus 21.9 kcal/mol for 1,2,4,5-tetrazines. Figure 2-3 shows the predicted relative rate constants for tetrazine or triazine cycloaddition with 3-carbamoyloxymethyl-1-methylcyclopropene, norbornene, or *trans*-cyclooctene, in water at 25 °C. 6-Aryl-1,2,4-triazine **67** react efficiently with *trans*-cyclooctene with a rate constant of 8.3×10^{-2} M^{-1} s^{-1}, which is much slower than that of 1,2,4,5-tetrazine **68**, with a rate constant of $\sim 4.9\times 10^{3}$ M^{-1} s^{-1}, while triazine remains inert to other bioorthogonal scaffolds.[85]

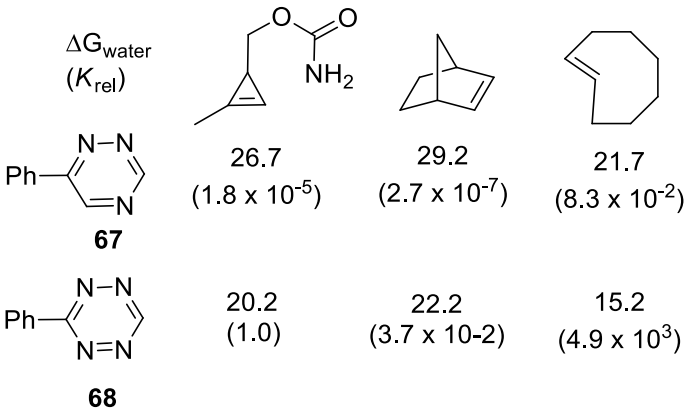

Figure 2-3. DFT-computed activation free energies (kcal/mol) and predicted relative rate constants (in parenthesis) for tetrazine or triazine cycloaddition with 3-carbamoyloxymethyl-1-methylcyclopropene, norbornene, or *trans*-cyclooctene, in water at 25 °C.[85]

2.3.2 Bioorthogonality and mutual orthogonality with other click reactions

A major advantage of IEDDA ligations over other click reactions such as CuAAC is that they do not require a metal catalyst making IEDDA highly suitable for biological applications.[86]

The ability to control chemical reactivity and selectivity, especially in chemically complex environments, is one of the most appealing features of IEDDA click chemistry.[87] The mutual orthogonality of IEDDA click chemistry, as shown in pathway **a** in Figure 2-4, with other click reactions, such as azide-alkyne click chemistry and thiol-ene click chemistry, as shown in pathway

b in Figure 2-4, enables the simultaneous multiple selective labeling reactions to connect complex functionalities in a facile fashion without the need for protecting groups.[66] This "one-pot approach" is very useful in many applications in the field of chemical biology, drug discovery,[88] and macromolecular chemistry.[89] However, there are some cyclooctynes which are prone to undergo both IEDDA and SPAAC **c** and **d** (Figure 2-4) , therefore, these two reactions cannot be performed simultaneously.[66]

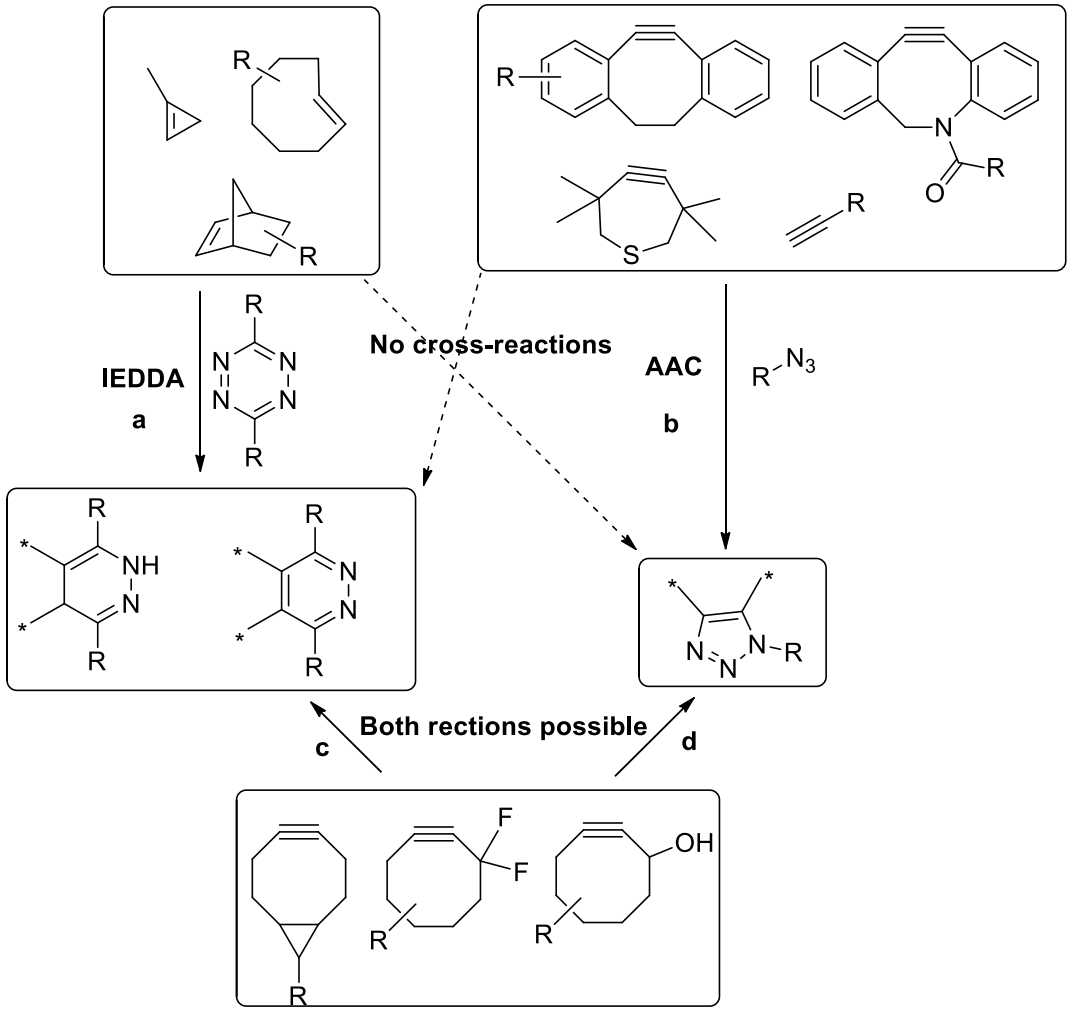

Figure 2-4. Suitable pairs for mutually orthogonal azide-alkyne/IEDDA click chemistry.[66]

2.4 Tetrazine probes

Since the unmodified tetrazines could not be applied directly to bioconjugation, as they were not stable in water,[90] a considerable number of different unsymmetric and symmetric tetrazine analogues with various functionalities have been prepared.[91] A straightforward two-step procedure for synthesizing tetrazines involves the reaction of nitriles **69** or analogues, such as nitrile imines or aldehydes with hydrazine (both anhydrous and hydrated hydrazine may be used) (Scheme 2-4a). For unsymmetrically substituted tetrazines, formamidine acetate **72** is used as a reagent (Scheme 2-4b).[91] The resulting dihydrotetrazines **70** and **73** can be further oxidized into the fully aromatic tetrazines **71** and **74** by HONO. Either sulfur[74] or Lewis acids such as nickel triflate or zinc triflate can be used as catalysts in this reaction. High yields can be obtained by using a pressure tube at higher temperature.[90]

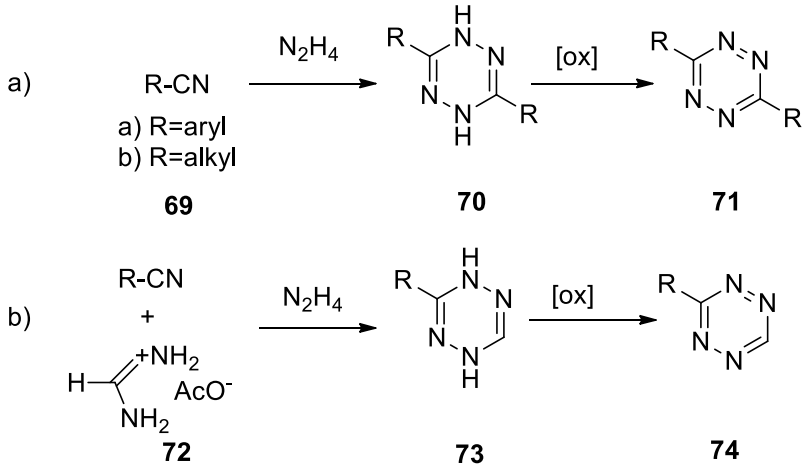

Scheme 2-4. Synthetic strategies for tetrazines using a) hydrazine or b) formamidine acetate as reagents.[92]

Another important route toward the preparation of differently functionalised tetrazines is through nucleophilic aromatic substitution (S_NAr)[65, 90, 91] of precursors such as 3,6-bis(3,5-dimethyl-1H-pyrazol-1-yl)-*s*-tetrazine **75**,[93] and 3,6-dichloro-*s*- tetrazine **76**[94] (Scheme 2-5).

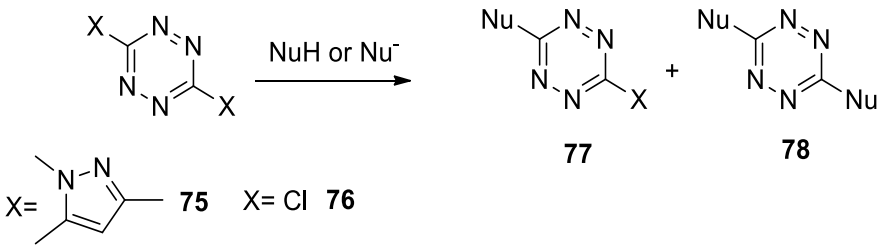

Scheme 2-5. General approach for the nucleophilic substitution of *s*-tetrazine.[91]

The color of most tetrazines ranges from orange to red due to the weak n→π* transition excited by light with wavelength around 520 nm.[91] In addition, some suitably substituted tetrazines are fluorescent, however, the fluorescence of these tetrazine analogues are weak in general due to the low molar extinction coefficient of the associated absorption band (*ca*. 1000 M^{-1}•cm^{-1}).[95]

Since tetrazines absorb light in the visible region, they are considered as chromophores, thus they can act as quenchers towards a series of fluorophores[96] based on the resonance energy transfer (RET) theory as supported by the studies of Dumas-Verdes *et al*.[97] and Weissleder *et al.*[98] On the other hand, upon reaction of tetrazines with an IEDAA partner, fluorescence can be restored, thus providing excellent "turn-on" probes with minimal background signal in biomolecule labeling experiments. Figure 2-5 shows examples of some tetrazine probes which have been used for IEDDA cycloadditions.

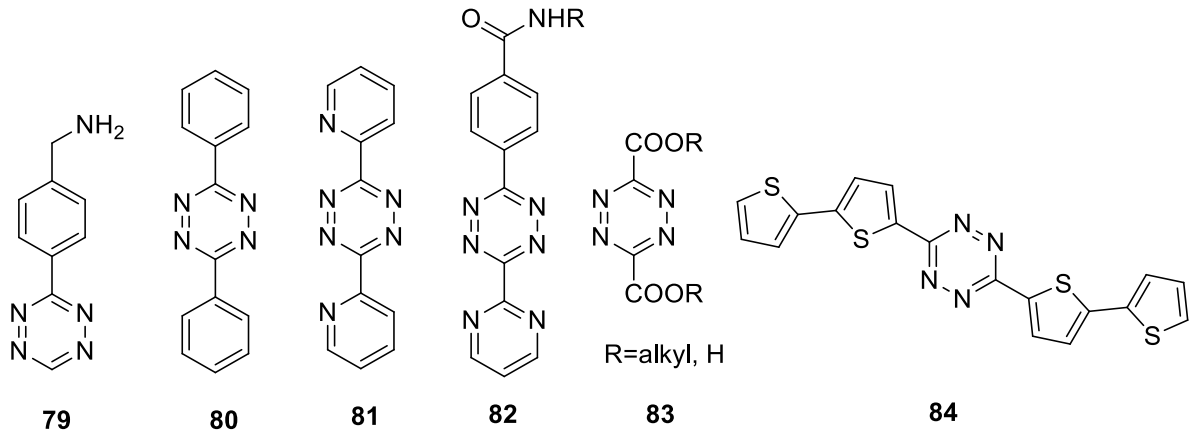

Figure 2-5. Examples of symmetrical and unsymmetrical aromatic *s*-tetrazines used for IEDDA.[99,100]

Several factors have to be taken into considerations regarding the quenching mechanism.[96] The spectral overlap between the emission of the fluorophore and the absorption of the tetrazine, and the close proximity of the fluorophore and the quencher results in a through-space energy transfer mechanism which is generally known as a florescence resonance energy transfer (FRET) (Figure 2.6a).[96, 101] If the fluorophore is connected to the acceptor via electronically conjugated linkers, the energy transfer in such a system occurs through-bonds (TBET) and through-space (FRET) (Figure 2-6b).[96, 97, 101]

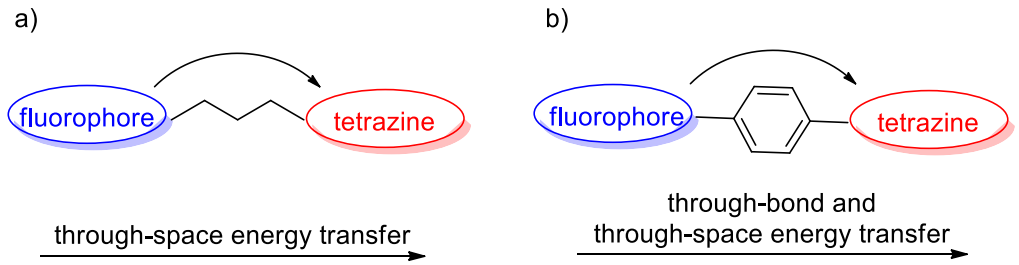

Figure 2-6. a) Through-space and b) through-bond and through space energy transfer cassettes.[101]

When tetrazine undergoes IEDDA reaction, it is converted to a (dihydro)pyridazine derivative. This reaction is accompanied by a drastic change in electronic and spectroscopic properties. Therefore, the fluorescence is restored.[96]

Another possible mechanism for the quenching process results from photoinduced electron transfer (PET) between the fluorophore and tetrazine. Before IEDDA reaction, the $HOMO_{tetrazine}$ lies higher in energy than that of the $HOMO_{florophore}$, thus an electron from $HOMO_{tetrazine}$ can be transferred to $HOMO_{florophore}$. This process competes with radiative decay of the excited fluorophore to the ground state, thus diminishing the fluorescence. Reaction of tetrazine through IEDDA makes $HOMO_{tetrazine}$ lower than $HOMO_{phrorophore}$, preventing electron transfer, thus fluorescence is restored (Figure 2-7).[102]

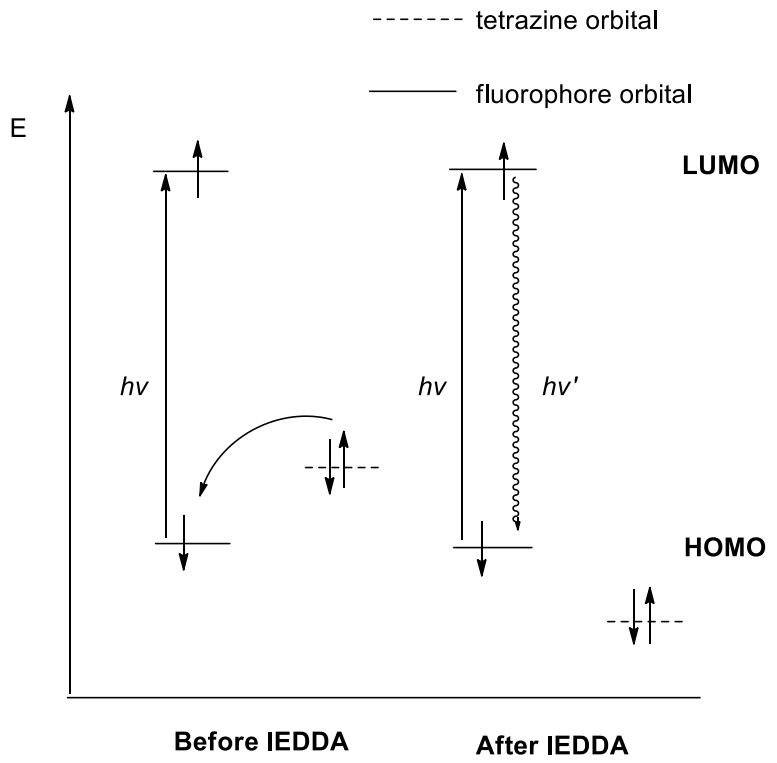

Figure 2-7. Energy level diagrams illustrating PET from the frontier molecular orbital perspective.[102]

Weissleder and coworkers designed a series of tetrazine-fluorophore probes where the fluorescence of these molecules was efficiently quenched by tetrazine via FRET, with up to a 20-fold enhancement in fluorescence after destruction of the tetrazine upon IEDDA cycloaddition. For instance, the green-emitting tetrazine dye, tetrazine-BODIPY FL **85** (Figure 2-8a) showed fluorescence enhancement of approximately 15-fold upon cycloaddition.[98, 103]

In a separate study, Chin *et al.* demonstrated that tetrazines can also quench near-IR-emitting fluorophores such as tetramethylrhodamine **87** (Figure 2-8b). However, the fluorescence enhancement was only about 5-fold due to the large separation in space between the FRET pair.[80]

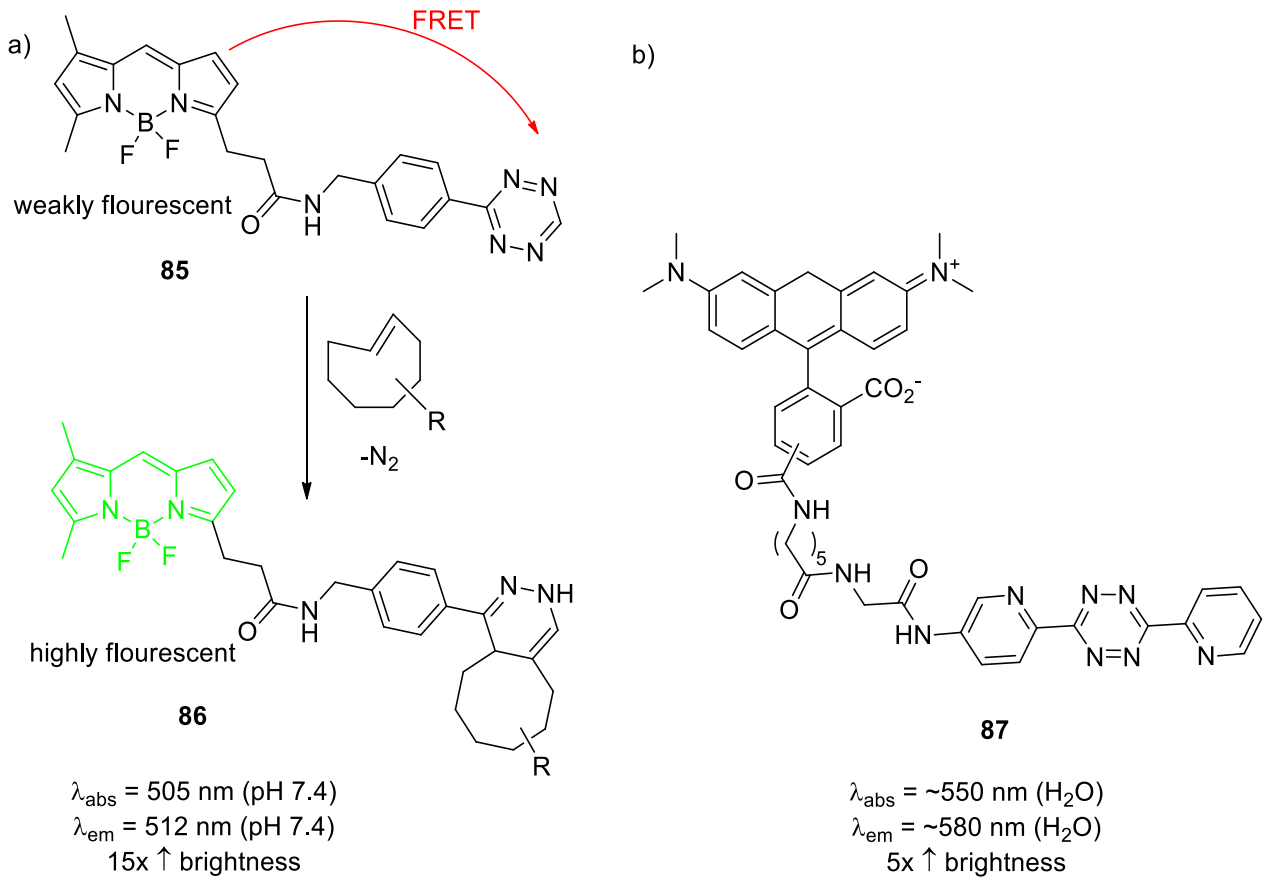

Figure 2-8. Tetrazine "turn-on" probes. a) BODIPY FL–tetrazine conjugate and b) tetramethylrhodamine-tetrazine conjugate.[103]

FRET efficiency can be increased dramatically by reducing the distance between tetrazine and the fluorophore. Moreover, the close proximity of the FRET pair may allow for other quenching pathways, such as through-bond energy transfer (TBET).[101, 103] To raise the possibility of the latter pathway, the conjugated linker between tetrazine and the fluorophore should not be flexible, and must prevent tetrazine and the fluorophore to be co-planar, otherwise the system would behave as a single conjugated dye.[101] The first explanation of this phenomenon was provided by Carlson *et al.* who synthesised a series of virtually non-fluorescent BODIPY-tetrazine conjugates **88**, **89**, and **90** (Figure 2-9), where the tetrazine was attached to the BODIPY core via a rigid phenyl linker.[104] BODIPY-tetrazine conjugate **88** exhibits a 90 degree rotation between the BODIPY and tetrazine

ring which prevents pi-system conjugation and increases the efficiency of the FRET quenching. Indeed, reaction of **88** with *trans*-cyclooctenol in water gave a turn-on ratio of 900- fold.

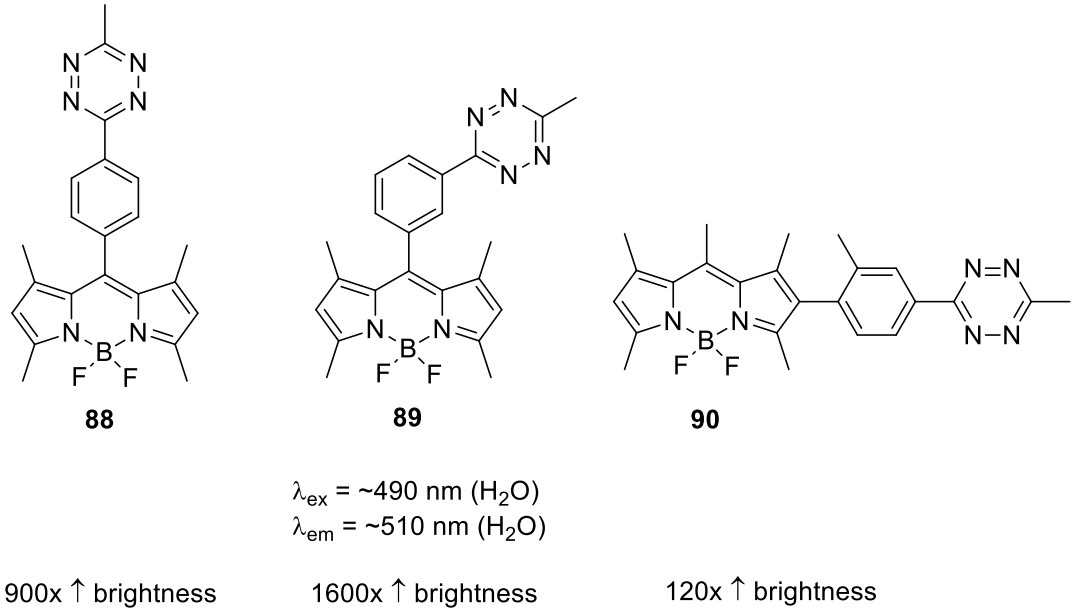

Figure 2-9. BODIPY-tetrazine probes connected with rigid linkers.[104]

Moving the attachment position of the tetrazine from *para*- to *meta*- on the phenyl ring, such as in conjugate **89**, exhibited even greater turn-on ratio, e.g. 1600-fold in water.[104] To demonstrate that TBET was operative in the quenching, BODIPY-tetrazine conjugate **90** was synthesized. In this derivative, the BODIPY and tetrazine groups were arranged such that their transition dipoles are nearly perpendicular which prevents efficient FRET. In addition, conjugation of the phenyl linker was minimized by the *ortho*-methyl group. Surprisingly, a 120-fold enhancement in fluorescence was still observed upon reaction of **90** with *trans*-cyclooctenol, suggesting that FRET is not the only quenching pathway in these conjugates, and tetrazine-TBET quenching mechanism may be taken into consideration. PET quenching mechanism was ruled out as the fluorescence emission intensity of these compounds was found to be independent of solvent polarity. After cycloaddition, the fluorescence quantum yields of these compounds reached up to 0.8, indicating that quenching was fully relieved. Excellent signal intensity, reduced background fluorescence

and no requirement for washing steps in the labeling process make BODIPY-terazine conjugates very attractive molecules for biological applications. Indeed, these compounds were successfully applied for imaging *trans*-cyclooctene-functionalized antibodies on both fixed and live cells.[103, 104]

The approach described above was expanded to multicolor imaging.[103] Coumarin-tetrazine conjugates, such as **91**, were designed (Figure 2-10).[105] In these compounds, transition dipoles of the coumarin fluorophore and the tetrazine align significantly to maximize contribution from FRET in addition to TBET, resulting in an up to an impressive 11000-fold enhancement in fluorescence to final quantum yields of 0.5 upon tetrazine ligation. These compounds, named HELIOS probes, were used for efficient detection of a variety of *trans*-cyclooctene-functionalized molecules in fixed and live cells.[103, 105]

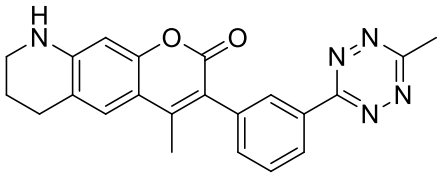

91

λ_{ex} = 388 nm (pH 7.4)
λ_{em} = 482 nm (pH 7.4)

11000x ↑ brightness

Figure 2-10. Cumarin-tetrazine probe.[105]

2.5 IEDDA for site-specific labeling of nucleic acids

Labeling of oligonucleotides (RNA or DNA) with a molecule of interest (e.g., a fluorescent dye or affinity tag) helps in understanding their functions. Recently, IEDDA between tetrazines and olefins has been used for this application.

In 2010, Jäschke *et al.* introduced norbornene moieties as dienophiles into DNA sequences at both terminal and internal positions during solid-phase synthesis, and the deprotected oligomers are then conjugated with water-stable tetrazine (Scheme 2-6).[106] In this study, when norbornene

moiety **94** was introduced to 19-mers ODN as shown in Figure 2-11, followed by treatment with equimolar amounts of tetrazine probe **95** at room temperature, 50% conversion was obtained after only 12 min. Higher conversion (up to 90%) was obtained by increasing the reaction time to 3 h with a rate constant ~ 20 ± 2 M^{-1} s^{-1}.[106]

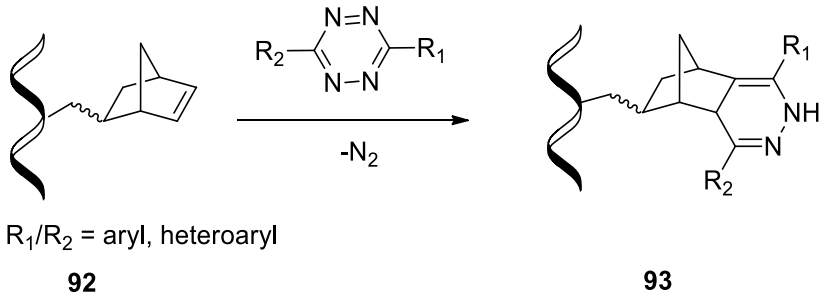

Scheme 2-6. General scheme for IEDDA between norbornene modified DNA and tetrazine derivative.[106]

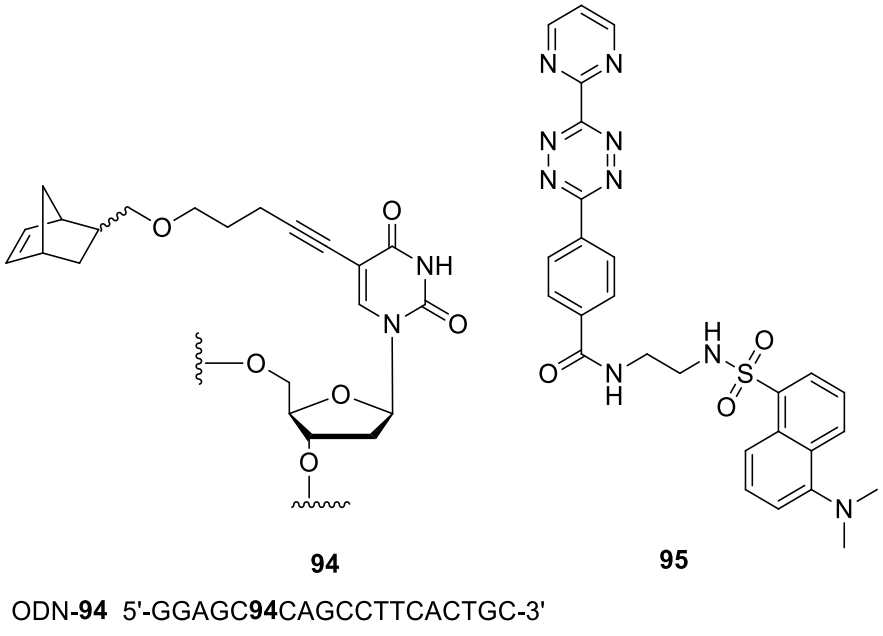

Figure 2-11. Norbornene building block **94** and tetrazine probe **95** for fluorescent labeling of DNA.[106]

This approach was further expanded to RNA molecules via both chemical and enzymatic routes.[107] First, a 5'-norbornene-modified 19mer RNA **96** was synthesized by solid phase synthesis using a norbornene phosphoramidite.[106] After **96** was incubated with a dansyl-modified tetrazine **97** at room temperature for 90 min, ~90% of the RNA was converted to the Diels-Alder product

98 (Scheme 2-7a) as determined by LC-MS analysis.[107] In addition, an "initiator" **99**, *i.e.* guanosine modified with norbornene at the 5'-position, was synthesized[108] in order to label RNA molecules that are enzymatically transcribed. T7 RNA polymerase efficiently transcribed the DNA template using a defined promoter, having a guanosine nucleotide as +1 base, which is the transcription start site(Scheme 2-7b).[109] Upon IEDDA, conversions of norbornene-labelled RNA to IEDAA product were found to be comparable to those obtained for chemically modified RNA and the labeling efficiency was found to depend on both the incubation time and the excess of dansyl-tetrazine reagent.[107]

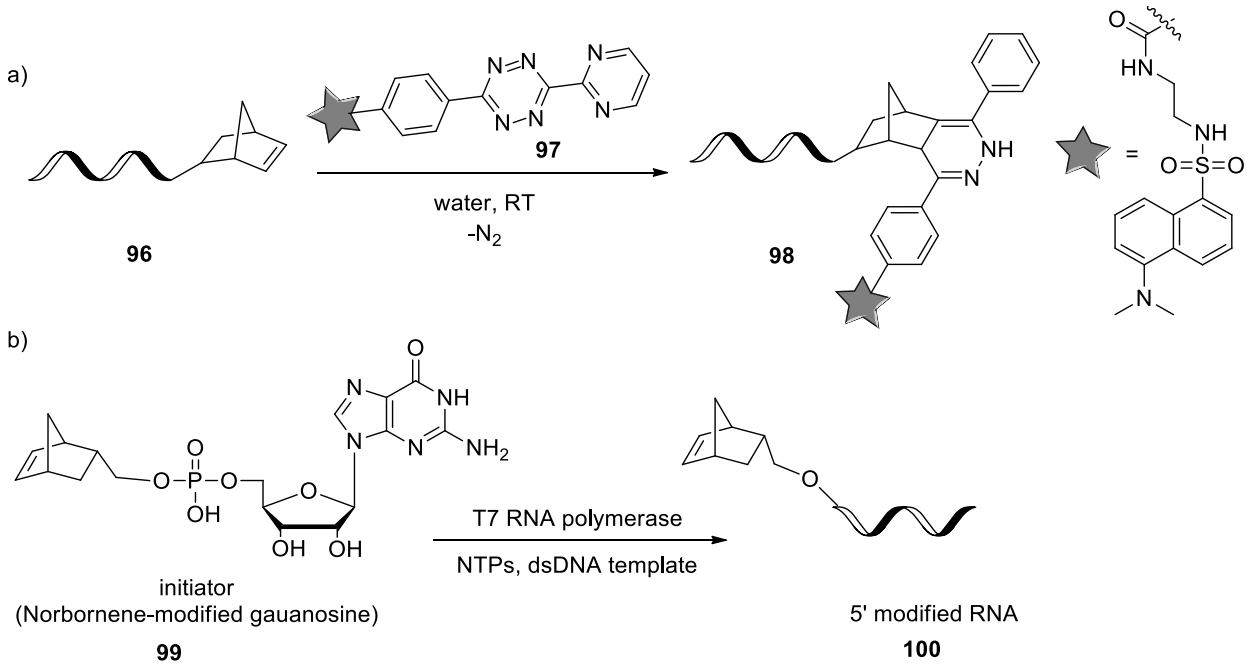

Scheme 2-7. a) IEDDA reaction of a norbornene-modified RNA with Dansyl-modified tetrazine and b) incorporation of the initiator nucleotide into transcribed RNA by T7 RNA polymerase.[107]

A successful combination of CuAAC and IEDDA for simultaneous site-specific double-labeling of DNA oligonucleotides in a one-pot reaction has been reported.[83] In this study, three different *trans*-cyclooctene-based alcohols were synthesized as dienophiles moieties. These moieties include two diastereomers of (*E*)-cyclooct-4-enol and endo-(*E*)-bicyclo[6.1.0]non-4-en-

9-yl methanol, which were converted into corresponding phosphoramidite **101**, **102** and **103** respectively (Figure 2-12).[83] Doubly modified oligonucleotides were synthesized by introducing one of the reactive dienophiles at 5'-end, while the alkynyl residue was attached to an internal position. CuAAC and IEDDA reactions were carried out simultaneously (by incubation of the oligonucleotide with Alexafluor-594 azide, $CuSO_4$, tris-(benzyltriazolylmethyl)amine (TBTA), sodium ascorbate, and tetra-methylrhodamine-tetrazine (TAMRA-tetrazine) **104** as shown in Scheme 2-8. Neither the primary mass spectra nor the MS/MS spectra indicated the presence of multiply or cross-functionalized fragments that would indicate cross-reactivity. In addition, IEDDA proceeded with rate constants up to 380 000 M^{-1} s^{-1} which are ~8 orders of magnitude more reactive than CuAAC reactions.[83]

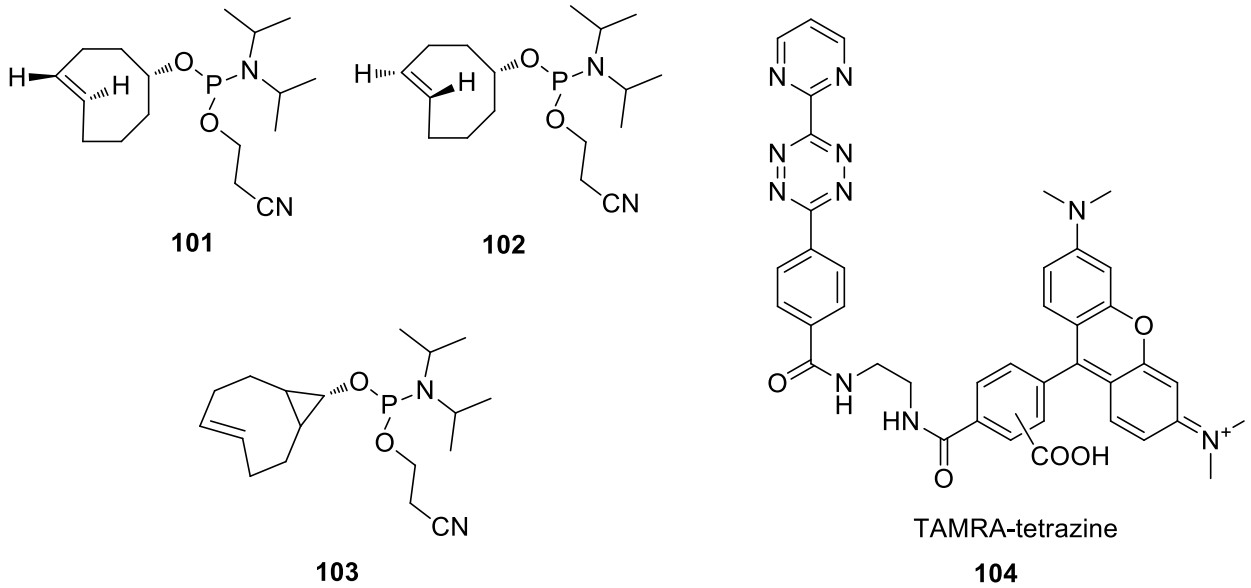

Figure 2-12. *Trans*-cyclooctene-derivative phosphoramidies **101**, **102**, **103** and TAMRA-tetrazine **104** used for site specific one-pot dual labeling of DNA.[83]

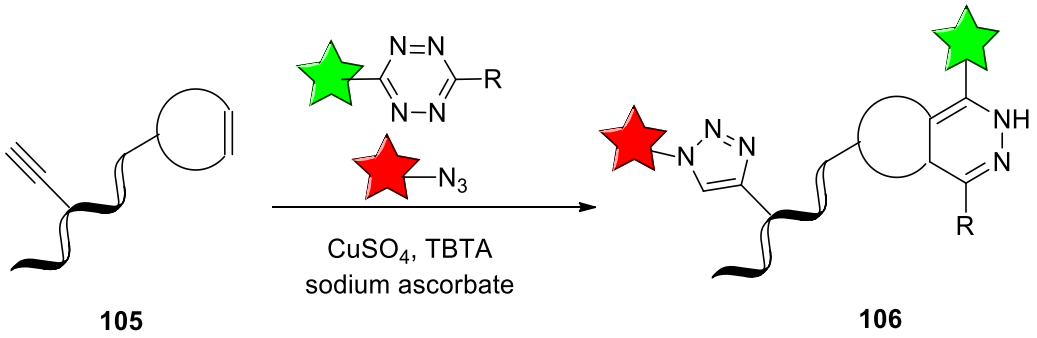

Scheme 2-8. Double modification of a DNA oligonucleotide by simultaneous IEDDA and CuAAC reaction.[83]

In 2014, Royzen *et al.* reported the site-specific fluorescent labelling of RNA using a cytidine triphosphate (CTP) analogue **107** (Figure 2-13) derivatized with a *trans*-cyclooctene at the 5-position of the cytosine to minimally alter the electrostatics of cytosine, which is important to preserve enzymatic recognition.[110, 111] This modified CTP was incorporated into an RNA strand by *in vitro* transcription using DNA template with the sequence: 5'-ACAAACACCATTGTCACACTCCACCTGTCTC-3'. The transcription generates the RNA product 5'-GGGAGACAGGUGGAGUGUGACAAUGGUGUUUGU-3' where *trans*-cyclooctene modified cytodine is incorporated at the two underlined positions. The transcription efficiency of the CTP analogue was calculated to be 60 ± 5%, suggesting that this modification does not disrupt the recognition of the nucleotide by T7 RNA polymerase.[110] Bioorthogonal reactions of the modified RNA with fluorescein-labelled tetrazine **108** achieved 60% conversion. This approach could be potentially used for fluorescent labeling of any RNA molecules. Further, it could also allow for *in vivo* imaging of nucleic acids of interest in real time.[110]

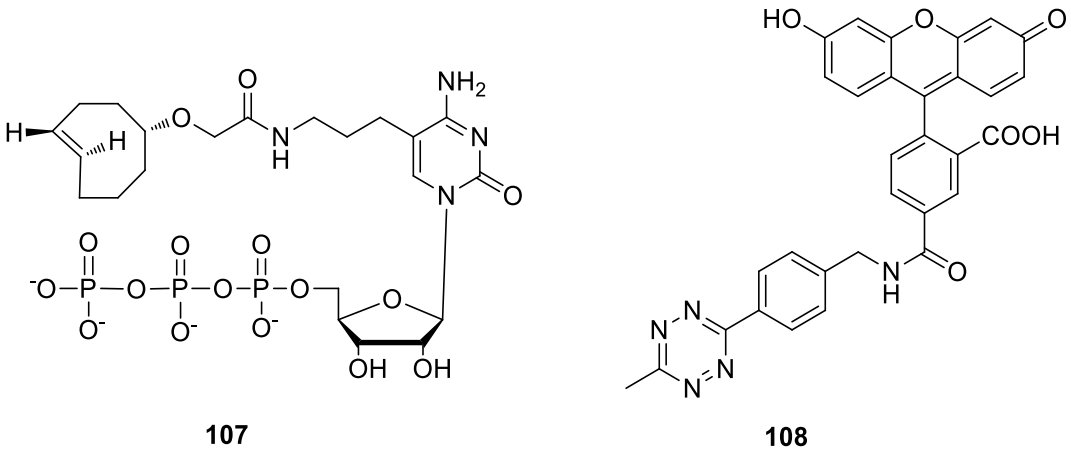

Figure 2-13. The bio-orthogonal pair utilized for site-specific fluorescence labelling of RNA.[110]

2.6 Objectives of this project

The main goal of this project is the site-specific fluorescent labeling of DNA oligonucleotides by IEDDA cycloaddition of *trans*-cyclooctene derivatives and BODIPY-tetrazine **89**. The attractive features of this reaction have been discussed previously in this chapter. *Trans*-cyclooctene derivatives will be introduced through an alkyne linker to the 5-position of 2'-deoxyuridine through the Sonogashira coupling reaction, followed by conversion to corresponding phosphoramidites. Using solid phase DNA synthesis, these phosphoramidites will be incorporated into DNA sequences for labeling with BODIPY-tetrazine **89** *via* the IEDDA.

CHAPTER 3: Results and discussions

(Photoregulation of DNA functions by cyclic azobenzene derivatives)

3.1 Synthesis of cyclic azobenzene phosphoramidite

Cyclic azobenzene phosphoramidite monomer was synthesised by following the previously reported procedure[55, 112] with some modifications. First, cyclic azoxybenzene **110** was synthesized in moderate yields (62%) (Scheme 3-1) by the treatment of 2,2'-dinitrodibenzyl **109** with lead powder and sodium carbonate. Under this condition, this reaction was completed in 24 h, even on larger scales (e.g. 20 g of dinitrodibenzyl) and without the need for addition of extra portions of lead powder. This transformation was previously carried out in the presence of triethylammonium acetate buffer[55] which was quite often difficult to reproduce, especially on larger scales.

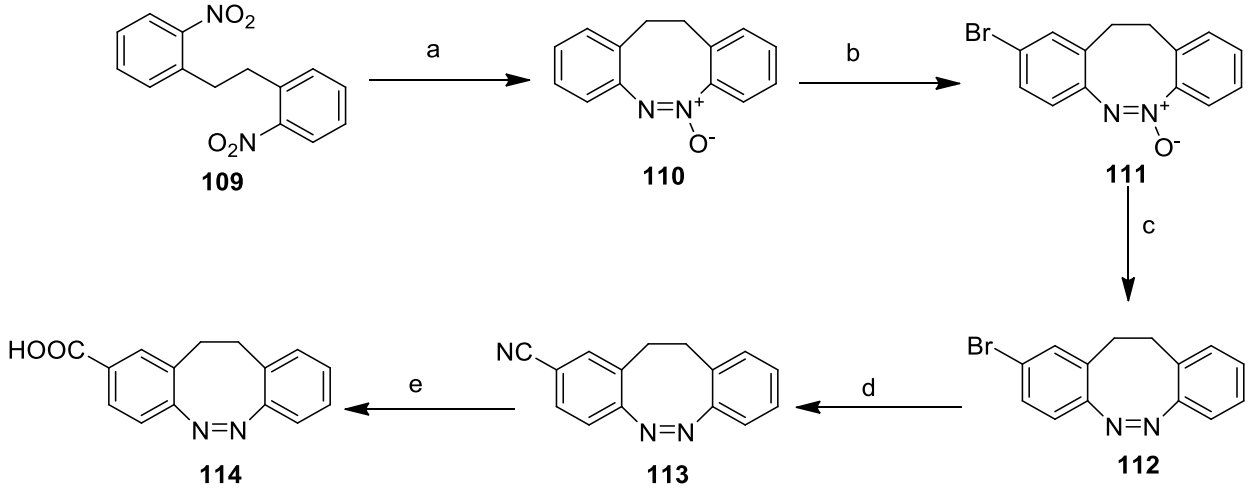

Scheme 3-1. *Reagents and conditions*: (a) Pb, Na_2CO_3, MeOH, 62%; (b) Br_2, CH_3COOH, 69%; (c) PCl_3, dry benzene, 50%; (d) CuCN, dry DMF, 61%; (e) KOH, H_2O, EtOH, 96%.

Electrophilic aromatic bromination of cyclic azoxybenzene **110** with bromine in the presence of acetic acid gave the corresponding bromoazoxybenzene **111** in 69% yield. The latter compound

underwent deoxygenation when treated with freshly distilled phosphorus trichloride in dry benzene to give the corresponding bromoazobenzene **112** in 50% yield.

Cyanoazobenzene **113** was obtained in 61% yield by treating bromoazobenzene **112** with copper (I) cyanide in dry dimethylformamide. Subsequent hydrolysis of nitrile group of **113** under alkaline conditions, *i.e*. potassium hydroxide solution in aqueous ethanol, gave the corresponding carboxylic acid **114** in 96% (Scheme 3-1).

The cyclic azobenzene carboxylic analogue **114** was then coupled with D-threoninol **115** using dicyclohexylcarbodiimide (DCC) as an activator in the presence of *N*-hydroxysuccinimide (NHS) to give D-threoninol-linked cyclic azobenzene amide **116** in 90% yield (Scheme 3-2). This compound was subsequently treated with dimethoxytrityl (DMTr) chloride in dry pyridine to give the corresponding DMTr-protected compound **117** in 83% yield.

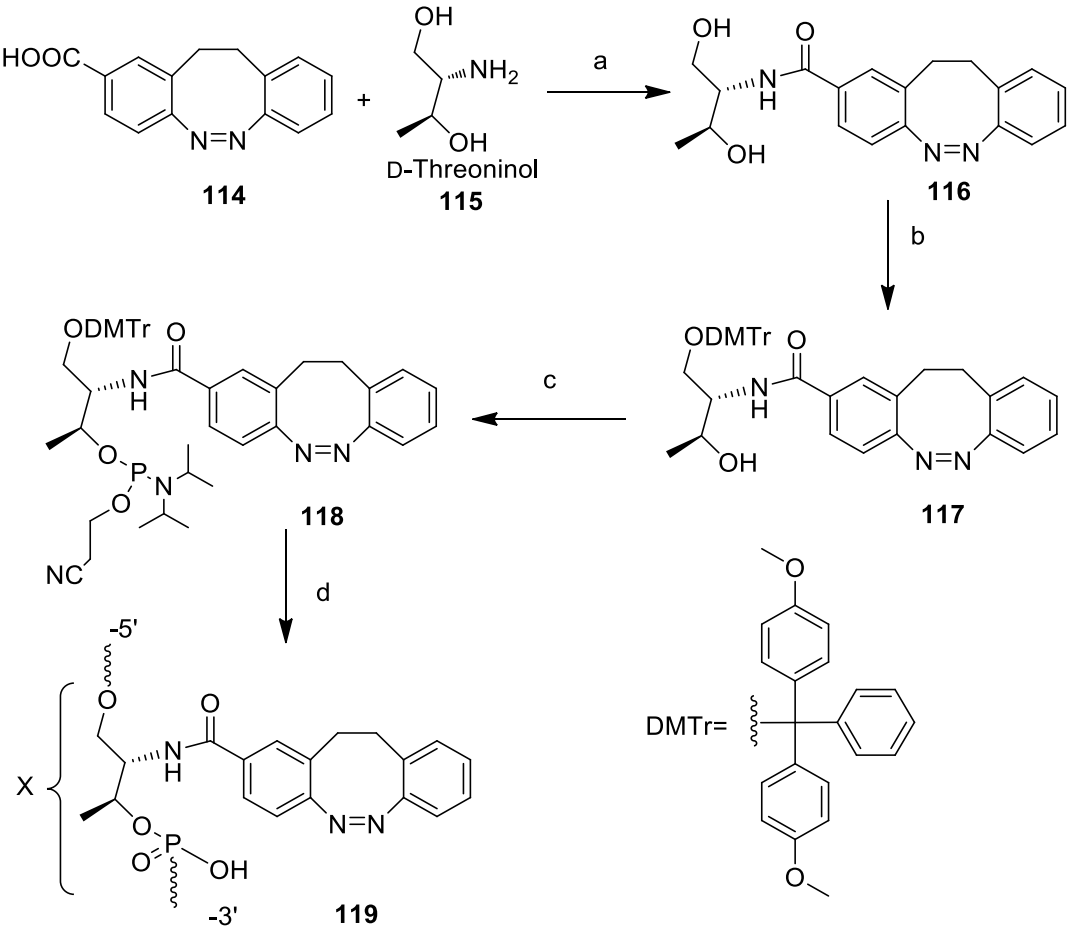

Scheme 3-2. *Reagents and conditions*: (a) DCC, NHS, DMF, 90%; (b) DMTr-Cl, pyridine, 83%; (c) (2-cyanoethyl) -*N*,*N*-diisopropylphosphochloridite, DIPEA, THF, 72%; (d) solid phase DNA synthesis.

Finally, cyclic azobenzene phosphoramidite **118** was synthesized in 72% yield by treating DMTr-protected D-threoninol-linked cyclic azobenzene derivative **117** with the phosphitylating reagent (2-cyanoethyl)-*N*,*N*-diisopropylphosphochloridite in the presence of *N*,*N*-diisopropyl ethylamine (DIPEA, or Hünig's base) in freshly distilled tetrahydrofuran (THF) (Scheme 3-2). Figure 3-1 shows the ^{31}P NMR spectrum of cyclic azobenzene phosphoramidite **118** as a mixture of two diastereomers.

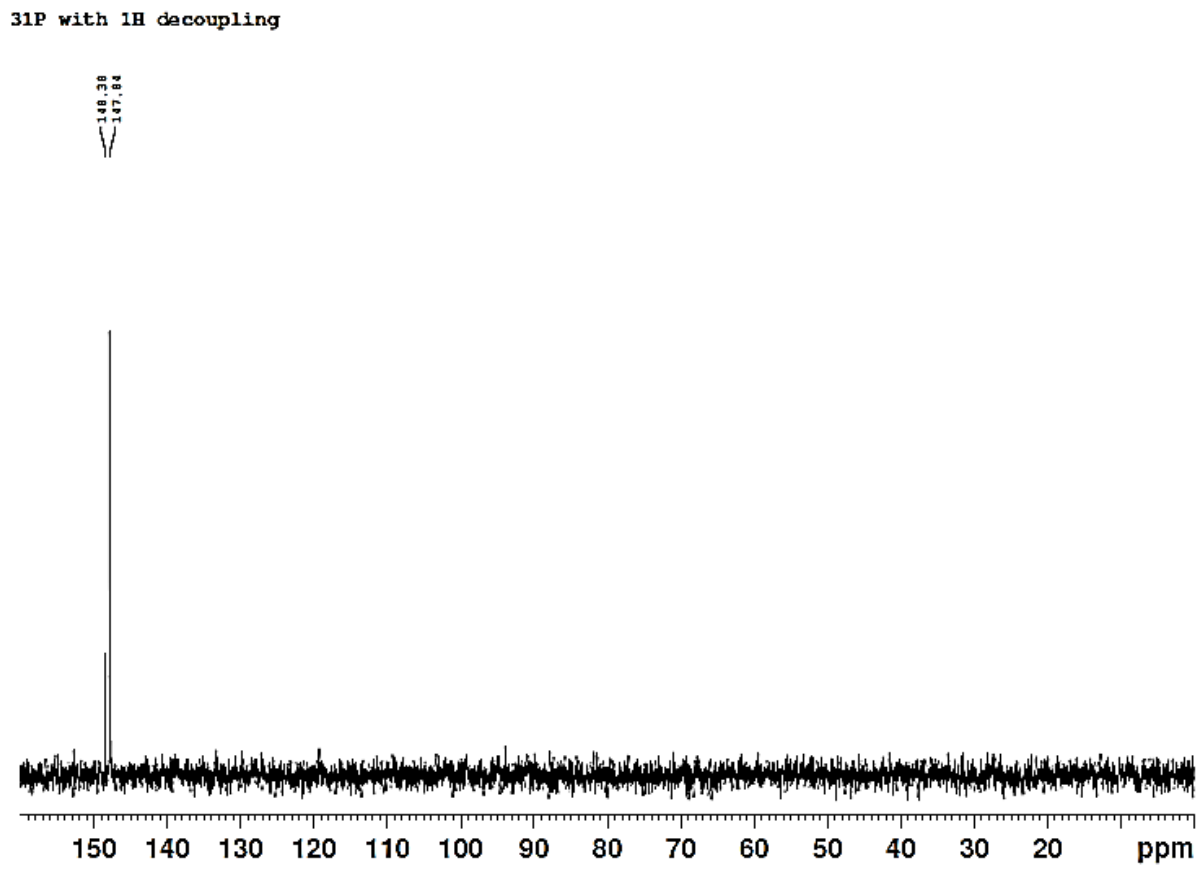

Figure 3-1. ^{31}P NMR spectrum of cyclic azobenzene phosphoramidite **118.**

Cyclic azobenzene phosphoramidite **118** was processed following the standard procedure used for drying phosphoramidite, and then shipped to Dr. Richard Pon's DNA lab (University of Calgary) for incorporation into DNA sequences using solid phase synthesis.

3.2 Synthesis of cyclic azobenzene-modified oligonucleotides

Using cyclic azobenzene phosphoramidite monomer **118** as a building block, a 20-mer DNA sequence was modified by the insertion of cAB-Thr at up to four different positions (Table 3-1). The standard ABI 0.2 μmol phosphate protocol was modified as follows: 10 min coupling at cAB position and 5 min coupling at the base immediately after cAB because the hydroxyl group on cAB phosphoramidite is quite shielded by cAB group which will interfere with the next coupling. All the modified sequences were attached to Black Hole Quencher-1 (BHQ-1, as shown in **120** in

Figure 3-2) at the 3'-end while fluorescein (6-FAM, as shown in **121** in Figure 3-2) was attached to the 5'-termini of the complementary strand (Figure 3-2). This FRET (Fluorescence Resonance Energy Transfer) pair will be used to evaluate the ability of these modified sequences to hybridize using the FRET technique. After solid phase synthesis, the products were deprotected and purified by gel electrophoresis. The optical density (OD_{260}) of the purified DNA sequences was quantified at 260 nm. DNA concentration was subsequently estimated using the following equation:[113]

1 OD = 33 µg/ml solution of ssDNA

Table 3-1. Cyclic azobenzene-modified oligonucleotide; where X= cAB phosphoramidite.

Oligo Name	Sequence 5' to 3'	Scale (µmol)	OD $_{260}$	MW Calculated[c]	MW Found[d]
AB_0	CTTTAAGAAGGAGATATACC-**BHQ-1**	1.0	56.8	6703.6	6703.8
FAM	**FAM**-GGTATATCTCCTTCTTAAAG	1.0	27.7	6620.2	6619.8
AB_1	CTTTAAGAAGXGAGATATACC-**BHQ-1**	0.2	9.7[a]	7104.9	7105.5
AB_{1-1}	CTXTTAAGAAGGAGATATACC-**BHQ-1**	0.2	5.5[b]	7104.9	7103.5
AB_{1-2}	CTTTAAGAAGGAGATATAXCC-**BHQ-1**	0.2	17.6[a]	7104.9	7104.0
AB_2	CTTTAXAGAAGGAGATXATACC-**BHQ-1**	0.2	2.7[b]	7506.3	7505.0
AB_{2-1}	CTXTTAAGAAGXGAGATATACC-**BHQ-1**	0.2	1.9[b]	7506.3	7506.0
AB_{2-2}	CTTTAAGAAGXGAGATATAXCC-**BHQ-1**	0.2	10.9[a]	7506.3	7505.5
AB_3	CTTTAXAGAAGXGAGATXATACC-**BHQ-1**	0.2	4.0[a]	7907.7	7907.0
AB_4	CTTTXAAGAXAGGAXGATAXTACC-**BHQ-1**	0.2	6.1[a]	8309.0	8308.5

[a] Deprotected by incubation with aqueous dimethylamine-concentration ammonium hydroxide (1:1, v/v) at 60°C for 20 min. [b]Deprotected by incubation with concentrated ammonium hydroxide at 55°C for 15 h. [c]M.W. of neutral species. [d]Mass deconvoluted for neutral species.

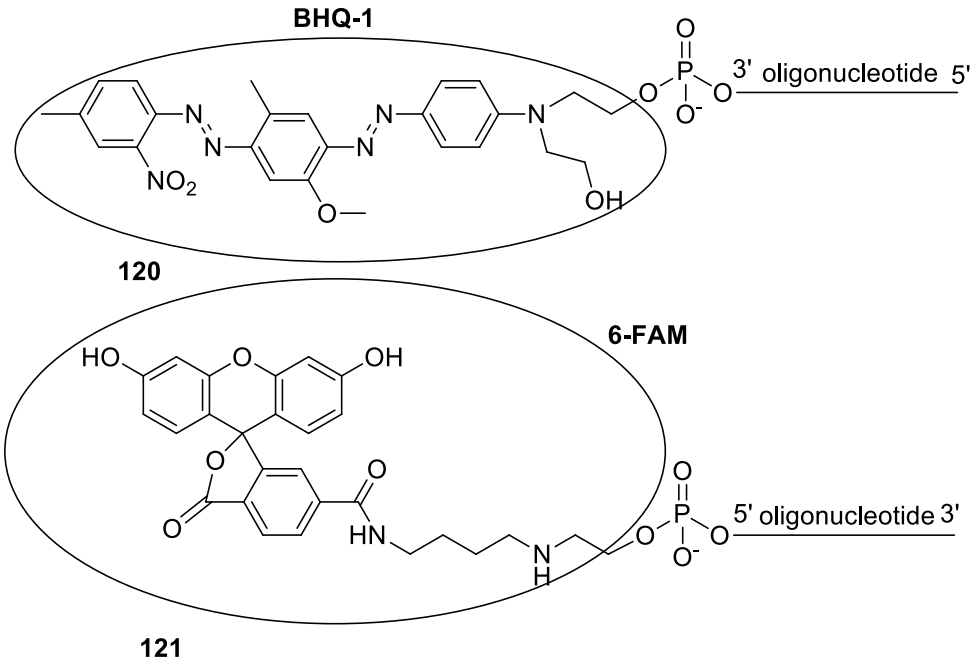

Figure 3-2. Structures of BHQ-1 **120** and 6-FAM **121**.

It is clear from the OD values of the purified oligonucleotides that the synthesis yields of some cAB-modified DNA sequences were quite low in general. This is particularly the case when cAB-Thr is incorporated into multiple positions of oligonucleotides. It is possible that the low overall yields are due to cleavage of the amide bond in cAB-Thr during deprotection under basic conditions (as shown in **119**, Figure 3-3a). This cleavage is also dependent on deprotection conditions, as deprotection using a AMA solution (aq. NH_4OH-methylamine 1:1, v/v) gave higher yields (as can be seen in Figure 3-3b), probably due to the much shortened deprotection time, i.e. 20 min at 60°C as compared with heating overnight at 55°C in aq. NH_4OH solution.

a)

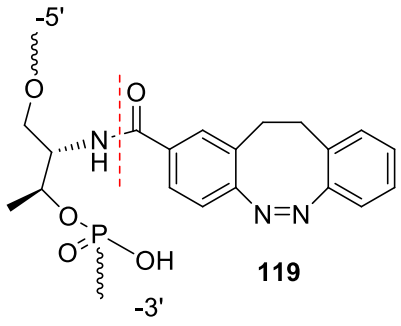

119

b)

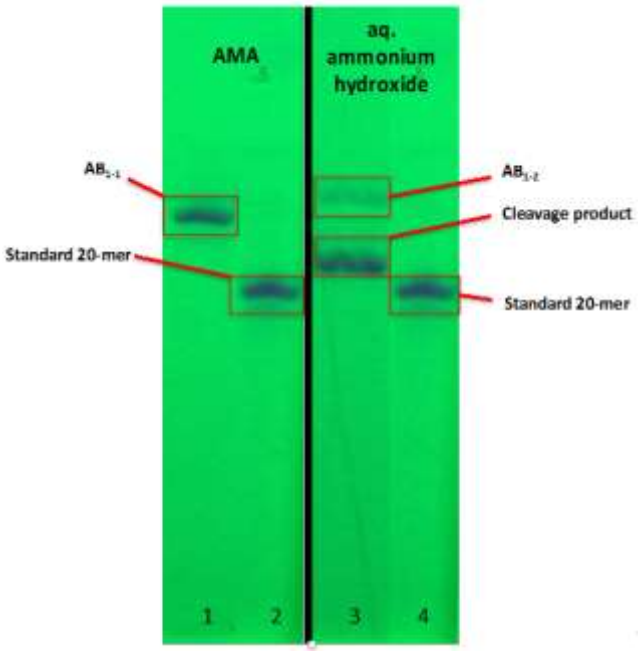

Figure 3-3. a) Structure **119** shows the cleavage position, b) lane 1) CTT TAA GAA GGA GAT ATA XCC deprotected by AMA at 60°C for 20 min; lane 2) 20-mer control; lane 3) CTX TTA AGA AGG AGA TAT ACC deprotected by aq. ammonium hydroxide at 55°C o/n; lane 4) 20-mer control.

The hypothesized cleavages of amide bond is also supported by the differences seen in the trityl assay and mass spectroscopic data of the AB_1 sequence. The trityl assay for the synthesis of AB_1 (Figure 3-5) shows that the coupling efficiency of cyclic azobenzne was reasonably good (>92%); however, the mass spectrum of HPLC-purified AB_1 (Figure 3-4) shows that in addition to the desired sequence, which has a molecular weight of 7105 Daltons, there is major truncated sequence with a molecular weight of 3590 Daltons, which corresponds to the cleavage fragment **124** shown in Scheme 3-3. Thus, it can be assumed that if cyclic azobenzene is cleaved at the amide bond during deprotection, the resulting NH_2 can attack the phosphodiester bond, leading to chain cleavage (Scheme 3-3).

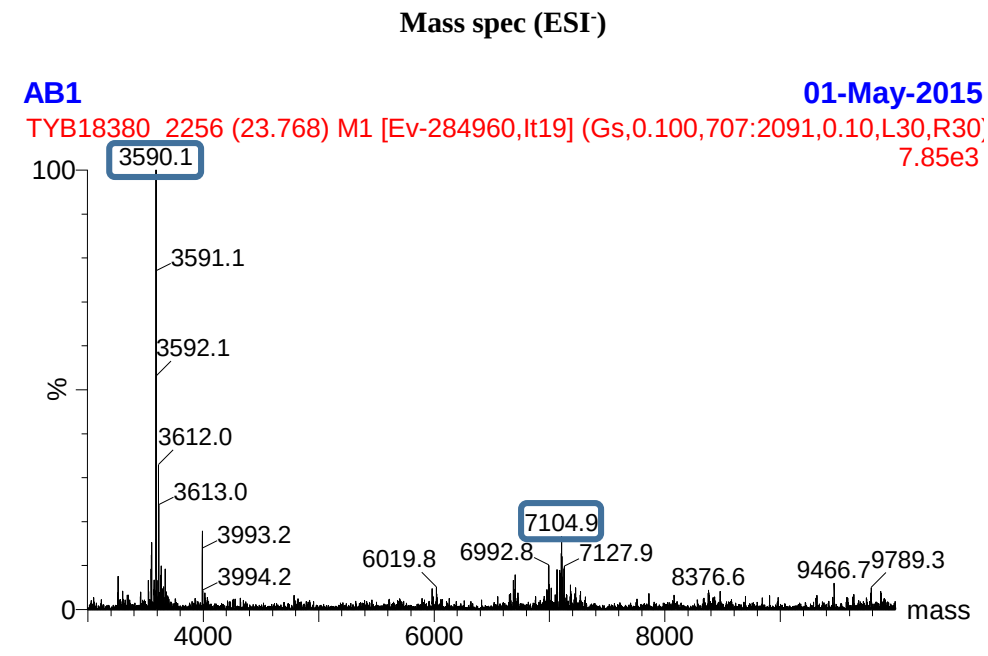

Figure 3-4. Mass spectroscopy of AB_1 (5'-CTTTAAGAAGXGAGATATACC-3'BHQ-1).

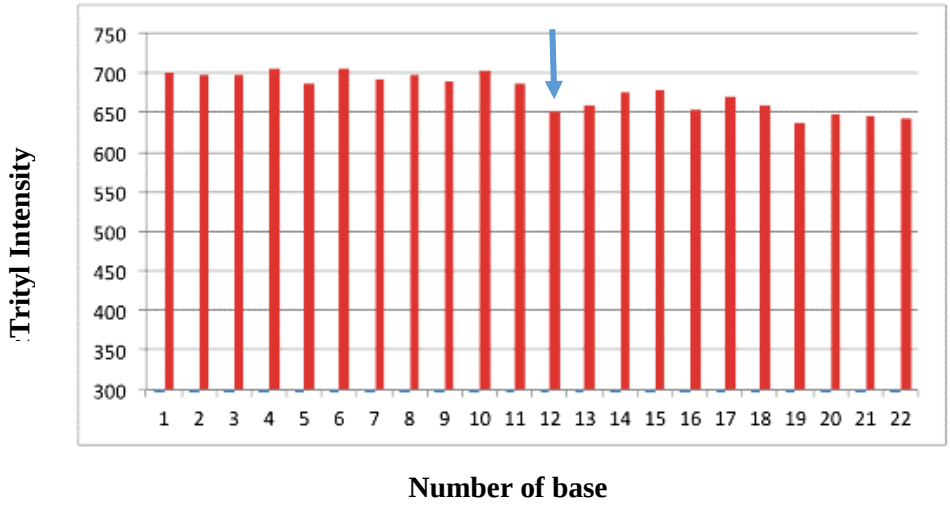

Figure 3-5. Trityl assay of AB_1 (5'-CTTTAAGAAGXGAGATATACC-3'BHQ-1) synthesis.

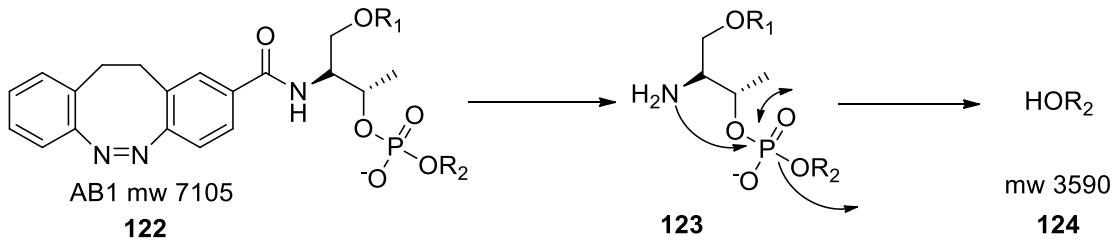

Scheme 3-3. The postulated mechanism for the amide bond cleavage of cAB phosphoramidite.

To improve the yield of the synthesis, AMA solution was used for deprotecting of AB_1, AB_{1-2}, AB_{2-2}, AB_3 and AB_4 resulting in better yields compared to the other sequences. In future experiments, combination of ultramild phosphoramidites[114, 115] and the Q-linker[116] will be used for the synthesis of cAB-modified oligonucleotides, as cleavage from solid support and deprotection can be accomplished under very mild alkaline conditions, *i.e*. incubation with aqueous ammonium hydroxide for 2 h at room temperature.

3.3 Thermal back isomerizatiom studies of *trans*-cyclic azobenzene

Thermal back isomerization experiments were performed using UV-vis spectrophotometer at different temperatures (25-95°C), in order to investigate the stability of *trans*-cAB at elevated temperatures. First, the *cis*-cAB **47** which is the thermodynamically stable isomer, was isomerized to *trans*-cAB **48** in DMSO at 25°C by exposure to purple light (395 nm) for 2 h. The absorbance of the isomerized products was recorded in the range of 350-650 nm. Then the absorption spectra were recorded with every 10°C increase in temperature. The sample was kept for ~5 min prior to next measurement. This experiment was performed twice, one with samples exposed to light (395 nm) throughout the experiment (Figure 3-6a), and another with light off (Figure 3-6b). It is clear from both graphs that the light does not have measurable effects and that temperatures dominate the back isomerization process.

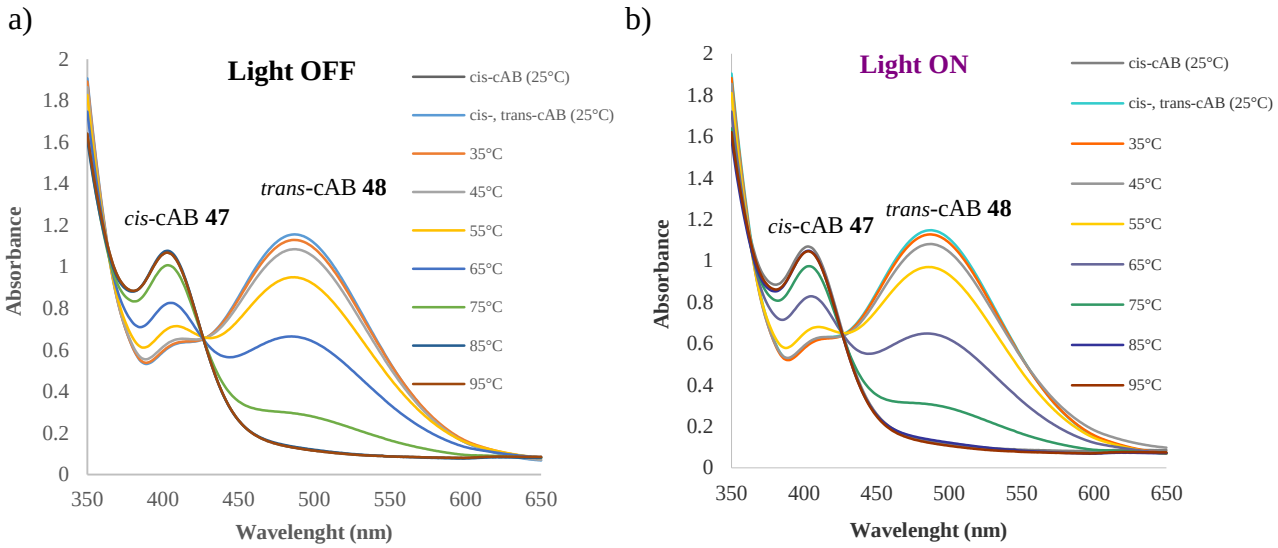

Figure 3-6. UV-vis spectra of cAB **47** in DMSO (1.5 mg/1.5 ml), a) thermal back isomerization of *trans*-cAB with the purple light (395 nm) on, b) the same experiment but the light off.

Thermal back isomerization experiment was performed also at fixed temperatures 25, 37 and 55°C. While Figure 3-7c suggests that *trans*-cAB completely isomerizes back to the *cis*-form in about 100 min at 55°C, this process takes over 100 and 24 h at 25 and 37°C, respectively (Figure 7-3 a, b)

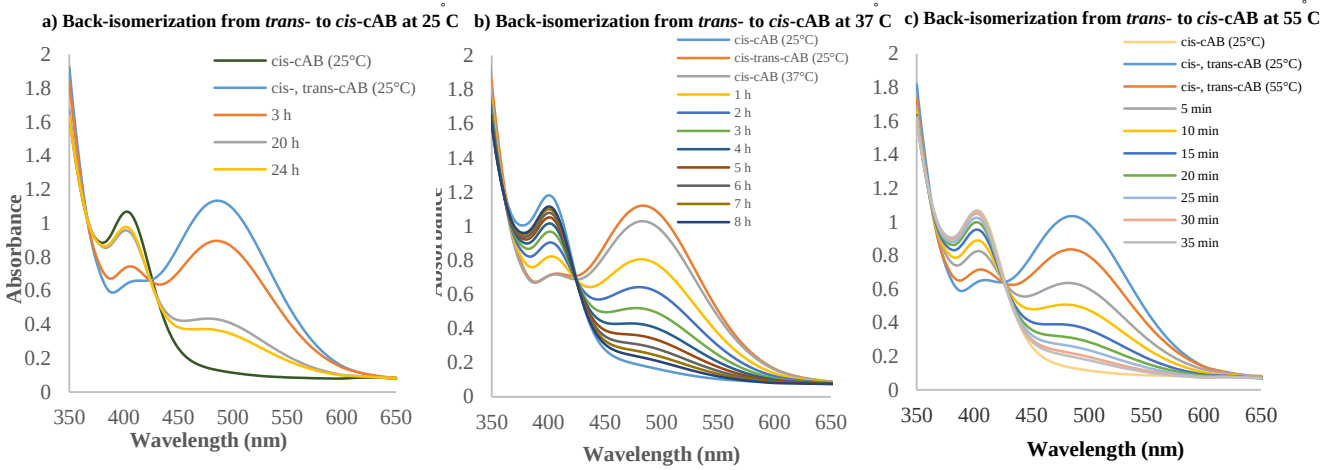

Figure 3-7. Back-isomerization of *trans*- to *cis*-cAB in DMSO (1.5 mg/1.5 ml) at a) 25°C, b) 37°C, and c) 55°C.

From these observations, it can be concluded that the back isomerization process of *trans*-cAB is temperature-dependent. These results are useful in experimental design and interpreting

the results of the melting temperature (T_m) measurement of the cAB-modified DNA duplexes, as T_m measurement requires heating samples to elevated temperatures, *e.g*. 95°C.

3.4 Photoregulation of DNA melting temperature (T_m)

T_m is defined as the temperature at which half of a DNA duplex is denaturated. In order to determine the ability of cAB-tethered DNA sequences to hybridize, T_ms of these modified sequences in the presence of the complementary strand were measured and compared with the unmodified duplex. It is hypothesized that *cis*-cAB will disturb the DNA duplex due to its non-planarity, as a result, lowering the T_m values; while *trans*-cAB will intercalate into and stabilize DNA duplexes, leading to T_m values higher than the corresponding dsDNA with *cis*-cAB.

The final concentration for each component used in this experiment is shown in (Table 3-2). For annealing the strands, samples were placed in the heating block at 95°C for ~3-5 min and then cooled down slowly to room temperature, which typically took 45-60 min.

Table 3-2. Final concentrations for each component used for the melting temperature experiments.

Component	Concentration
FAM-DNA	2 µM
BHQ-1-DNA	2 µM
Tris-HCl (pH 8.0)	10 mM
NaCl	50 mM

The T_m measurement was performed using UV-vis spectrophotometer equipped with temperature control. It can be concluded from the T_m results (Table 3-3) that there is a decrease by 5-8°C in the T_m values for each cAB unit incorporated into the DNA sequence when cAB exists in the *cis*-form. For example, incorporation of one cAB to the middle of the sequence (AB_1) lowers the T_m value by 5°C to 43°C as compared to 48°C for the unmodified one (AB_0). Going from AB_1 to AB_4, which contains four cAB units, a 27°C decrease in the T_m value can be seen, suggesting

that the more cAB units incorporated, the lower the T_m value. All of these results are in agreement with what was expected.

For $AB_{1\text{-}1}$ and $AB_{1\text{-}2}$ where cAB is incorporated to a position close to 5'- and 3'-end of the BHQ strand, respectively, the T_m values do not significantly differ from that of AB_1, suggesting that the way that cAB affects DNA hybridization might be independent of the position of incorporation. Similar results were found for $AB_{2\text{-}1}$ and $AB_{2\text{-}2}$.

As *trans*-cAB is not stable thermodynamically, as it was shown previously in this chapter, it was not possible to perform the same experiment to measure the T_m values of the DNA duplexes containing *trans*-cAB.

Table 3-3. The melting temperature (T_m) values for cAB-modified DNA Duplexes.

Name	Duplexes	T_m°C[a] (*cis*-cAB)
AB_0-FAM	CTTTAAGAAGGAGATATACC-**BHQ-1** GAAATTCTTCCTCTATATGG-**FAM**	48
AB_1-FAM	CTTTAAGAAGXGAGATATACC-**BHQ-1** GAAATTCTTC CTCTATATGG-**FAM**	43
$AB_{1\text{-}1}$-FAM	CTXTTAAGAAGGAGATATACC-**BHQ-1** GA AATTCTTCCTCTATATGG-**FAM**	44
$AB_{1\text{-}2}$-FAM	CTTTAAGAAGGAGATATAXCC-**BHQ-1** GAAATTCTTCCTCTATAT GG-**FAM**	42
AB_2-FAM	CTXTTAAGAAGGAGATATAXCC-**BHQ-1** GA AATTCTTCCTCTATAT GG-**FAM**	36
$AB_{2\text{-}1}$-FAM	CTXTTAAGAAGXGAGATATACC-**BHQ-1** GA AATTCTTC CTCTATATGG-**FAM**	37
$AB_{2\text{-}2}$-FAM	CTTTAAGAAGXGAGATATAXCC-**BHQ-1** GAAATTCTTC CTCTATAT GG-**FAM**	36
AB_3-FAM	CTTTAXAGAAGXGAGATXATACC-**BHQ-1** GAAAT TCTTC CTCTA TATGG-**FAM**	28
AB_4-FAM	CTTTXAAGAXAGGAXGATAXTACC-**BHQ-1** GAAA TTCT TCCT CTAT ATGG-**FAM**	21

[a]Temperature ramp 1°C/min.

3.5 Circular Dichroism (CD) experiment

CD measurement was performed for AB_0 and modified DNA duplexes in order to study the secondary structure of cAB-modified DNA duplexes, as CD of nucleic acids is commonly used to provide a signature for their secondary structures. The common features of B-DNA duplexes include the following, a positive band at 275 nm, a negative band near 250 nm, and a cross-over point (from positive to negative intensity) at 260 nm.

Concentrations of each component used for CD measurement are shown in Table 3-4. Strands are annealed following the same procedures described previously for T_m measurement in section 3.4.

Table 3-4. Final concentration for each component used for the CD experiment.

Component	Concentration
FAM-DNA	1.6 µM
BHQ-1-DNA	1.6 µM
Tris-HCl (pH 8.0)	10 mM
NaCl	50 mM

The results of this experiment were in agreement with those of T_m experiments, that is, incorporation of cAB units into DNA destablizes the DNA secondary structure (Figure 3-9). In this respect, AB_0 showed the typical CD signature that corresponds to B-form duplexes. The typical CD transition bands are weakened with the increase in the number of cAB incorporated into the sequences. AB_4, for example, which has a T_m below room temperature (21°C), the intensities of the transitions are much weaker than those of AB_0 (Figure 3-8).

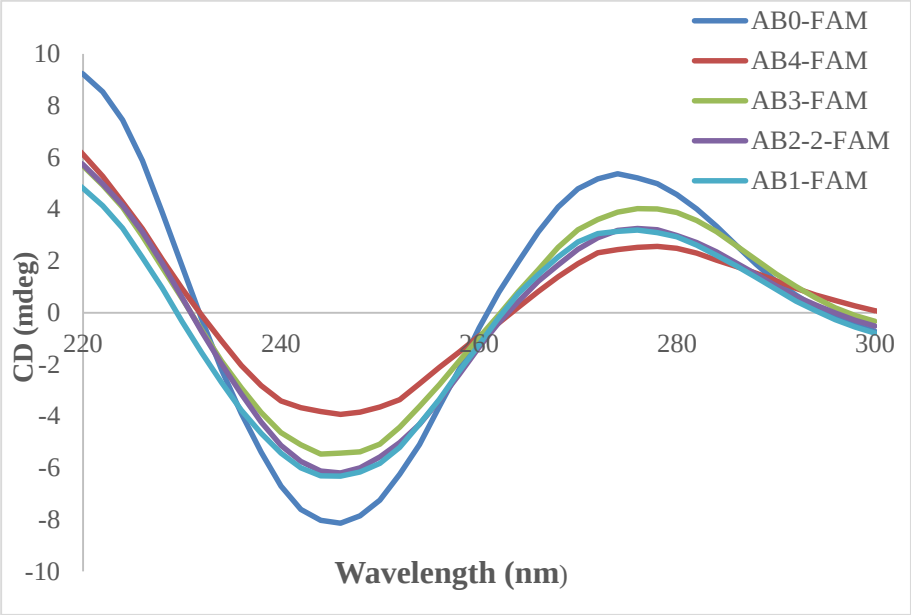

Figure 3-8. CD profiles for unmodified and cAB-modified DNA duplexes.

3.6 Fluorescence Resonance Energy Transfer (FRET) experiment

The possibility for *trans*-cAB to be accommodated in DNA duplexes was assessed by fluorescence Resonance Energy Transfer (FRET) experiments. Thus, FAM and 9 AB sequences (AB0-AB4) were individually prepared using the conditions summarized in Table 3-5. Strands were annealed following the same procedures described previously for T_m measurement in section 3.4.

Table 3-5. Final concentration for each component used for the FRET experiment.

Component	Concentration
FAM-DNA	80 nM
BHQ-1-DNA	120 nM
Tris-HCl (pH 8.0)	10 mM
NaCl	50 mM

The Fluorescence of each duplex was measured when cAB exists in the *cis*-form. The results are shown in Figure 3-9 which represent the average of two independent experiments.

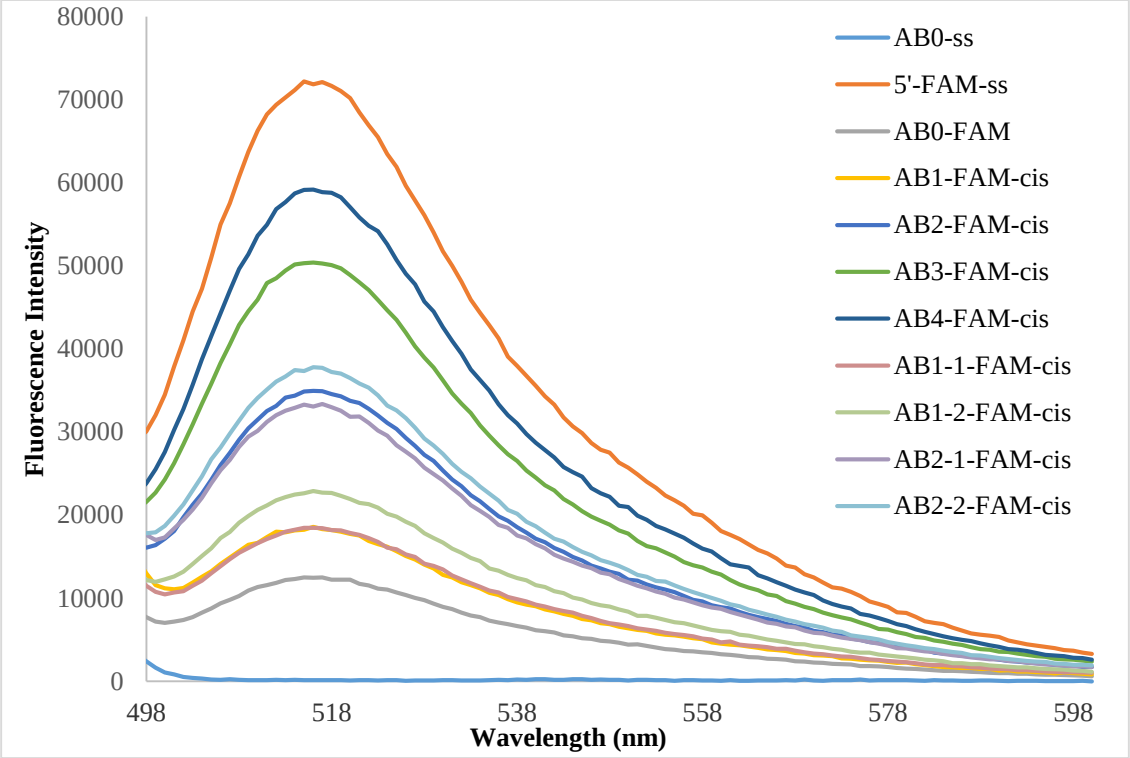

Figure 3-9. FRET experiment results for cAB-modified DNA duplexes where cAB exists in the *cis*-form.

It is clear from these results that the fluorescence intensity observed for the DNA duplexes is dependent on the number of cAB units that are incorporated, *i.e.* the more *cis*-cAB units attached to the DNA template, the higher the fluorescence intensity at 515 nm, which is a result of duplex destabilization, leading to the spacial separation of the FRET pair (fluorescein–Black Hole Quencher pair).

Then, the eight cAB-modified duplexes (AB_1-AB_4) were individually subjected to isomerization by exposure to purple light at 395 nm for 2 h, and the fluorescence of each duplex was determined as shown from Figure 3-10 to Figure 3-17.

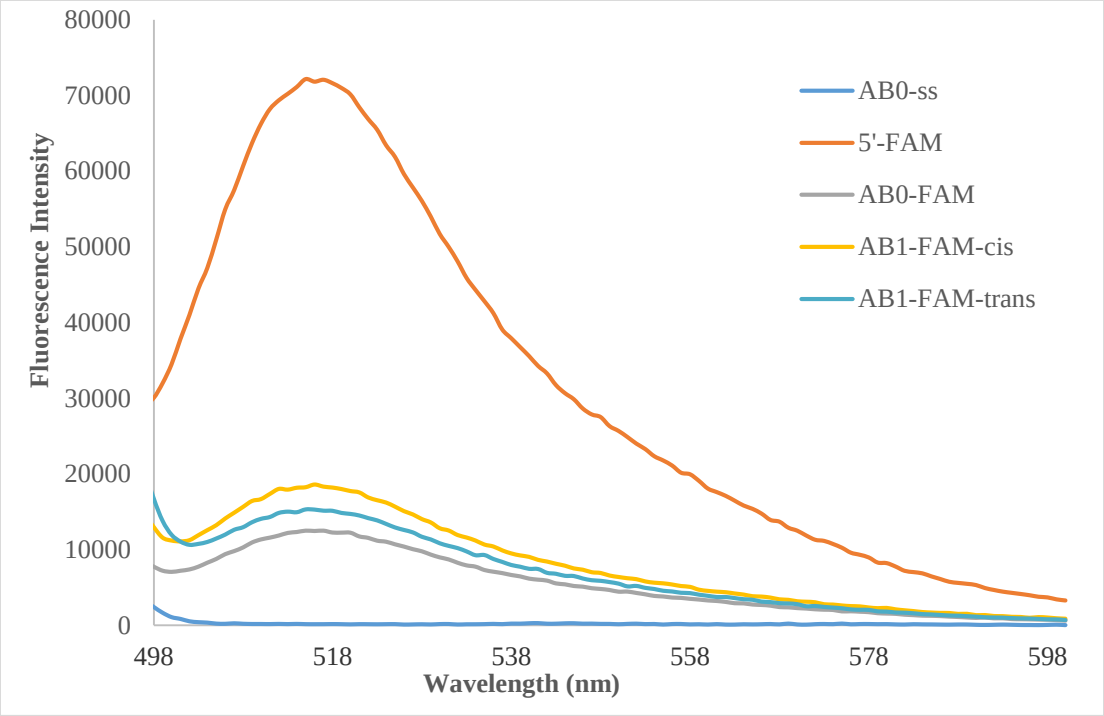

Figure 3-10. FRET experiment results for AB_1-FAM duplex.

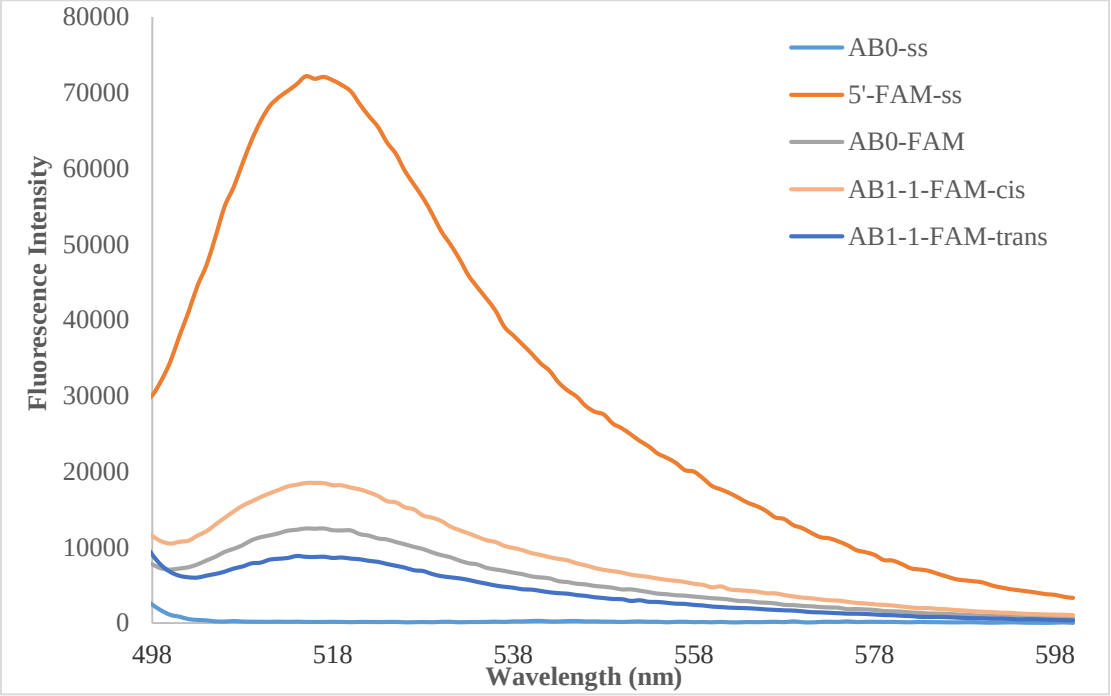

Figure 3-11. FRET experiment results for $AB_{1\text{-}1}$-FAM duplex.

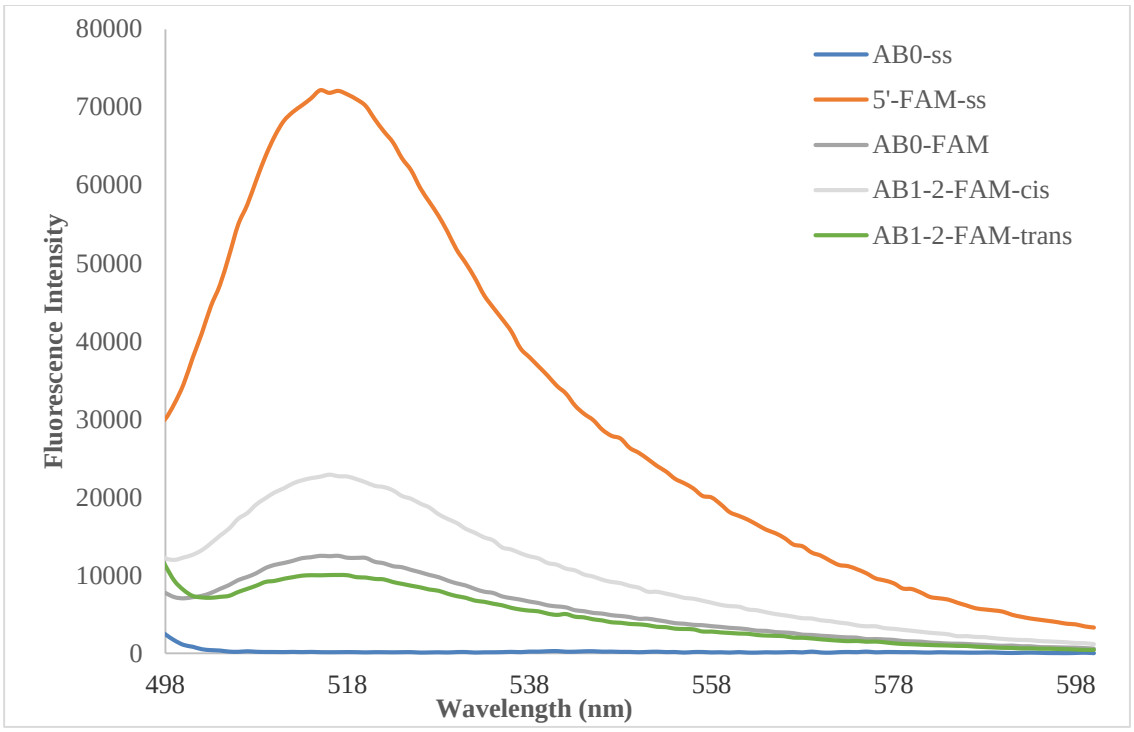

Figure 3-12. FRET experiment results for $AB_{1\text{-}2}$-FAM duplex.

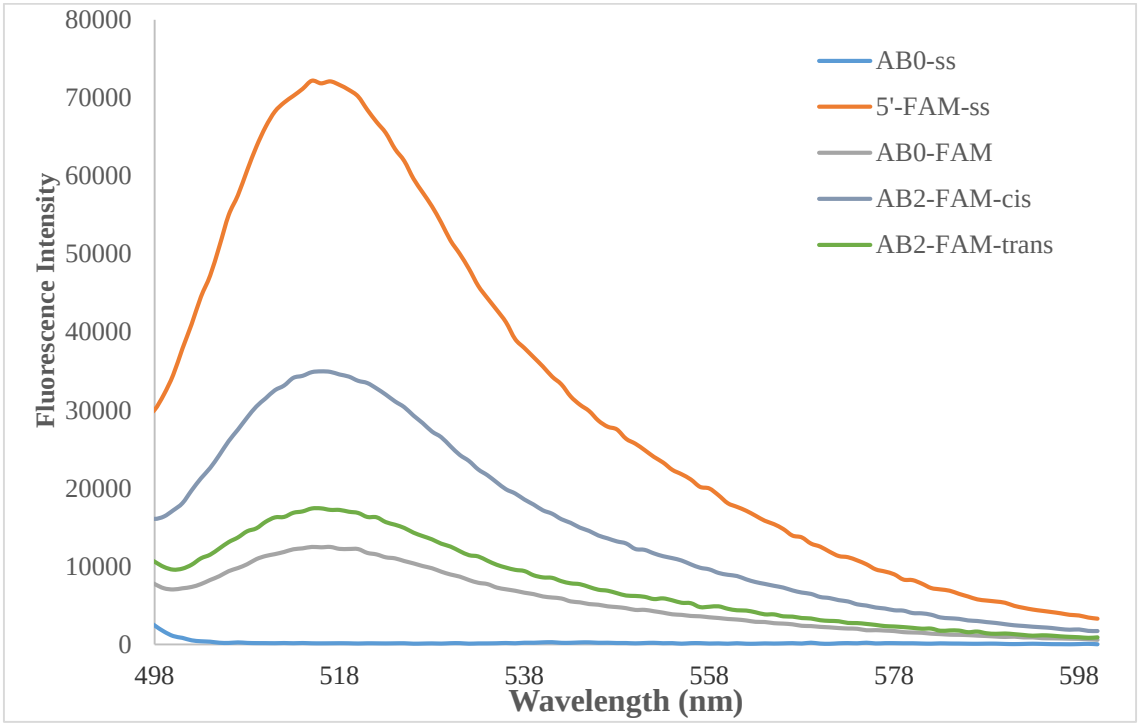

Figure 3-13. FRET experiment results for AB_2-FAM duplex.

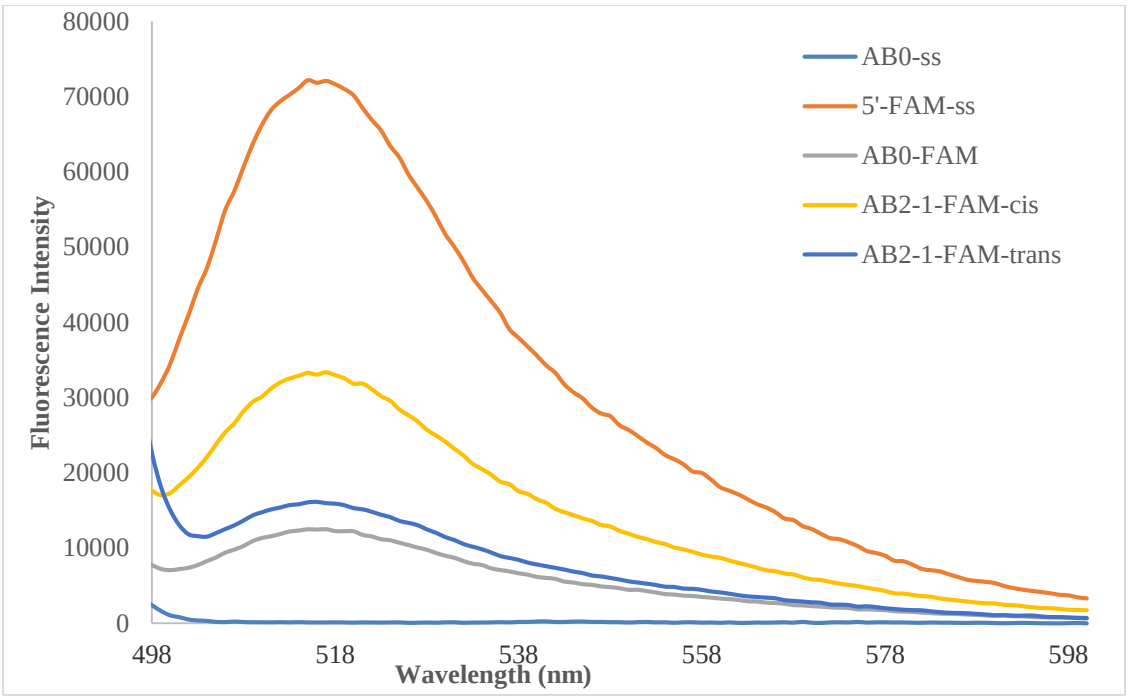

Figure 3-14. FRET experiment results for $AB_{2\text{-}1}$-FAM duplex.

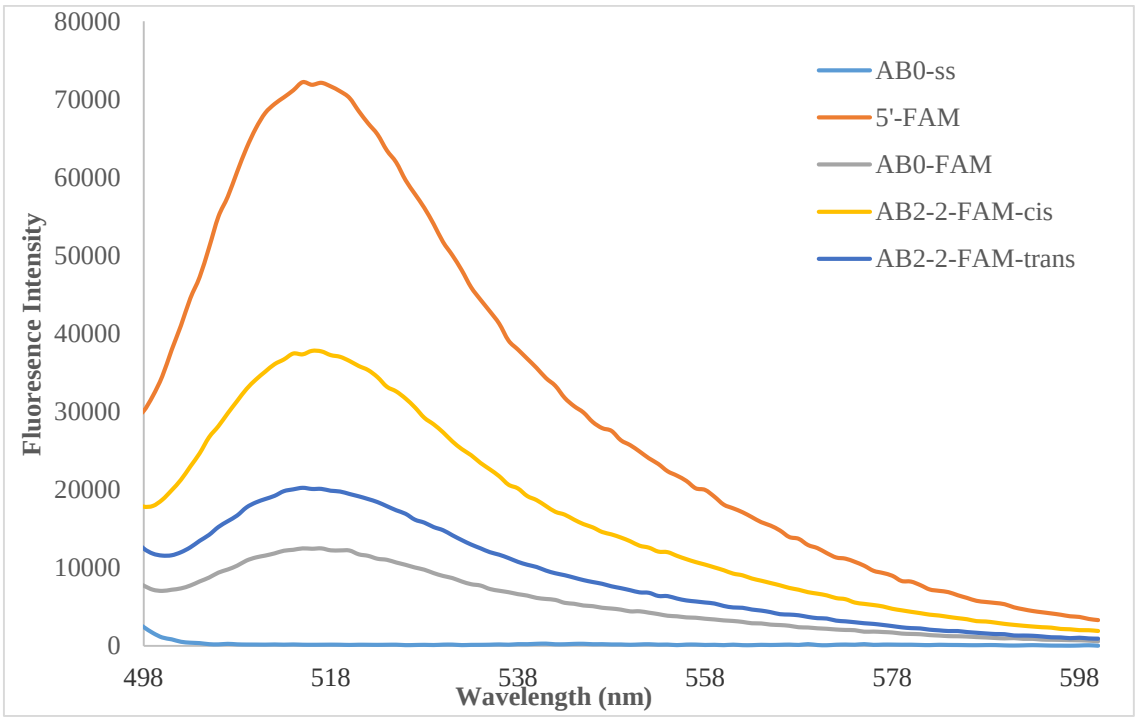

Figure 3-15. FRET experiment results for $AB_{2\text{-}2}$-FAM duplex.

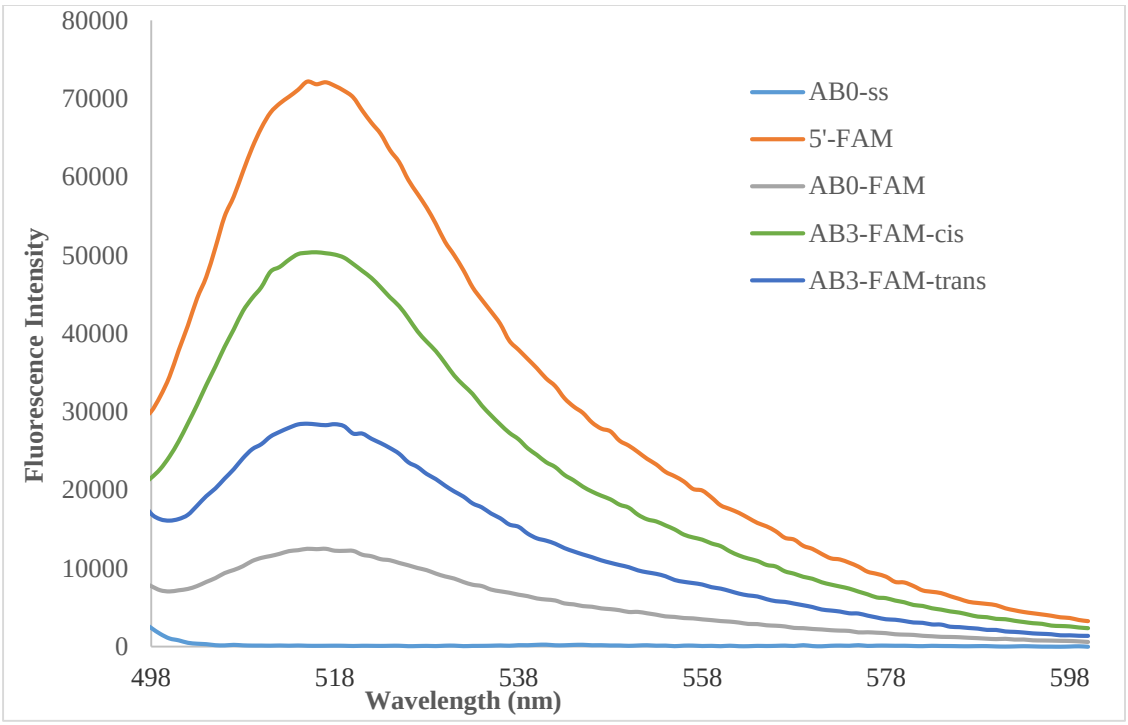

Figure 3-16. FRET experiment results for AB_3-FAM duplex.

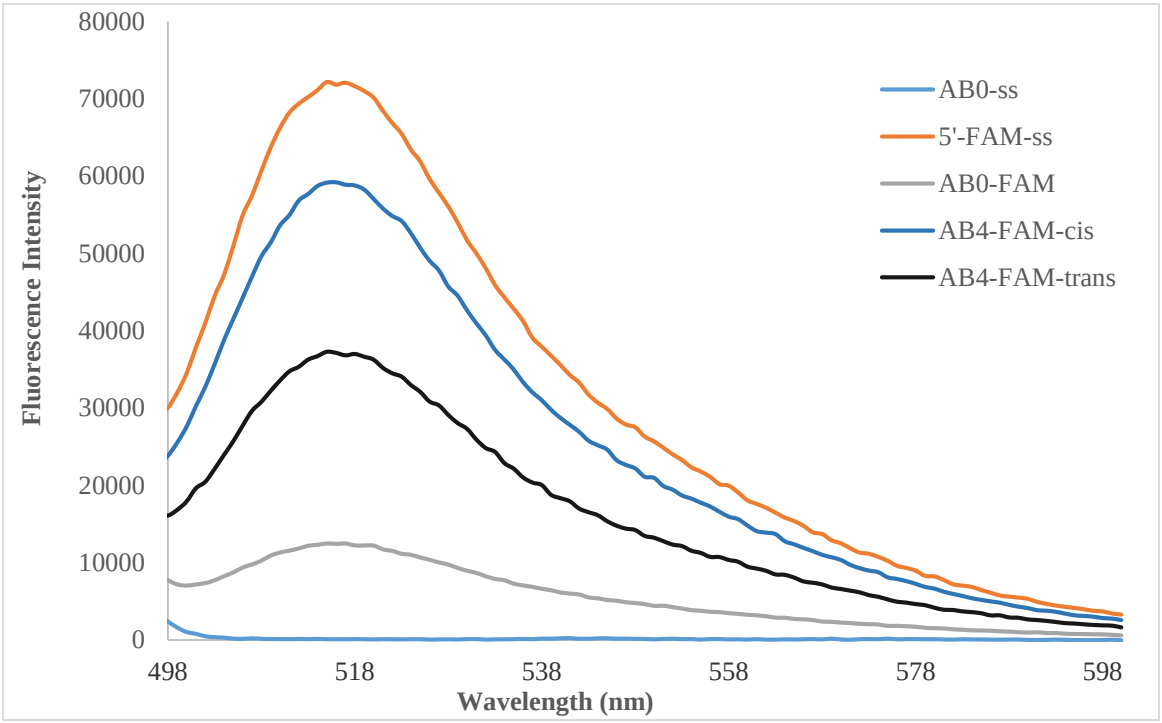

Figure 3-17. FRET experiment results for AB_4-FAM duplex.

The FRET quenching of the FAM/BHQ-1 FRET pair was used as an indication for the degree of hybridization, which is measured by equations (1 for *cis*-cAB) and (2 for *trans*-cAB) (F.I.: fluorescent intensity), where (FAM-ss) is the FAM single strand, (AB_x-FAM) is cAB-modified DNA duplexes and (AB_0-FAM) is the unmodified duplex. The values for each of the duplexes are summarized in Table 3-6.

$$\%\text{quenching } (cis) = \frac{\text{F. I. (FAM-ss)-F. I.}(cis\text{-AB}_x\text{-FAM})}{\text{F. I. (FAM-ss)-F. I.}(\text{AB}_0\text{-FAM})} \text{ x } 100\% \qquad (1)$$

$$\%\text{quenching } (trans) = \frac{\text{F. I. (FAM-ss)-F. I.}(trans\text{-AB}_x\text{-FAM})}{\text{F. I. (FAM-ss)-F. I.}(\text{AB}_0\text{-FAM})} \text{ x } 100\% \qquad (2)$$

Table 3-6. Fluorescent quenching as a measure of degree of hybridization for the DNA duplexes incorporating cAB.

Entry	Duplex	%Quenching (*cis*-)	%Quenching (*trans*-)	%Difference (*trans*-*cis*)
1	AB_0-FAM	-	-	-
2	AB_1-FAM	90	95	5
3	$AB_{1\text{-}1}$-FAM	90	106	16
4	$AB_{1\text{-}2}$-FAM	83	104	21
5	AB_2-FAM	63	90	27
6	$AB_{2\text{-}1}$-FAM	65	94	29
7	$AB_{2\text{-}2}$-FAM	58	87	29
8	AB_3-FAM	37	73	36
9	AB_4-FAM	22	58	36

As Table 3-6 shows, compared with *cis*-cAB, *trans*-cAB is better accommodated in DNA duplexes. AB_3 and AB_4 duplexes gave the highest difference values of 36%, indicating that the more cAB unit incorporated, the bigger the difference in fluorescence quenching between duplexes with *cis*- and *trans*-cAB and the better the system for the photoregulation of DNA hybridization. Although this difference might appear to be moderate, it should be borne in mind that the *cis*-*trans* isomerization in cAB will likely to be useful as a "turn-on", instead of a "turn-off", switch.

It is also worth mentioning that $AB_{1\text{-}2}$-FAM system gave better FRET results than its analogues AB_1-FAM and $AB_{1\text{-}1}$-FAM. As cAB is positioned closer to the quencher, $AB_{1\text{-}2}$-FAM

system gave 21% difference in fluorescence quenching between *cis*- and *trans*-duplexes which is 5 and 16% higher than that of $AB_{1\text{-}1}$-FAM and AB_1-FAM, respectively. These results suggest that $AB_{1\text{-}2}$-FAM system has more impact on the hybridization affinity than its analogues although these results are not in agreement with those obtained from T_m experiment which suggest the this process is independent of cAB-position. This discrepancy can be explained in that T_m represents the overall structure of the DNA duplex, while FRET experiments results are more dependent on the spacial separation of the FRET pair.

3.7 Conclusions and future work

cAB-Thr was successfully incorporated into oligonucleotides (Figure 3-18). T_m results showed a decrease by 5-8°C in the T_m values for each cAB unit incorporated into the DNA sequence when cAB exists in the *cis*-form. However, it was not possible to measure the T_m for *trans*-isomer, as *trans*-cAB is not stable thermally. In addition, the typical CD transition bands are weakened with the increase in the number of cAB incorporated into the sequences. And finally, FRET experiments revealed that AB_3 and AB_4 duplexes gave the biggest difference in fluorescence quenching between duplexes with *cis*- and *trans*-cAB.

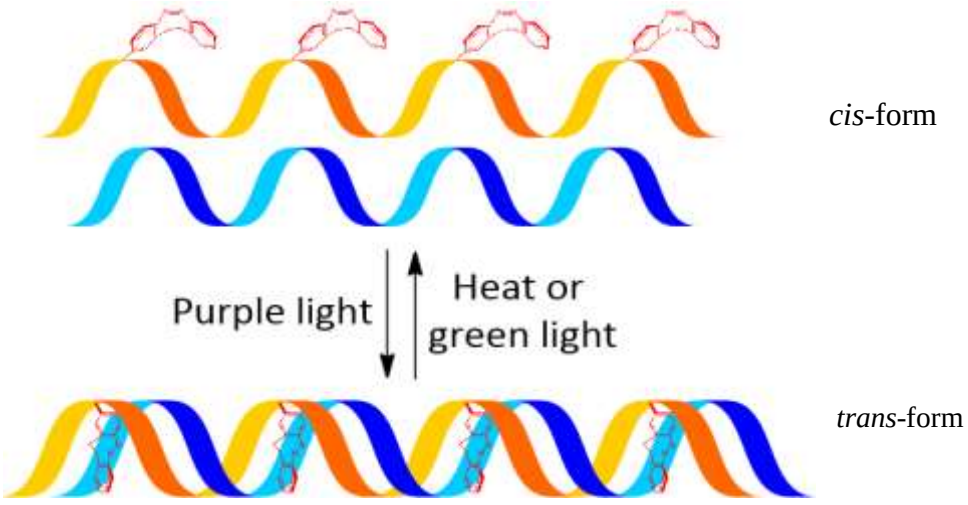

Figure 3-18. Schematic representation of the photoregulation of DNA hybridization with cAB.

Taken together, these results do suggest that cyclic azobenzene could be used for spatiotemporal regulation of DNA functions such as transcription, in a turn-on fashion. This can be achieved by tethering cAB units to specific positions on the T7 promoter, then the transcription by the T7-RNA polymerase can be reversibly photoregulated by *cis-trans* isomerization of cAB.

CHAPTER 4: Results and discussions

(Site-specific labeling of DNA by IEDDA)

4.1 Overview of the synthesis of *trans*-cyclooctene derivatives

The main goal of this project is to synthesize *trans*-cyclooctene derivatives for introduction into DNA sequences, such as **125** and **126** (Scheme 4-1), using the phosphoramidite chemistry based solid phase synthesis, followed by Inverse Electron Demand Diels Alder reaction (IEDDA) with BODIPY-tetrazine **89**, leading to the formation of fluorescently labeled DNA sequences **127** and **128**.

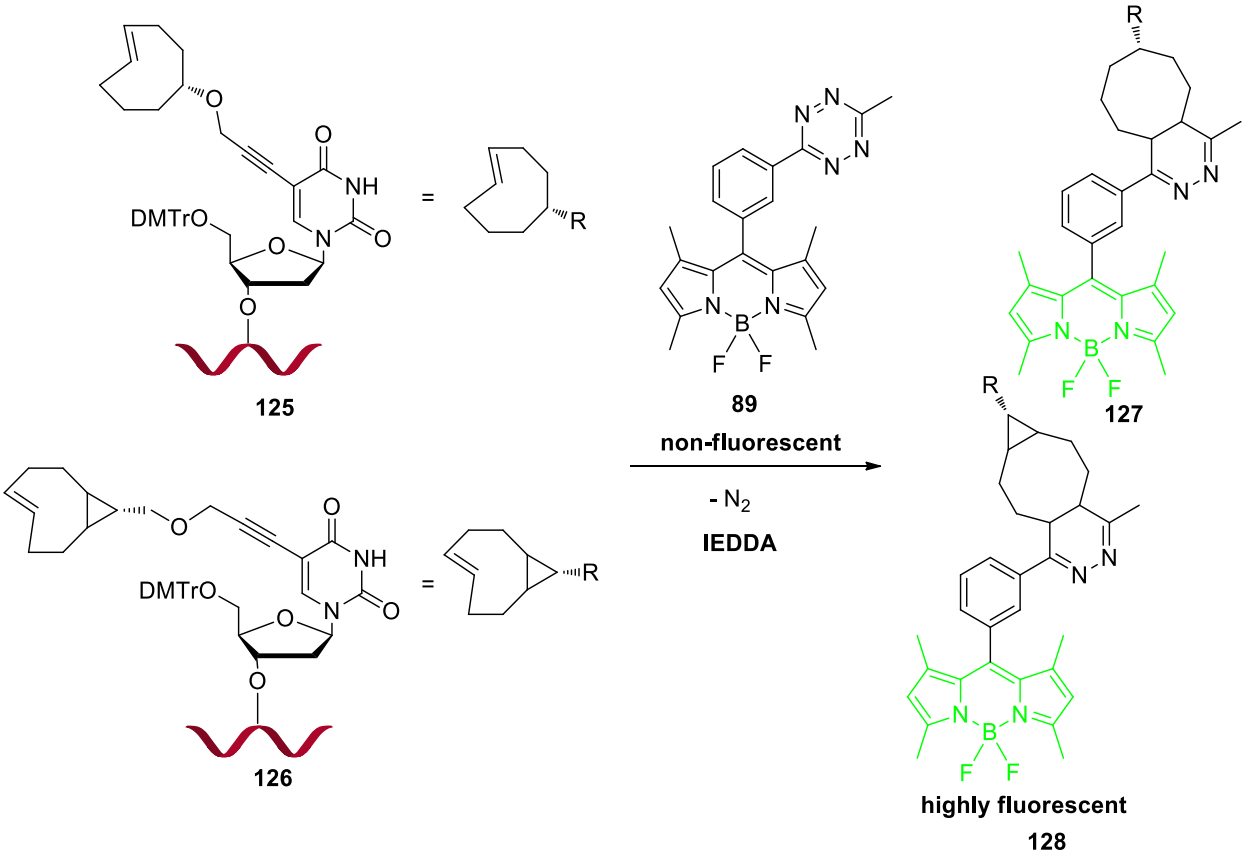

Scheme 4-1. The general scheme for site-specific labeling of DNA using IEDDA between *trans*-cyclooctene derivative and BODIPY-tetrazine adduct.

Commercially available 5-iododeoxyuridine **129** was first protected at 5'-OH with a DMTr group in order to increase its solubility. The protected compound **130** was obtained in 80% yield (Scheme 4-2).

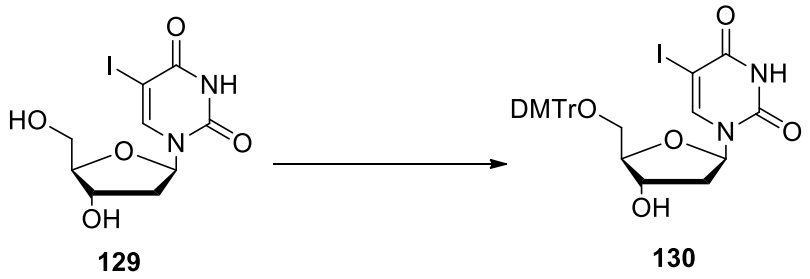

Scheme 4-2. *Reagents and conditions*: DMTr-Cl, pyridine, 80%.

In order to synthesize the first *trans*-cyclooctene derivative **134**, 1,5-cyclooctadiene **131** was treated with *meta*-chloroperbenzoic acid (*m*-CPBA) to give the corresponding epoxide **132** in a moderate 69% yield (Scheme 4-3). Nucleophilic substitution using lithium aluminum hydride $LiAlH_4$ was then performed to open the epoxide ring and gave (*Z*)-cyclooct-4-enol **133** in 52% yield.[117] Isomerization of **133** in a UVP-CL-500-ultraviolet crosslinker reactor at 254 nm in the presence of methyl benzoate as a sensitizer gave two isomers, (*E*)-cyclooct-4-enol **134-a** as a major product in 32% and (*E*)-cyclooct-4-enol **134-b** as a minor in 13% yield (Scheme 4-3). Separation of these two *trans*-isomers from the *cis*-cyclooctene **133** was performed by passing the reaction mixture through a column packed with $AgNO_3$-impregnated silica gel. *Trans*-Cyclooctenes form water-soluble complexes with $AgNO_3$, whereas *cis*-cyclooctene binds only weakly to $AgNO_3$, so it can be eluted by a mixture of hexane-diethylether (1:9, v/v), while *trans*-cyclooctene is retained by the $AgNO_3$-impregnated silica gel. Subsequent elution of the silica gel with aqueous ammonium hydroxide releases *trans*-cyclooctene from the silica gel.

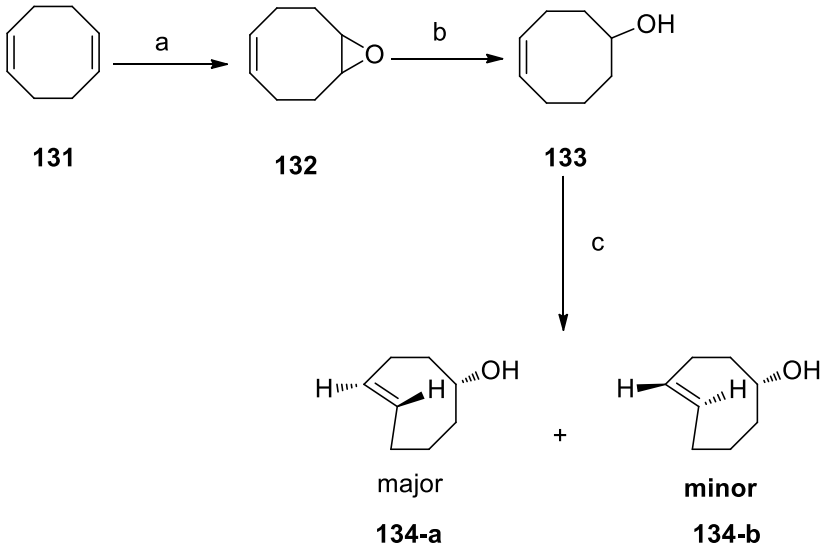

Scheme 4-3. *Reagents and conditions*: a) *m*-CPBA, DCM, 69%; b) $LiAlH_4$, THF, 52%; c) $C_6H_5COOCH_3$, ether-hexane (9:1), 45%.

The two *trans*-cyclooctenes **134-a** and **134-b** can be distinguished by NMR spectroscopy. Examination of the crown conformation structure of both isomers (Figure 4-1)[118] clearly reveals that the hydrogen labeled as Ha is axially substituted and positioned close to the transannular alkene of the major isomer **134-a**. This explains the relatively upfield chemical shift for Ha (3.36-3.40 ppm) due to shielding by the alkene (Figure 4-2a). While for the minor isomer **134-b**, Ha is equatorial and therefore distant from the alkene. As a result, NMR signal is more down field (3.98-4.03 ppm) (Figure 4-3a).

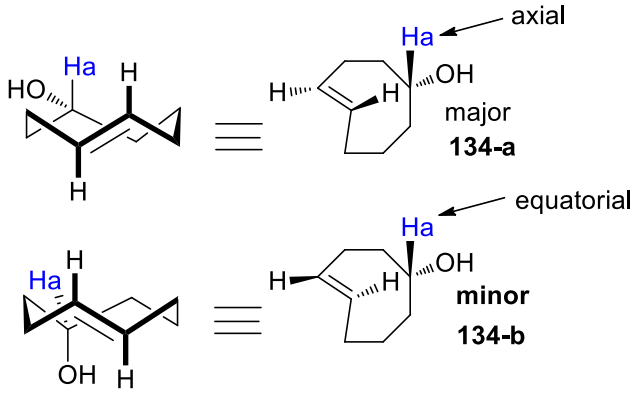

Figure 4-1. The crown conformation structure of major **134-a** and minor **134-b** isomers.

The stereochemistry of the two isomers was further confirmed by NOE experiments. When Ha is irradiated, a corresponding NOE signal was seen in the alkenic region of the major isomer **130-a**, indicating the close proximity of those two protons (Figure 4-2b). However, NOE was not observed for the minor isomer **130-b** (Figure 4-3b).

a)

b)

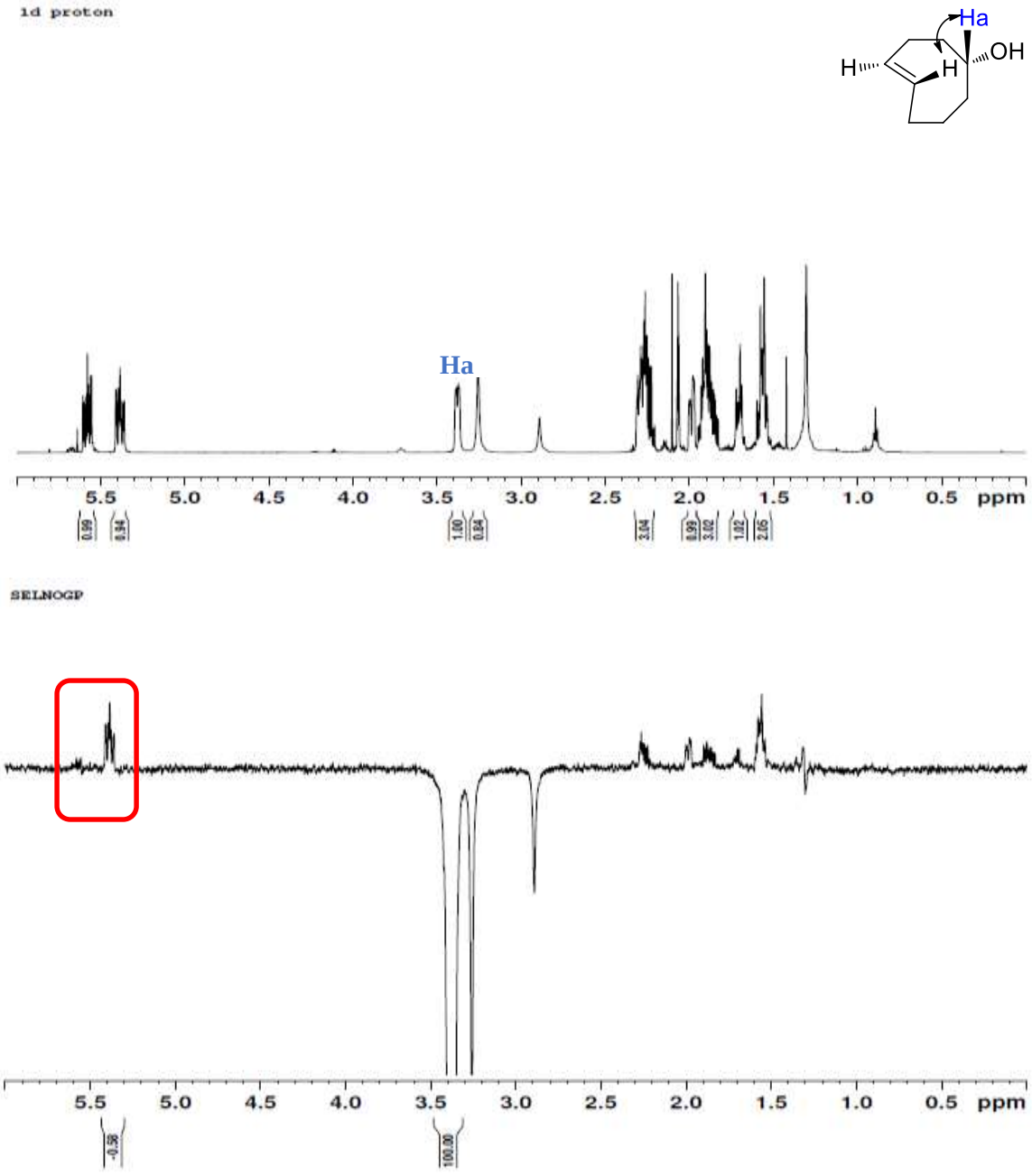

Figure 4-2. a) ^{1}H NMR spectrum of major **134-a**, b) NOE spectrum of the same compound in acetone-d_6.

a)

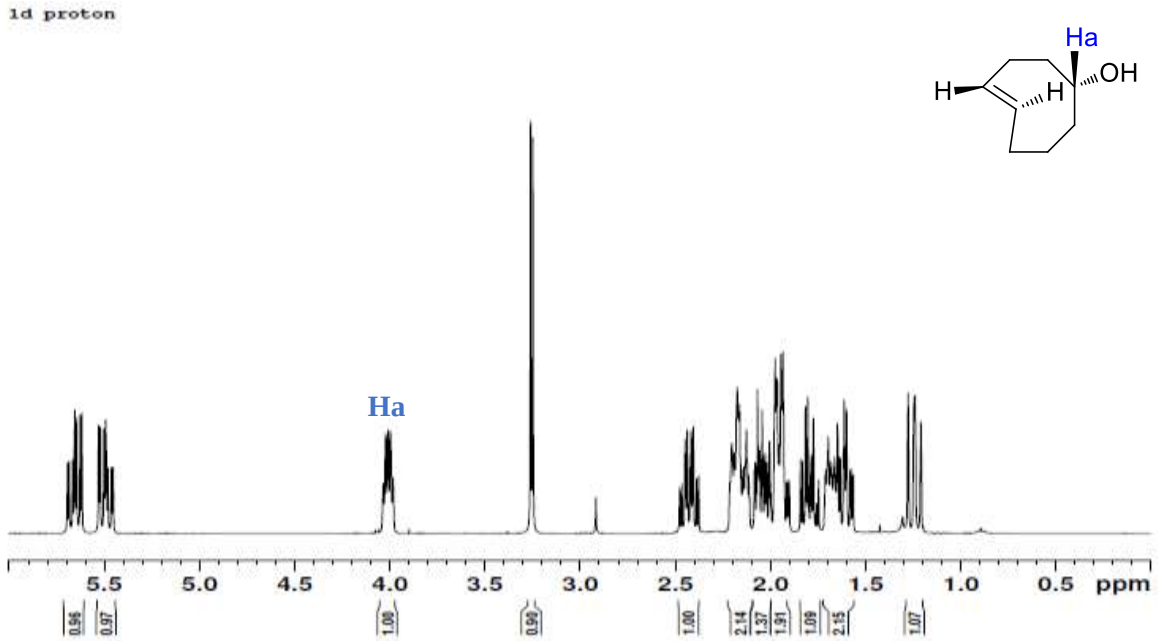

b)

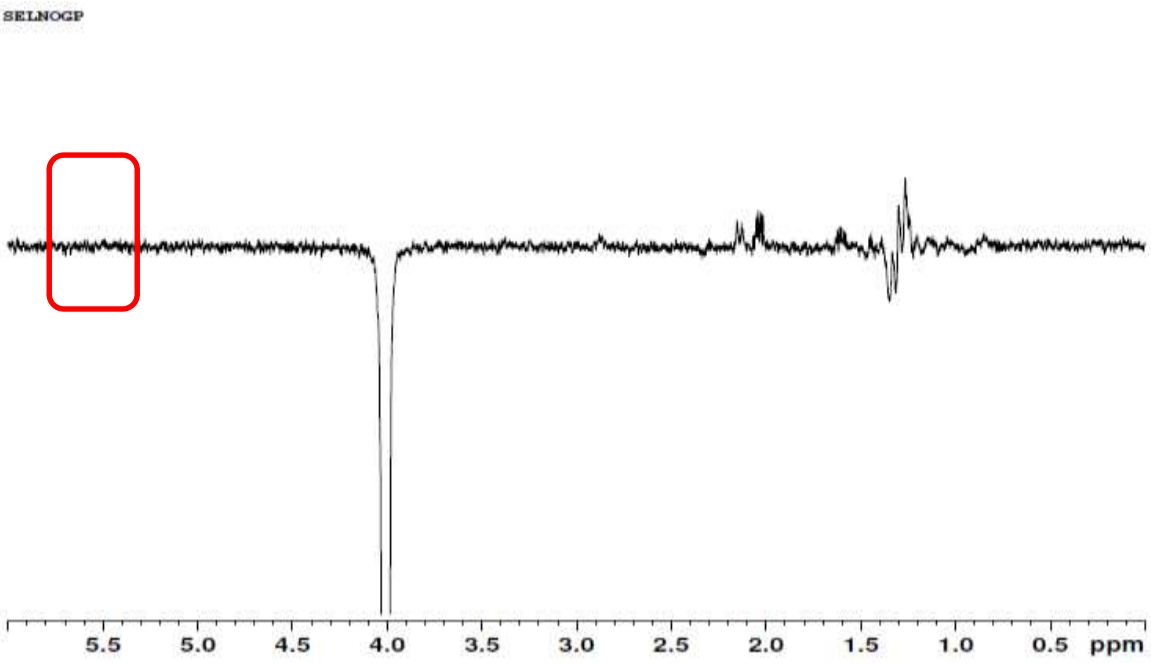

Figure 4-3. a) ^{1}H NMR spectrum of minor **134-b**, b) NOE spectrum of the same compound in acetone-d_6.

The major isomer **134-a** was further treated with propargyl bromide to afford the propargylated compound **135** in a moderate yield 61%. NOE experiments was performed for the propargylated compound **135**. When Ha is irradiated, a corresponding NOE signal was seen in the

alkenic region, indicating the close proximity of those two protons (Figure 4-4a and b). This observation also indicates that the propargylation reaction did not affect the stereochemistry of the compound.

a)

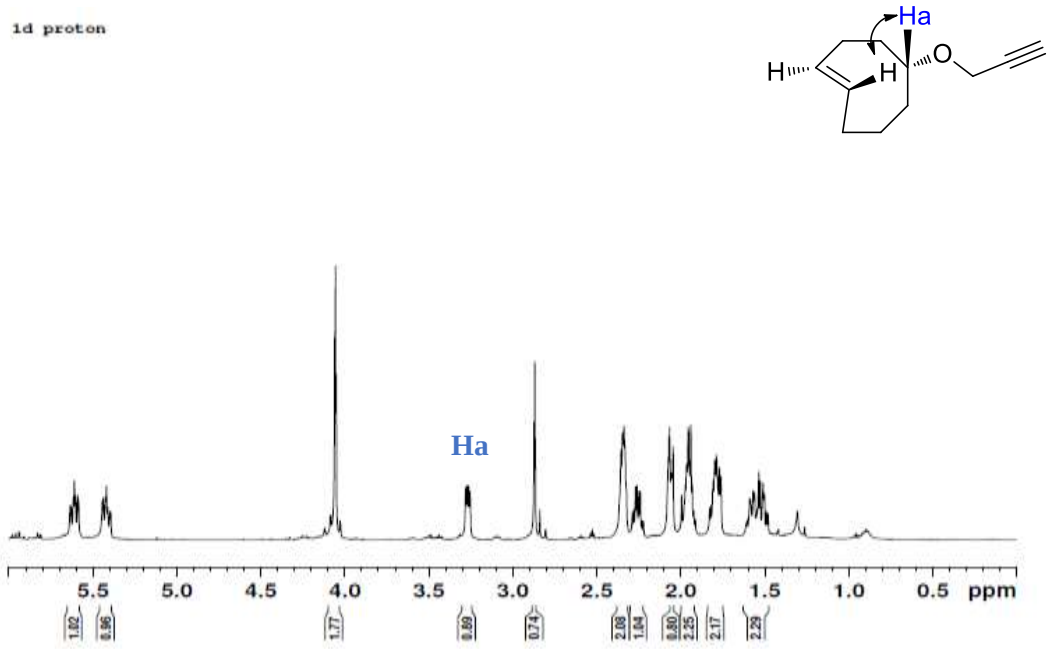

b)

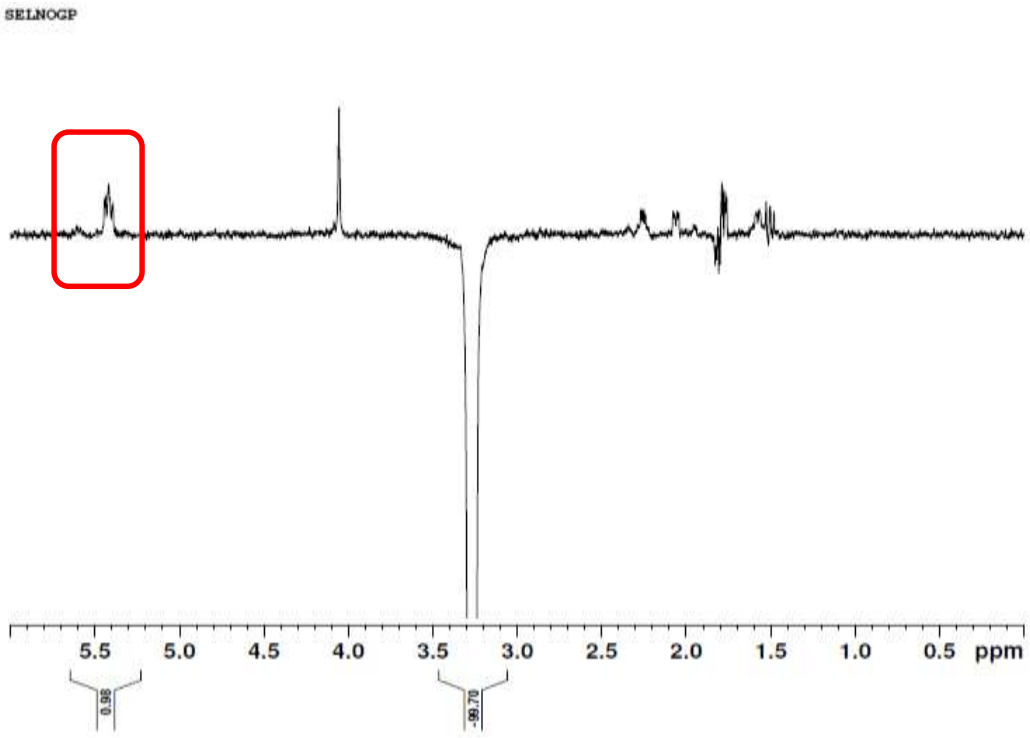

Figure 4-4. a) ^{1}H NMR spectrum of **135**, b) NOE spectrum in acetone-d_6.

Reaction of **135** with the previously prepared 5'-*O*-DMTr-protected 5-iododeoxyuridine **130** in the presence of copper (I) iodide, tetrakis(triphenylphosphine)palladium and DIPEA was expected to give Sonogashira coupling product **136**, however, at this writing, this reaction has failed to give the desired product under various condition. Future work will further investigate this reaction. Once the desired product **136** is obtained, it will be transformed into the corresponding phosphoramidite for incorporation into DNA sequences **125** by solid phase synthesis (Scheme 4-4).

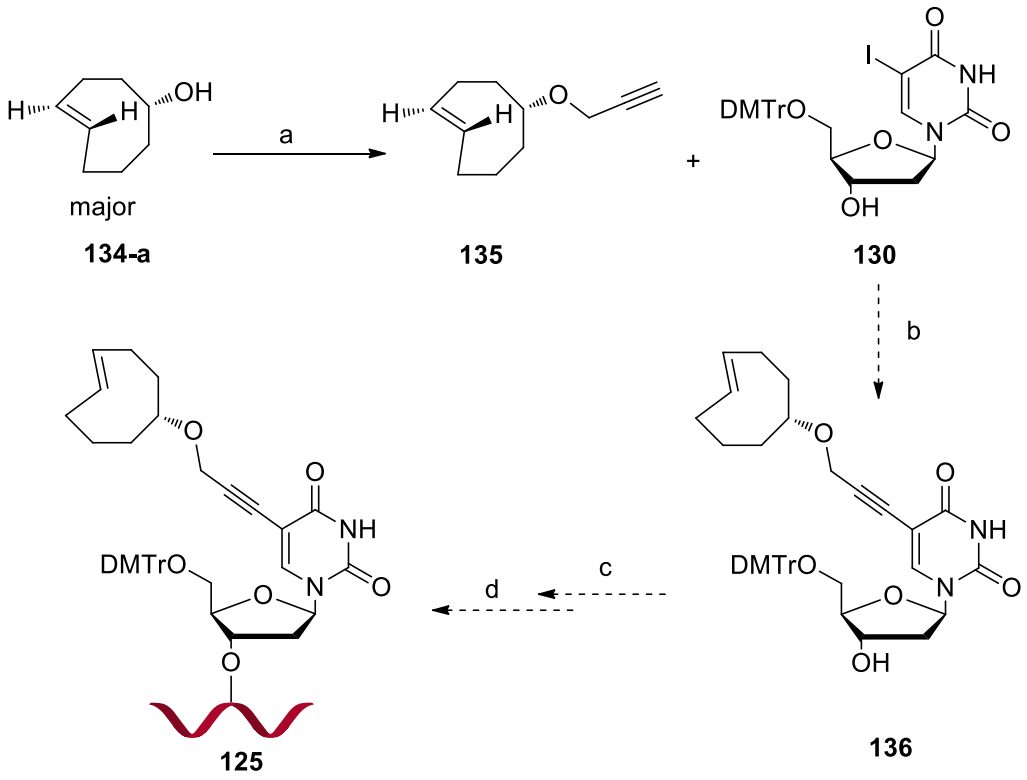

Scheme 4-4. *Reagents and conditions*: a) propargyl bromide, NaH, THF, 61%; b) CuI, $[Pd(PPh)_3]_4$, DIPEA; c) (2-cyanoethyl) -*N*,*N*-diisopropylphosphochloridite, DIPEA, THF; (d) Solid phase DNA synthesis.

The other *trans*-cyclooctene derivatives **139** and **141** were synthesized from the same starting material 1,5-cyclooctadiene **131**. First, treatment of **131** with ethyl diazoacetate in the presence of catalytic amount of rhodium acetate $Rh_2(OAc)_4$ gave two isomers, *exo*-isomer **137-a** and *endo*-isomer **137-b** in 58 and 41% yields, respectively. Reduction of both isomers in separate reactions using diisobutylaluminium hydride (DIBAL) at -78°C gave the corresponding reduced compounds, **138** in 93% yield and **140** in 81%, respectively. Photoisomerization of **138** and **140** using the procedure previously described in this section gave the corresponding *trans*-isomers **139** (39% yield) and **141** (40% yield) (Scheme 4-5).

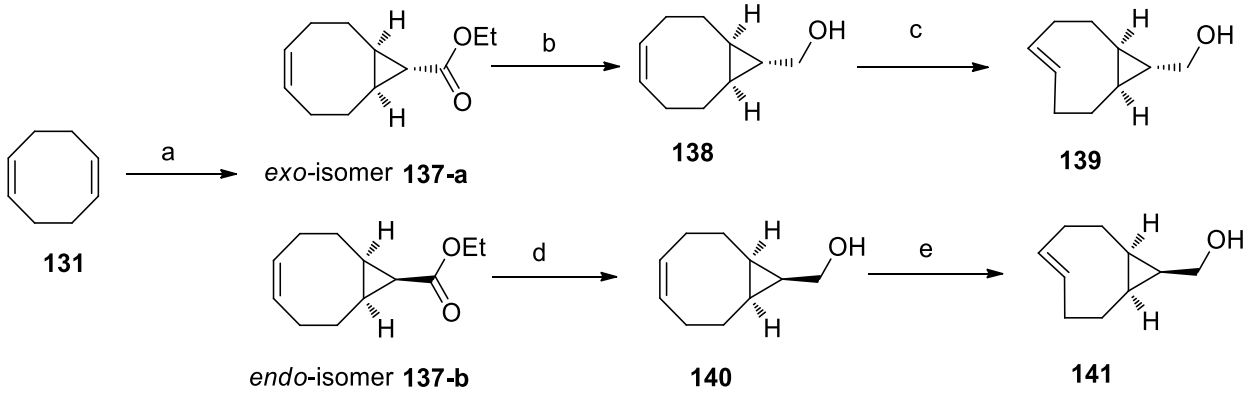

Scheme 4-5. *Reagents and conditions*: a) $Rh_2(OAc)_4$, ethyl diazoacetate, 58% *exo*, 41% *endo*; b) DIBAL, THF, 93%; c) $C_6H_5COOCH_3$, ether-hexane (9:1), 39% d) DIBAL, THF, 81%; e) $C_6H_5COOCH_3$, ether-hexane (9:1), 40%.

Propargylation reaction of **141** using propargyl bromide in the presence of sodium hydride gave the corresponding product **142** in 64% yield. In future work, the latter compound **142** will be treated with 5'-*O*-DMTr-5-iododeoxyuridine **130** under the Sonogashira coupling conditions to furnish the compound **143** which will then be transformed into the corresponding phosphoramidite for incorporation into DNA sequences **126** using solid phase synthesis (Scheme 4-6).

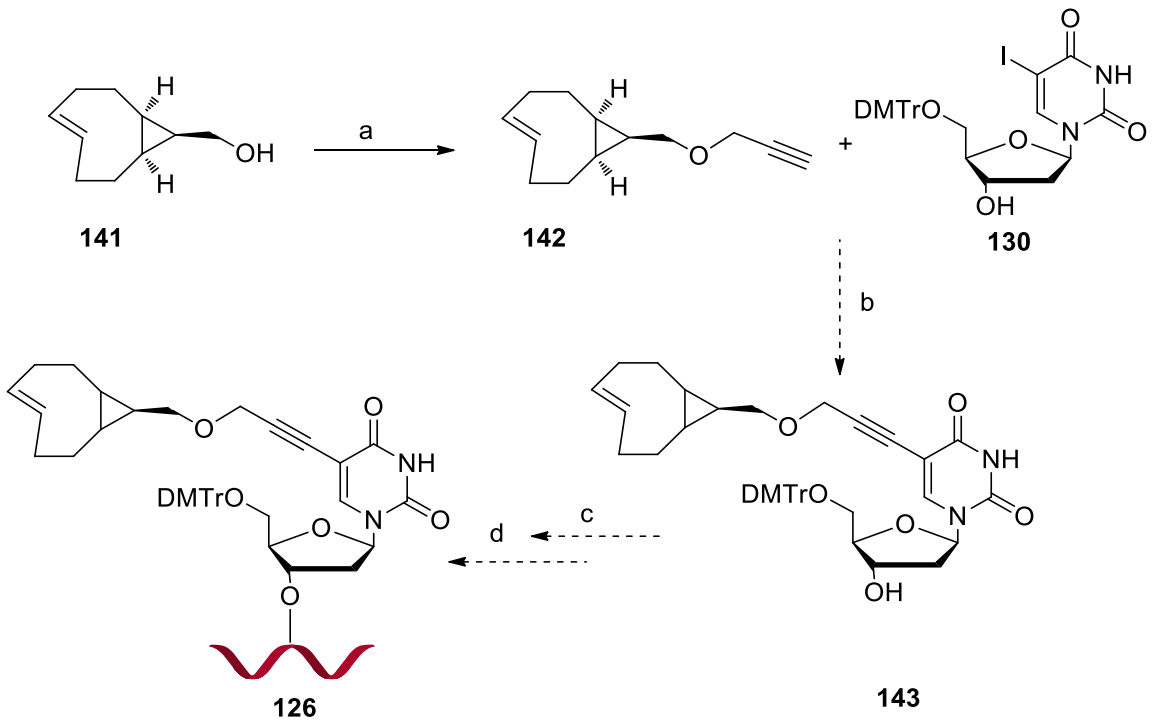

Scheme 4-6. *Reagents and conditions*: a) propargyl bromide, NaH, THF, 64%; b) CuI, $[Pd(PPh)_3]_4$, DIPEA; c) (2-cyanoethyl) -*N*,*N*-diisopropylphosphochloridite, DIPEA, THF; (d) Solid phase DNA synthesis.

4.2 BODIPY-tetrazine synthesis

The first attempt to synthesize BODIPY-tetrazine **89** followed a previously reported procedure (Scheme 4-7).[104]

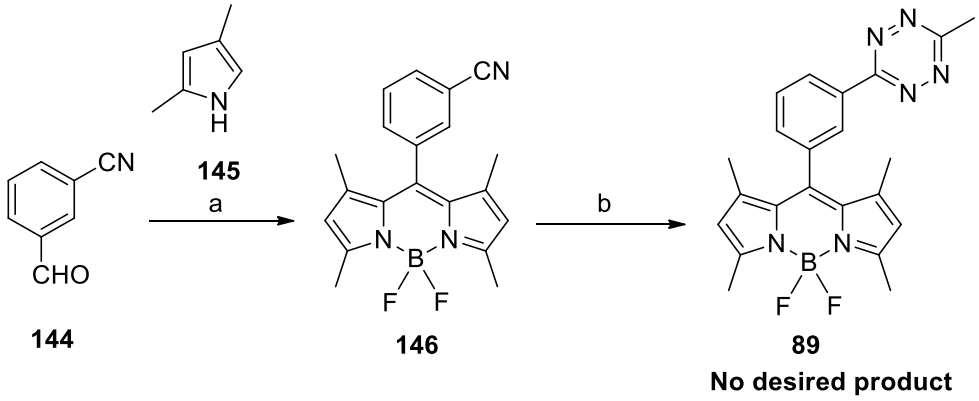

Scheme 4-7. *Reagents and conditions*: a) i. TFA, DCM, ii. DDQ, iii. DIPEA, iv. BF_3•OEt_2, 35%; b) $Zn(OTf)_2$, NH_2NH_2 hydrate, CH_3CN, DMF.

Thus BODIPY **146** was prepared in 35% yield by first reacting 3-formyl benzonitrile **144** with 2,4-dimethylpyrrole **145** in the presence of trifluoroacetic acid TFA, followed by oxidation with 2,3-dichloro-5,6-dicyanobenzoquinone DDQ, and then complexation with $BF_3.OEt_2$ in the presence of DIPEA, However, the following transformation to introduce the tetrazine ring as in **89** failed under various conditions (Table 4-1).

Table 4-1. The various conditions used for Bodipy-tetrazine synthesis.

Reagent	Conditions	Results
$Zn(OTf)_2$	60°C, microwave, 18 h	No desired product
$Zn(OTf)_2$	60°C, 24 h	No desired product
$Zn(OTf)_2$	100°C, 18 h	No desired product
$Ni(OTf)_2$	60°C, 24 h	No desired product
Sulfur	78°C (reflux), overnight	No desired product

Consequently, another synthetic approach was used (Scheme 4-8). Thus, the aldehyde group of 3-formyl benzonitrile **144** was first protected as acetal by the treatment with ethylene glycol in the presence of (±)-camphor-10-sulfonic acid (CSA) to give **148** in 95% yield. The corresponding tetrazine compound **149** was obtained in 41% yield by the reaction of **148** with acetonitrile in the presence of $Ni(OTf)_2$ and hydrazine hydrate. Aqueous toluene sulfonic acid was subseqently used to deprotect the acetal protecting group to give tetrazine benzaldehyde **150** in 98% yield. Finally, following the same reaction sequence that was used for synthesizing **146**, a product was isolated in 33% yield as a single spot on the TLC. Although this non-fluorescent compound has the characteristic color of tetrazines and ^{11}B NMR and ^{19}F NMR signals that correspond to BODIPY compounds, the identity of this compound could not be confirmed at this writing.

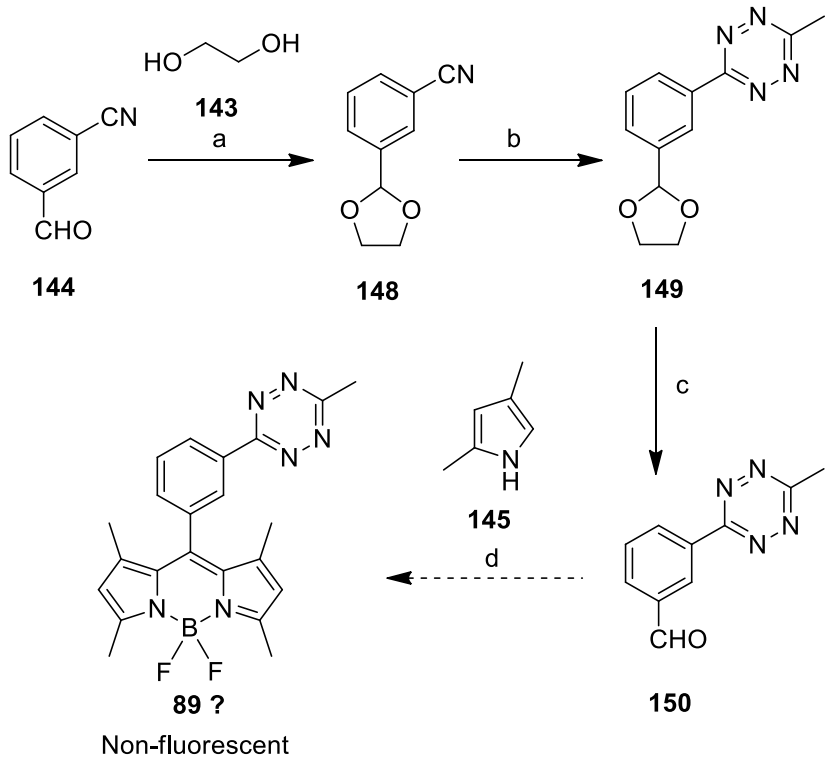

Scheme 4-8. *Reagents and conditions*: a) HOC_2H_4OH, CSA, benzene, 95%; b) $Ni(OTf)_2$, NH_2NH_2 hydrate, CH_3CN, DMF, 41%; c) TsOH, H_2O, MeOH, 98%; d) i. TFA, DCM, ii. DDQ, iii. DIPEA, iv. BF_3•OEt_2, 33%.

4.3 Conclusions and future work

Two different *trans*-cyclooctene derivatives **135** and **142** were synthesized in moderate yields from the same starting material 1,5-cyclooctadiene **131**. In addition, an alternative synthesis approach was pursued for the preparation of BODIPY-tetrazine compound.

Future work of this project will explore conditions for the Sonogashira coupling reactions towards the synthesis of 2'-deoxyuridine derivatives **136** and **143** containing *trans*-cyclooctene derivatives. The latters will be transformed into corresponding phosphoramidite for incorporation into oligonucleotides to study the IEDAA reaction for labeling purposes. Future work will also aim to confirm the identity of the BODIPY-tetrazine product **89**, and to develop this approach as a general method for synthesizing BODIPY-tetrazine conjugates. These conjguates will find

applications in labeling biomolecules through the IEDAA reactions, leading to fluorescent “turn on” with very low background noise.

CHAPTER 5: Experimental

5.1 Instrumentation

^{1}H NMR spectra were measured at 300, 400 and 600 MHz with Bruker Avance 300, 400 and 600 Digital NMR spectrometers with 7.05, 9.4 and 14.1 Tesla Ultra shield magnets, respectively. Tetramethylsilane was used as an internal standard. ^{13}C NMR spectra were measured at 75 MHz or 100 MHz, ^{31} P at 162 MHz, ^{11}B at 128 MHz, and ^{19}F at 376 MHz with the same instrument. Chemical shifts and coupling constants (*J* values) are given in ppm and Hz, respectively. The following deuterated solvents from C/D/N isotopes Inc. were used for preparation of NMR samples: dimethyl-d_6 sulfoxide with 0.05% tetramethylsilane internal standard (99.9 atom % D), deuterated chloroform (99.9 atom % D), and deuterated oxide (99.9 atom % D). Low resolution mass spectra were obtained with a Bruker HCT Ultra LC/MS system with ESI interfaces, and the data were processed using Bruker Data Analysis software. UV/Vis spectra and melting temperature curves were recorded with Cary 4000 UV/Visible spectrophotometer. Fluorescence spectra were measured using QuantaMaster model QM-2001-4 cuvette-based L-format scanning spectrofluorometer from Photon Technology International (PTI) interfaced with FeliX32 software. Photoisomerization reactions were performed using Hoefer UVC 500 Ultraviolet Crosslinker. Circular Dichroism (CD) spectra were recorded using Jasco J-600 Circular Dichroism Spectrometer.

5.2 Chromatography

Silica gel (EMD, >230 mesh) was used for flash chromatography. Silver nitrate-impregnated silica gel was prepared using the following procedure.[118]

Flash silica gel (90.00 g) was suspended in water (100 ml) in a 2 L round bottom flask. The flask was covered with aluminum foil and a solution of silver nitrate (10 g) in water (10 ml) was added. The resulting mixture was thoroughly mixed. Water was evaporated under reduced pressure on a rotary evaporator (bath temperature ~ 65 °C) using a bump trap equipped with a coarse fritted disk. After the bulk water was removed, the residue was co-evaporated with toluene (2×200 ml) to remove the remaining trace amount of water. The silver nitrate impregnated silica gel was furthere dried *in vacuo* overnight at room temperature.

Thin layer chromatography was performed on Silicycle SilicaPlate F-254 TLC plates using the following solvent mixtures:

System A: hexane-diethyl ether (90:10, v/v)

System B: hexane-diethyl ether (50:50, v/v)

System C: hexane-diethyl ether (30:70, v/v)

System D: dichloromethane-methanol (95:5, v/v)

5.3 Solvents and chemicals

Benzene, toluene and tetrahydrofuran THF were dried by heating under reflux over sodium in the presence of benzophenone for 4 h and then distilled. *N*,*N*-Diisopropylethylamine, and pyridine were dried by heating under reflux over calcium hydride for 2 h and then distilled in an atmosphere of nitrogen. Dimethylformamide (DMF) was dried by heating at 60°C for 2 h in the presence of calcium hydride, followed by distillation under reduced pressure. Dichloromethane and chloroform were dried by heating under reflux over phosphorus pentoxide for 2 h and then distilled in an atmosphere of nitrogen. All the distilled solvents were stored over activated 4 Å molecular sieves. All other reagents were purchased from Sigma-Aldrich or VWR Canlab without further purification prior to use unless stated otherwise.

5.4 Preparation of compounds

11, 12-Dihydrodibenzo[*c, g*] [1, 2] diazocine-5-oxide 110

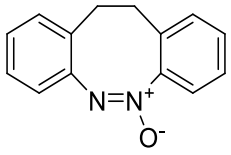

2,2'-Dinitrodibenzyl **109** (6.09 g, 22.38 mmol) was dissolved in methanol (250 ml) followed by addition of sodium carbonate (18.68 g, 176.2 mmol) and lead powder (18.26 g, 88.13 mmol, 200 mesh). The reaction mixture was stirred vigorously under reflux for 24 h, then the products were filtered and washed with dichloromethane. The filtrate and washing were combined and concentrated under reduced pressure. The residue was re-dissolved in dichloromethane (100 ml) and washed with saturated sodium bicarbonate (3×50 ml). The organic layer was dried ($MgSO_4$) and concentrated under reduced pressure. The residue was purified by column chromatography on silica gel. The appropriate fractions, which were eluted with dichloromethane-hexane (40:60 v/v), were pooled and concentrated under reduced pressure to give the *title compound* as a pale yellow solid (3.09 g, 62 %).

$\delta_H(CDCl_3)$: 2.88 (1 H, ddd, *J* = 5.9, 9.6 and 14.4), 2.98 (1 H, ddd, *J* = 5.2, 10.0, and 14.9), 3.22 (1 H, ddd, *J* = 5.1, 10.1, 14.6), 3.37(1 H, ddd, *J* = 5.9, 10.1, 15.0), 6.94(1 H, d, *J* = 7.8), 7.02 (2 H, d, *J* = 4.0), 7.04 (1 H, d, *J* =7.6), 7.10-7.20 (4 H, m).

These values are in agreement with the previously reported data.[55]

2-Bromo-11,12-dihydrodibenzo[*c,g*][1,2]diazocine-6-oxide 111

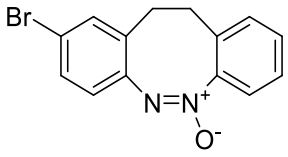

To a solution of 11,12-dihydrodibenzo[*c*,*g*][1,2]diazocine-5-oxide **110** (1.60 g, 7.14 mmol) in acetic acid (16.0 ml), bromine (1.60 ml, 31.04 mmol) was added drop-wise. After the reaction mixture was heated at 50°C in a sealed flask for 2 days, the reaction was quenched by a drop-wise addition of sodium thiosulfate solution (40%) until the color changed from brown to pale yellow. The mixture was then extracted with dichloromethane (3×50 ml). The organic layers were combined and washed with water (2×50 ml) and saturated aqueous sodium bicarbonate solution (2×50 ml). The organic layer was dried ($MgSO_4$) and concentrated under reduced pressure. The residue was purified by column chromatography on silica gel. The desired product was obtained upon evaporation of appropriate fractions, which were eluted with dichloromethane-hexane (40:60 v/v), as a light brown solid (1.48 g, 69%).

$\delta_H(CDCl_3)$: 2.84 (1 H, ddd, *J* = 5.9, 9.6, and 14.8), 2.98 (1 H, ddd, *J* = 5.1, 9.9 and 14.8), 3.21 (1 H, ddd, *J* = 5.1, 10.1, and 14.8), 3.36 (1 H, ddd, *J* = 5.9, 9.9, and 15.0), 6.82 (1 H, d, *J* = 8.4), 7.07 (1 H, d, *J* = 7.5), 7.16–7.22 (3 H, m), 7.24–7.26 (2 H, m).

These values are in agreement with the previously reported data.[55]

2-Bromo-11,12-dihydrodibenzo[*c*,*g*][1,2]diazocine 112

Phosphorus trichloride (8.30 ml, 95.1 mmol) was added slowly to a solution of 2-bromo-11,12-dihydrodibenzo[*c*,*g*][1,2]diazocine-6-oxide **111** (1.80 g, 5.96 mmol) in dry benzene (25 ml) and the reaction mixture was heated under reflux for 24 h. Upon cooling, the reaction mixture was evaporated under reduced pressure. To the dark residue, hydrochloric acid (0.1 *M*, 10 ml) was added, followed by extraction with diethyl ether (3×50 ml). The organic layers were combined and

washed with saturated aqueous sodium bicarbonate (2×50 ml) and the organic layers were dried ($MgSO_4$) and evaporated to dryness under reduced pressure. The residue was purified by column chromatography on silica gel. The desired product was obtained upon evaporation of appropriate fractions, which were eluted with dichloromethane-hexane (30:70 v/v), as a pale yellow solid (0.850 g, 50%).

$\delta_H(CDCl_3)$: 2.76 (2 H, m), 2.99 (2 H, br, m), 6.73 (1 H, d, *J* = 8.4), 6.85 (1 H, d, *J* = 7.8), 7.02 (1 H, d, *J* = 7.5), 7.07 (1 H, t, *J* = 7.4), 7.15 (1 H, d, *J* = 1.6), 7.18 (1 H, t, *J* = 7.5), 7.26 (1 H, dd, *J* = 1.7 and 8.4).

These values are in agreement with the previously reported data.

11,12-Dihydrodibenzo[*c*,*g*][1,2]diazocine-2-carbonitrile 113

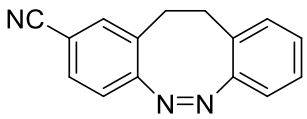

To a solution of 2-bromo-11,12-dihydrodibenzo[*c*,*g*][1,2]diazocine **112** (1.15 g, 4.02 mmol) in dry *N*,*N*-dimethyl formamide (10 ml), copper (I) cyanide (0.54 g, 6.03 mmol) was added. After the reaction mixture was heated under reflux overnight, the products were cooled to room temperature, followed by addition of ethylenediamine (10% aqueous solution, 50 ml). The mixture was extracted with dichloromethane (3×50 ml). The organic layer was separated and successively washed with saturated aqueous sodium bicarbonate solution (3×50 ml) and water (3×50 ml). The organic layer was dried ($MgSO_4$) and concentrated under reduced pressure. The residue was purified by column chromatography on silica gel. The desired product was obtained upon evaporation of appropriate fractions, which were eluted with dichloromethane-hexane (60:40 v/v) as a pale yellow solid (0.57 g, 61%).

$\delta_H(CDCl_3)$: 2.78–2.87 (2 H, m), 3.00–3.07 (2 H, m), 6.87 (1 H, d, *J* = 7.7), 6.92 (1 H, d, *J* = 8.1), 7.01 (1 H, d, *J* = 7.5), 7.08 (1 H, dt, *J* = 1.2 and 7.5), 7.19 (1 H, t, *J* = 7.5), 7.32 (1 H, d, *J* = 1.2), 7.44 (1 H, dd, *J* = 1.4 and 8.0).

These values are in agreement with the previously reported data.[112]

11,12-Dihydrodibenzo[*c*,*g*][1,2]diazocine-2-carboxylic acid 114

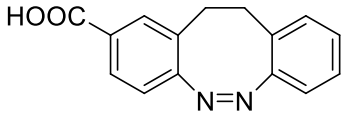

The carbonitrile **113**(200 mg, 0.80 mmol) was placed in a solution of potassium hydroxide (6.00 g) in ethanol (60 ml) and water (15 ml) and heated under reflux for 4 h. Ethanol was removed under reduced pressure and the residue was treated with aqueous hydrochloric acid (6 *M*) until the mixture turned acidic (pH 4). The mixture was extracted with ethyl acetate (3×50 ml). The combined organic layers were washed with brine (2×30 ml), dried ($MgSO_4$), and concentrated under reduced pressure to give the crude carboxylic acid which was purified by column chromatography on silica gel. The appropriate fractions, which were eluted with dichloromethane-methanol (95:5 v/v), were combined and concentrated under reduced pressure to give the *title compound* as a light yellow solid (196 mg, 96%).

$\delta_H(CDCl_3)$: 2.83 (1 H, m), 2.89 (1 H, m), 3.04 (2 H, m), 6.87 (1 H, d, *J* = 7.8), 6.92 (1 H, d, *J* = 8.1), 7.00 (1 H, d, *J* = 7.6), 7.05 (1 H, t, *J* = 7.7), 7.17 (1 H, t, *J* = 7.5), 7.76 (1 H, d, *J* = 1.2), 7.87 (1 H, dd, *J* = 1.3 and 8.1).

These values are in agreement with the previously reported data.[55]

(*Z*)-*N*-((2*S*,3*S*)-1,3-Dihydroxybutan-2-yl)-11,12-dihydrodibenzo[*c*,*g*][1,2]diazocine-2-carboxamide 116

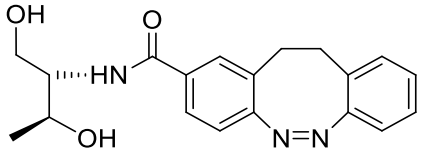

To a solution of 11,12-dihydrodibenzo[*c*,*g*][1,2]diazocine-2-carboxylic acid **114** (200 mg, 0.79 mmol) in dry *N*,*N*-dimethyl formamide (4.0 ml), D-threoninol **115** (70 mg, 0.67 mmol), *N*,*N*-dicyclohexylcarbodiimide (164 mg, 0.79 mmol) and *N*-hydroxysuccinamide (92 mg, 0.79 mmol) were added. After the reaction mixture was stirred for 5 h at room temperature under a nitrogen atmosphere, the precipitate was removed by filtration and the filtrate was evaporated under reduced pressure. The oily residue was purified by column chromatography on silica gel. Evaporation of appropriate fractions, which were eluted by dicholoromethane-methanol (95:5 v/v), gave the *title compound* as a pale yellow foam (240 mg, 90%).

δ_H (DMSO-d_6): 1.01 (3 H, t, *J* = 6.1), 2.83-2.86 (2 H, m), 2.88-2.91 (2 H, m), 3.40-3.45 (1 H, m), 3.51-3.55 (1 H, m), 3.81-3.84 (1 H, m), 3.85-3.88 (1 H, m), 4.56-4.61 (2 H, m, br, OH, ex), 6.88 (1 H, d, *J* = 7.8), 6.92 (1 H, d, *J* = 8.1), 7.07 (1 H, t, *J* = 7.3), 7.10 (1 H, d, *J* = 7.2), 7.19 (1 H, dt, *J* = 7.19) (1 H, t, *J* = 7.2), 7.60 (1 H, d, *J* = 2.9), 7.66 (1 H, d, *J* = 8.1), 7.71 (1 H, d, *J* = 8.3, NH, ex).

These values are in agreement with the previously reported data.[55]

(*Z*)-*N*-((2*R*,3*S*)-1-(bis(4-methoxyphenyl)(phenyl)methoxy)-3-hydroxybutan-2-yl)-11,12-dihydrodibenzo[*c*,*g*][1,2]diazocine-2-carboxamide 117

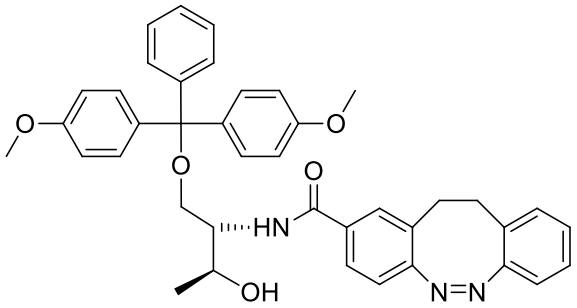

(*Z*)-*N*-((2*S*,3*S*)-1,3-Dihydroxybutan-2-yl)-11,12-dihydrodibenzo[*c*,*g*][1,2]diazocine-2-carboxamide **116** (70 mg, 0.21 mmol) was azeotroped with dry toluene (5 ml) and then dry pyridine (2×5 ml). The residue was dissolved in dry pyridine (10 ml) and then azeotroped to a volume of approximately 5 ml, followed by addition of 4,4'-dimethoxytrityl chloride (84 mg, 0.25 mmol) under nitrogen. The reaction mixture was stirred at room temperature for 1 h and triethylamine (1 ml) was added. The products were poured into saturated aqueous sodium bicarbonate (20 ml) and extracted with dichloromethane (3×20 ml). The organic layers were combined, dried ($MgSO_4$) and evaporated to dryness to give an oily product. The oily residue was purified by column chromatography on silica gel. The desired product was obtained upon evaporation of appropriate fractions, which were eluted with methanol-dichloromethane (1:99 v/v), as a pale yellow foam (110 mg, 83 %).

δ_H(DMSO-d_6): 0.97 (3 H, d, *J* = 6.0), 2.85-2.93 (5 H, m), 3.14-3.19 (1 H, m), 3.72 (6 H, s), 3.97-4.06 (2 H, m), 4.53 and 4.55 (both d, *J* = 6.0, together 1 H, OH), 6.80-6.84 (4 H, m), 6.88 (1 H, d, *J* = 7.8), 6.96 (1 H, d, *J* = 8.0), 7.05 (1 H, t, *J* = 7.3), 7.10 (1 H, t, *J* = 7.3), 7.16-7.23 (8 H, m), 7.34-7.38 (2 H, m), 7.63 (1 H, d, *J* = 10.2), 7.70 (1 H, ddd, *J* = 1.4, 1.4 and 6.9), 8.00 and 8.03 (both d, *J* = 8.5, together 1 H)

These values are in agreement with the previously reported data.[112]

(2*S*,3*R*)-4-*O*-Dimethoxytrityl-3-((*Z*)-11,12-dihydrodibenzo[*c*,*g*][1,2]diazocine-2-carboxamido)butan-2-yl(2-cyanoethyl) diisopropylphosphoramidite 118

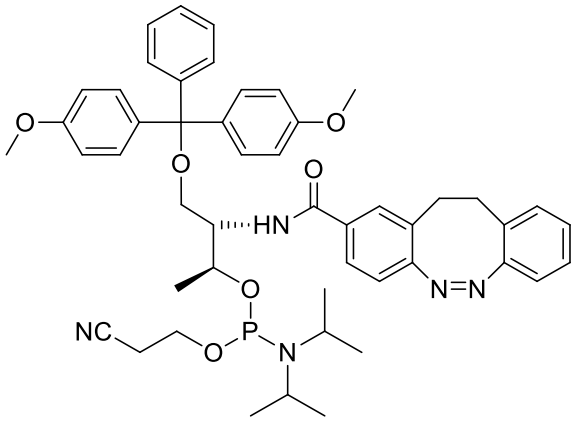

(Z)-*N*-((2*R*,3*S*)-1-*O*-Dimethoxytrityl-3-hydroxybutan-2-yl)-11,12-dihydrodibenzo[*c*,*g*][1,2] diazocine-2-carboxamide **117** (200 mg, 0.31mmol) was azeotroped with dry toluene (2×5 ml) and dissolved in dry tetrahydrofuran (3 ml), followed by addition of dry *N*,*N*-diisopropyl ethylamine (Hünigs base, DIPEA, 0.16 ml, 0.94 mmol), and (2-cyanoethyl)-*N*,*N*-diisopropyl phosphochloridite (110 mg, 0.47 mmol). The reaction mixture was stirred at room temperature for 30 min. Triethylamine (2 ml) were added and the products were evaporated under reduced pressure. The residue was purified by column chromatography on silica gel. The desired product was obtained upon evaporation of appropriate fractions, which were eluted with hexane-dichloromethane-triethylamine (28:70:2 v/v), as a pale yellow color glass (197 mg, 72%).

δ_H($CDCl_3$ containing trace amount of triethylamine) include the following signals: 0.98 (2 H, t, *J* = 5.9), 2.28–2.32 (1 H, m, br), 2.80–2.87 (2 H, m, br), 2.98–3.03 (2 H, m, br), 3.17–3.32 (2 H, m, br), 3.50 (3 H, br), 3.79 (6 H, s), 3.31–4.44 (1 H, m, br), 6.22, 6.26, 6.40, 6.45 (four sets of doublets that represent the NH proton, two diastereomers + rotamers, d, *J* = 8.8), 6.78–6.80 (4 H, br), 6.86

(d, *J* = 7.5) and 6.90 (d, J = 7.9) (these two sets of signals integrate together 2 H), 6.99 (t, *J* = 7.3) and 7.03 (t, *J* = 7.4) (these two sets of signals integrate together 2 H), 7.40 (2 H, t, *J* = 8.3).

δp [$CDCl_3$]: 147.84 and 148.38.

These values are in agreement with the previously reported data.[112]

5′-*O*-(4,4′-Dimethoxytrityl)-5-iodo-2′-deoxyuridine 130

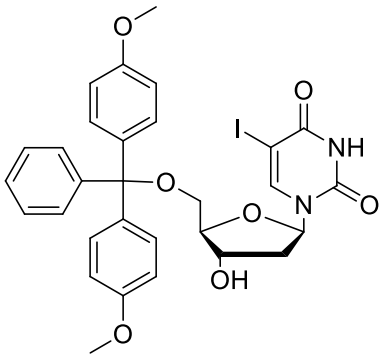

5-Iodo-2′-deoxyuridine **129**(1.00 g, 2.82 mmol) was azeotroped with dry toluene (2×10 ml). The residue was dissolved in dry pyridine (20 ml) and azeotroped to a volume of approximately 10 ml. To the solution, 4,4'-dimethoxytrityl chloride (1.15 g, 3.39 mmol) was added under nitrogen. After the reaction mixture was stirred for 1 h at room temperature, ice-cold water (25 ml) was added. The products were extracted with dichloromethane (3×30 ml). The organic layers were combined, dried over $MgSO_4$, and evaporated to dryness to obtain an oily product. The oily residue was purified by column chromatography on silica gel. The desired product was obtained upon evaporation of appropriate fractions, which were eluted with methanol-dichloromethane (2:99 v/v), as a while foam (1.48 g, 80 %).

R_f (System D): 0.40

δ_H ($CDCl_3$): 2.28-2.39 (1 H, m), 2.46-2.52 (1 H, m), 3.38-3.46 (2 H, m), 3.82 (6 H, s), 4.07 (1 H, m), 4.55-4.57 (1 H, m), 6.32 (1 H, dd, *J* = 7.6 and 6.0), 6.87 (4 H, d, *J* = 8.8), 7.25-7.36 (9 H, m), 8.14 (1 H, s).

δ_C ($CDCl_3$): 41.4, 55.2, 63.5, 69.8, 72.2, 85.3, 86.2, 86.9, 113.3, 127.0, 128.0, 130.0, 130.1, 135.4, 135.5, 143.8, 144.4, 151.6, 158.6, 162.2.

(*Z*)-9-Oxabicyclo[6.1.0]non-4-ene 132[117]

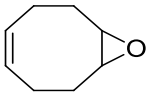

1,5-Cyclooctadiene **131** (30.0 g, 0.277 mol) was dissolved in dry dichloromethane (350 ml), followed by drop-wise addition of a solution of *meta*-chloroperoxybenzoic acid (55.47 g, 0.2911 mol) in dry dichloromethane (650 ml). After the addition was complete, the reaction mixture was stirred for 4 h at room temperature. The products were then filtered and the filtrate was washed successively with 5% aqueous sodium hydroxide solution (3×100 ml), sodium bicarbonate solution (3×100 ml) and water (3×100 ml). The organic phase was dried ($MgSO_4$) and evaporated under reduced pressure to remove dichloromethane. Distillation of the crude mixture under reduced pressure (b.p 86–88°C/9 mmHg) gave the *title compound* as a colorless oil (23.76 g, 69%).

R_f (System A): 0.45

δ_H ($CDCl_3$): 1.98-2.10 (4 H, m), 2.11-2.16 (2 H, m), 2.35-2.46 (2 H, m), 3.00-3.04 (2 H, m), 5.52-5.60 (2 H, m).

δ_C ($CDCl_3$): 23.6, 28.1, 56.6, 128.8.

(*Z*)-Cyclooct-4-enol 133[117]

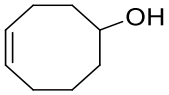

(*Z*)-9-Oxabicyclo[6.1.0]non-4-ene **132** (23.40 g, 0.1884 mol) was added drop-wise to a suspension of lithium aluminium hydride (4.04 g, 0.106 mol) in dry tetrahydrofuran (400 ml) at 0°C. The reaction mixture was stirred under reflux overnight. After the reaction was cooled to room temperature, water (20 ml) and dry $MgSO_4$ (2.00 g) were added and the mixture was stirred for 20 min. The mixture was then filtered and washed with diethyl ether. The filtrate and the washing were dried ($MgSO_4$) and evaporated under reduced pressure to remove the solvent. Distillation of the crude mixture under reduced pressure (b.p 95–97°C/9 mmHg) gave the *title compound* as a colorless oil (12.28 g, 52%).

R_f (System C): 0.56

δ_H ($CDCl_3$): 1.48-1.56 (1 H, m, OH), 1.58-1.73 (1 H, m), 1.79-1.95 (4 H, m), 2.05-2.16 (4 H, m), 2.24-2.33 (1 H, m), 3.75-3.81 (1 H, m), 5.54-5.61 (1 H, m), 5.65-5.71 (1 H, m).

δ_C ($CDCl_3$): 22.7, 24.9, 25.6, 36.3, 37.6, 72.6, 129.5, 130.1.

***rel*-(1*R*-4*E*-p*R*)-Cyclooct-4-enol (major) 134-a and *rel*-(1*R*-4*E*-p*S*)-cyclooct-4-enol (minor) 134-b**

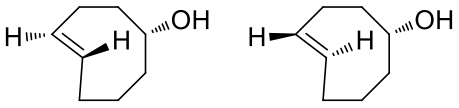

major **minor**

These compounds were synthesized from (*Z*)-cyclooct-4-enol by modification of a previously published procedure.[86]

(*Z*)-Cyclooct-4-enol **133** (1.00 g, 7.92 mmol) and methyl benzoate (1.10 g, 8.15 mmol) were dissolved in hexane-diethyl ether (200 ml, 1:9, v/v) and transferred in equal volumes to 4 Petri dishes (9.0 cm diameter). The Petri dishes were placed in a UVP-CL-500-ultraviolet crosslinker reactor and irradiated at 20×100 μJ/cm^2. At intervals of 25–30 min, the reaction mixture was passed through a column packed with 25 g of silica gel impregnated with 10% silver nitrate. The column was equilibrated with ether prior sample loading. The mixture passing through the column was placed back into the UV crosslinker for further irradiation. After total 7 h irradiation, the silica gel was transferred to a flask and stirred in an ammonium hydroxide solution (150 ml, 28%) for 5 min. Dichloromethane (150 ml) was added and stirring was continued for 5 min. The mixture was filtered and the aqueous layer was extracted with dichloromethane (3×50 ml). The combined organic phases were washed with water (3×50 ml) and dried ($MgSO_4$). After evaporation of the solvents, the two diastereomers of the product were isolated by column chromatography on silica gel (hexane-diethyl ether, 90:10 v/v) as colorless oils (major: 318 mg, 32%; minor: 126 mg, 13%).

Major **134-a**

R_f (System C): 0.55

δ_H ($CDCl_3$): 1.55-1.72 (3 H, m), 1.93-1.99 (4 H, m), 2.24-2.37 (3 H, m), 3.44-3.48 (1 H, m), 5.35-5.43 (1 H, m), 5.50-5.62 (1 H, m).

δ_C ($CDCl_3$): 31.2, 32.6, 34.3, 41.0, 44.5, 77.7, 132.7, 135.0.

Minor **134-b**

R_f (System C): 0.73

δ_H ($CDCl_3$): 1.22-1.32 (1 H, m), 1.63-1.71 (1 H, m), 1.77-1.91 (4 H, m), 2.08-2.19 (2 H, m), 2.21-2.29 (2 H, m), 2.34-2.44 (1 H, m), 4.04-4.07 (1 H, m), 5.53-5.64 (2 H, m).

δ_C ($CDCl_3$): 27.6, 29.3, 34.0, 34.1, 42.9, 67.4, 133.0, 134.2.

***rel*-(1*R*-4*E*-p*R*)-5-(Prop-2-yn-1-yloxy)cyclooct-1-ene 135**

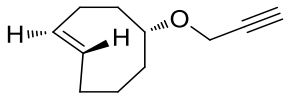

A solution of *rel*-(1*R*-4*E*-p*R*)-cyclooct-4-enol **134-a** (275 mg, 2.18 mmol) in dry tetrahydrofuran (3 ml) was added dropwise to a suspension of sodium hydride (60% in mineral oil, 260 mg, 6.54 mmol) in dry tetrahydrofuran (5 ml) at 0°C (ice-water bath). The mixture was stirred at room temperature for 30 min. Subsequently, propargyl bromide (519 mg, 4.36 mmol) was added dropwise at 0°C. After the mixture was stirred at room temperature overnight, the reaction was quenched by careful addition of brine (15 ml). The aqueous phase was extracted with diethyl ether (2×20 ml), and the organic extracts were dried with $MgSO_4$ and concentrated under reduced pressure. The residue was purified by column chromatography, eluting with hexane-diethyl ether (90:10 v/v) to afford the *title compound* (218 mg, 61%) as a pale yellow oil.

R_f (System A): 0.56

δ_H ($CDCl_3$): 1.46-1.59 (2 H, m), 1.78-1.88 (2 H, m), 1.89-2.02 (2 H, m), 2.09 (1 H, dd, *J* = 5.0 and 13.0), 2.22-2.32 (1 H, m), 2.35-2.41 (3 H, m), 3.21-3.25 (1 H, m), 4.06 (2 H, ddd, *J* = 4, 16 and 20), 5.37-5.45 (1 H, m), 5.55-5.63 (1 H, m).

δ_C ($CDCl_3$): 31.4, 32.8, 34.4, 37.5, 40.4, 55.2, 73.5, 80.4, 84.5, 132.3, 135.3.

Ethyl (1*R*,8*S*,9*R*,4*Z*)-bicyclo [6.1.0]non-4-ene-9-yl-10-ate (*exo*) 137-a and ethyl (1*R*,8*S*,9*S*,4*Z*)-bicyclo [6.1.0]non-4-ene-9-yl-10-ate (*endo*) 137-b[100]

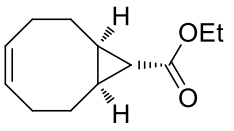

exo

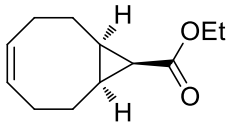

endo

1,5-Cyclooctadiene **131** (10 ml, 81.5 mmol) was added under nitrogen to a dry round-bottom flask containing rhodium(II) acetate (23.5 mg, 0.053 mmol) and the solution was stirred vigorously. Ethyl diazoacetate (8 ml, 1.00 mmol, 15% in toluene) was added to the solution via a syringe pump over 12 h. After the addition was complete, the reaction was stirred overnight and then transferred directly to a silica gel column and purified (0 to 1% diethyl ether/hexane), yielding 0.861 g (42%) of *endo*-ester and 1.182 g (58%) of *exo*-ester.

exo-ester **137-a**

R_f (System A): 0.55

δ_H ($CDCl_3$): 1.20 (1 H, t, *J* = 4.6), 1.27 (3 H, t, *J* = 7.2), 1.45-1.54 (2 H, m), 1.56-1.61 (2 H, m), 2.06-2.14 (2 H, m), 2.17-2.25 (2 H, m), 2.29-2.35 (2 H, m), 4.12 (2 H, q, *J* = 7.2), 5.61-5.69 (2 H, m).

δ_C ($CDCl_3$): 14.3, 26.6, 27.7, 27.8, 28.2, 60.2, 129.9, 174.4.

endo-ester **137-b**

R_f (System A): 0.69

δ_H ($CDCl_3$): 1.28 (3 H, t, *J* = 7.2), 1.38-1.44 (2 H, m), 1.72 (1 H, t, *J* = 8.8), 1.80-1.89 (2 H, m), 2.03-2.12 (2 H, m), 2.17-2.27 (2 H, m), 2.48-2.56 (2 H, m), 4.13 (2 H, q, *J* = 7.2), 5.59-5.66 (2 H, m).

δ_C ($CDCl_3$): 14.4, 21.2, 22.6, 24.1, 27.0, 59.7, 129.4, 172.3.

(1*R*,8*S*,9*R*,4*Z*)-Bicyclo [6.1.0]non-4-ene-9-ylmethanol 138[100]

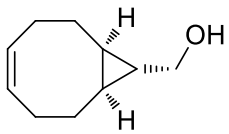

To a solution of ethyl (1*R*,8*S*,9*R*,4*Z*)-bicyclo [6.1.0]non-4-ene-9-yl-10-ate (*exo*) **137-a** (1.92 g, 9.84 mmol) in dry tetrahydrofuran (40 ml) in a round bottom flask cooled at -78°C (dry ice – acetone bath) was added a solution of diisobutylaluminium hydride (25 ml, 24.79 mmol, 80% in THF) dropwise via a syringe. After the reaction was stirred at -78°C for 30 min, the reaction was quenched by addition of a generous excess of brine solution (20 ml) and then warmed to room temperature. The resulting heterogeneous mixture was filtered, and the filter cake was washed with diethyl ether (15 ml). The filtrate and washing were combined and extracted with diethyl ether (3×20 ml). The organic layers were combined and concentrated under reduced pressure. The residue was purified through a short silica gel column eluting with hexane-diethyl ether (80:20 v/v) to yield *the title compound* as a colorless oil (1.397 g, 93%).

R_f (System C): 0.55

δ_H ($CDCl_3$): 0.64-0.70 (1 H, m), 0.75-0.83 (2 H, m), 1.38-1.47 (2 H, m), 2.04-2.22 (4 H, m), 2.27-2.34 (2 H, m), 3.49 (2 H, d, J = 7.2), 5.61-5.69 (2 H, m).

δ_C ($CDCl_3$): 22.1, 27.1, 28.9, 29.0, 67.3, 130.1.

(1*R*,8*S*,9*S*,4*Z*)-Bicyclo [6.1.0]non-4-ene-9-ylmethanol 140

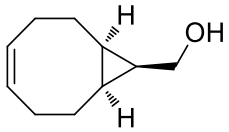

To a solution of ethyl (1*R*,8*S*,9*S*,4*Z*)-bicyclo[6.1.0]non-4-ene-9-yl-10-ate (*endo*) **137-b** (1.43 g, 7.32 mmol) in dry tetrahydrofuran (40 ml) in a round bottom flask at -78°C (dry ice–acetone) was added dropwise a solution of diisobutylaluminium hydride (18 ml, 18.31 mmol, 80% in THF). After the reaction mixture was stirred at -78°C for 30 min, the reaction was quenched by addition of a generous excess of brine solution (20 ml) and then warmed to room temperature. The resulting

heterogeneous mixture was filtered, and the filter cake was washed with ether (15 ml). The filtrate and washing were combined and extracted with diethyl ether (3×20 ml). The organic layers were combined and concentrated under reduced pressure. The residue was purified through a short silica gel column eluting with hexane-diethyl ether (85:15 v/v) to yield the *title compound* as a colorless oil (0.901 g, 81%).

R_f (System C): 0.60

MS-ESI$^+$ found 153.1 for $[M+H]^+$, $C_{10}H_{17}O^+$ required 153.2.

δ_H ($CDCl_3$): 0.99-1.06 (1 H, m), 1.10-1.19 (1 H, m), 1.35 (1 H, s), 1.54-1.64 (2 H, m), 1.96-2.16 (4 H, m), 2.27-2.34 (2 H, m), 3.49 (2 H, d, J = 7.2), 5.61-5.69 (2 H, m).

δ_C ($CDCl_3$): 19.0, 20.7, 23.8, 27.6, 60.3, 129.7.

rel-(1_R_,8_S_,9_R_,4_E_)-Bicyclo[6.1.0]non-4-ene-9-ylmethanol 139

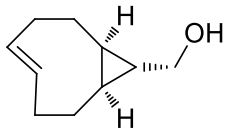

This compound was synthesized using a modified literature procedure.[86] A solution of (1*R*,8*S*,9*R*,4*Z*)-bicyclo [6.1.0]non-4-ene-9-ylmethanol **138** (0.690 g, 4.63 mmol) and methyl benzoate (1.23 g, 9.06 mmol) in hexane-diethyl ether (150 ml, 1:9 v/v) was transferred in equal volumes to 3 Petri dishes (9.0 cm diameter). The Petri dishes were placed in a UVP-CL-500-ultraviolet crosslinker reactor and irradiated at 20×100 μJ/cm^2. At intervals of 25-30 min, the reaction mixture was passed through a column packed with 25 g of silica gel impregnated with 10% silver nitrate. The column was equilibrated with ether prior to loading. The mixture passing through the column was placed back into the UV crosslinker for further irradiation. After total 7 h irradiation the silica gel was transferred to a flask and stirred in an ammonium hydroxide solution

(100 ml, 28%) for 5 min. Dichloromethane (100 ml) was added and stirring was continued for 5 min. The mixture was filtered and the aqueous layer was extracted with dichloromethane (3×30 ml). The combined organic phases were washed with water (3×30 ml) and dried ($MgSO_4$). After evaporation of the solvents, the product was isolated by flash chromatography on silica gel (hexane-diethyl ether 80:20 v/v) as colorless oil (270 mg, 39%).

R_f (System C): 0.53

δ_H ($CDCl_3$): 0.35-0.46 (2 H, m), 0.47-0.55 (1 H, m), 0.56-0.66 (1 H, m), 0.83-0.94 (1 H, m), 1.89-1.99 (2 H, m), 2.20-2.34 (3 H, m), 2.38-2.42 (1 H, m), 3.49-3.57 (2 H, m), 5.11-5.19 (1 H, m), 5.86-5.94 (1 H, m).

δ_C ($CDCl_3$): 20.6, 21.6, 27.7, 28.3, 32.7, 33.8, 38.4, 67.5, 131.2, 138.3.

rel-(1_R_,8_S_,9_S_,4_E_)-Bicyclo[6.1.0]non-4-ene-9-ylmethanol 141

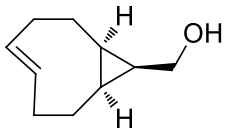

(1*R*,8*S*,9*S*,4*Z*)-Bicyclo [6.1.0]non-4-ene-9-ylmethanol **140** (0.704 g, 4.63 mmol) and (1.27 g, 9.34 mmol) methyl benzoate were dissolved in hexane-diethyl ether (150 ml, 1:9 v/v) and transferred in equal volumes to 3 Petri dishes (9.0 cm diameter). The Petri dishes were placed in an UVP-CL-500-ultraviolet crosslinker reactor and irradiated at 20×100 μJ/cm^2. At intervals of 25-30 min, the reaction mixture was passed through a column packed with 25 g of silica gel impregnated with 10% silver nitrate. The column was equilibrated with ether prior to loading. The mixture passing through the column was placed back into the UV crosslinker for further irradiation. After total 7 h irradiation the silica gel was transferred to a flask and stirred in an ammonium hydroxide solution (100 ml, 28%) for 5 min. Dichloromethane (100 ml) was added

and stirring was continued for 5 min. The mixture was filtered and the aqueous layer was extracted with dichloromethane (3×30 ml). The combined organic phases were washed with water (3×30 ml) and dried ($MgSO_4$). After evaporation of the solvents, the product was isolated by flash chromatography on silica gel (hexane-diethyl ether 80:20 v/v) as colorless oil (284 mg, 40%).

R_f (System C): 0.58

MS-ESI$^+$ found 153.1 for $[M+H]^+$, $C_{10}H_{17}O^+$ required 153.2.

δ_H ($CDCl_3$): 0.54-0.62 (1 H, m), 0.68-0.81 (2 H, m), 0.97-1.08 (1 H, m), 1.19-1.27 (1 H, m), 1.85-1.94 (2 H, m), 2.08-2.13 (1 H, m), 2.15-2.26 (2 H, m), 2.28-2.35 (1 H, m), 3.49-3.57 (2 H, m), 5.10-5.18 (1 H, m), 5.82-5.90 (1 H, m).

δ_C ($CDCl_3$): 18.0, 19.1, 20.9, 27.3, 27.5, 33.8, 34.3, 59.5, 131.2, 138.4.

rel-(1_R_,8_S_,9_S_,4_E_)-9-((Prop-2-yn-1-yloxy)methyl)bicyclo[6.1.0]non-4-ene 142

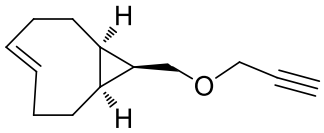

A solution of *rel*-(1*R*,8*S*,9*S*,4*E*)-bicyclo[6.1.0]non-4-ene-9-ylmethanol **141** (320 mg, 2.10 mmol) in dry tetrahydrofuran (3 ml) was added dropwise to a suspension of sodium hydride (60% in mineral oil, 252 mg, 6.31 mmol) in dry tetrahydrofuran (5 ml) at 0°C. The mixture was stirred at room temperature for 30 min. Subsequently, propargyl bromide (500 mg, 4.21 mmol) was added dropwise at 0°C. The mixture was stirred at room temperature overnight. The reaction was quenched by careful addition of brine (15 ml). The aqueous phase was extracted with diethyl ether (2×20 mL), the organic extracts were dried with $MgSO_4$ and concentrated under reduced pressure. The residue was purified by column chromatography, eluting with hexane-diethyl ether (90:10 v/v) to afford the *title compound* (255 mg, 64%) as a pale yellow oil.

R_f (System C): 0.58

δ_H ($CDCl_3$): 0.59-0.67 (1 H, m), 0.73-0.85 (2 H, m), 0.97-1.08 (1 H, m), 1.23-1.31 (1 H, m), 1.88-1.97 (2 H, m), 2.11-2.16 (1 H, m), 2.19-2.30 (2 H, m), 2.32-2.38 (1 H, m), 2.41 (1 H, t, *J* = 2.4), 3.46 (2 H, d, *J* = 7.6), 4.12 (2 H, d, *J* = 2.4), 5.13-5.21 (1 H, m), 5.85-5.93 (1 H, m).

δ_C ($CDCl_3$): 17.9, 19.0, 22.7, 27.4, 27.7, 33.8, 34.5, 57.7, 66.8, 74.1, 80.0, 131.3, 138.5.

10-(3-Cyanophenyl)-5,5-difluoro-1,3,7,9-tetramethyl-5H-dipyrrolo[1,2-c:2',1'-f][1,3,2]diazaborinin-4-ium-5-uide 146[104]

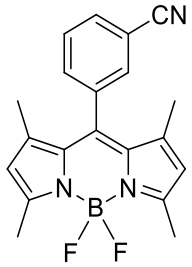

To a solution of 3-formylbenzonitrile **144** (1.00 g, 7.63 mmol) and 2,4-dimethylpyrrole **145** (1.70 ml, 16.5 mmol) in dry dichloromethane (50 ml) under a nitrogen atmosphere was added trifluoroacetic acid (20 µl, 0.261 mmol) and the reaction mixture was stirred at room temperature. After 30 min, TLC (solvent system: B) showed disappearance of 3-formylbenzonitrile. A solution of 2,3-dichloro-5,6-dicyanobenzoquinone (DDQ, 1.73 g, 7.60 mmol) in dry dichloromethane (50 ml) was added drop-wise followed by *N*,*N*-diisopropylethylamine (15.5 ml, 88.90 mmol) and $BF_3 \bullet OEt_2$ (15.5 ml, 125.6 mmol, ~45% BF_3 content). The reaction was allowed to stir overnight after which water (25 ml) was added and the aqueous phase was extracted with dichloromethane (3×25 ml). The combined organic extracts were dried with $MgSO_4$ and concentrated under reduced pressure. The crude mixture was purified using column chromatography (dichloromethane-hexane 40:60 v/v) to give the *title compound* (913 mg, 35%) as a red solid.

R_f (System B): 0.53

δ_H (DMSO-d_6): 1.33 (6 H, s), 2.46 (6 H, s), 6.22 (2 H, s), 7.76-7.79 (2 H, m), 8.02 (1 H, m), 8.04-8.07 (1 H, m).

δ_C (DMSO-d_6): 14.7 (4 C), 112.9, 118.6, 122.2, 130.9, 131.1, 132.3, 133.6, 133.7, 135.6, 139.5, 143.0, 156.0.

δ_B (DMSO-d_6): 0.57 (t, J = 33.3).

δ_F(DMSO-d_6): -143.57 (m).

3-(1,3-Dioxolan-2-yl)benzonitrile 148

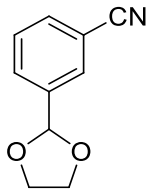

To a solution of 3-formylbenzonitrile **144** (1.00 g, 7.63 mmol) and (±)-camphor-10-sulfonic acid (0.354 g, 1.53 mmol) in dry benzene (50 ml) under a nitrogen atmosphere was added freshly distilled ethylene glycol **147** (1.42 g, 22.9 mmol). The reaction mixture was heated under reflux for 3 h. Upon cooling, a saturated aqueous sodium bicarbonate solution (50 ml) was added and the aqueous phase was back-extracted with dichloromethane (3×25 ml). The combined organic extracts were dried with $MgSO_4$ and concentrated under reduced pressure. Flash column chromatography eluting hexane-diethyl ether (50:50 v/v) gave the desired product as a colorless oil (1.27 g, 95%).

R_f (System B): 0.38

MS-ESI$^+$ found 176.0 for $[M+H]^+$, $C_{10}H_{10}NO_2^+$ required 176.2.

δ_H ($CDCl_3$): 4.04-4.08 (2 H, m), 4.09-4.14 (2 H, m), 5.83 (1 H, s), 7.49 (1 H, t, *J* = 7.6), 7.65 (1 H, d, *J* = 7.6), 7.71 (1 H, d, *J* = 7.6), 7.79 (1 H, s).

δ_C ($CDCl_3$): 65.4 (2 C), 102.2, 112.5, 118.5, 129.2, 130.2, 130.9, 132.6, 139.7.

3-(3-(1,3-Dioxolan-2-yl)phenyl)-6-methyl-1,2,4,5-tetrazine 149

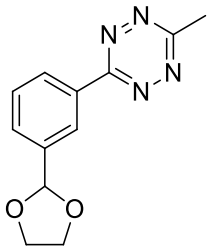

3-(1,3-Dioxolan-2-yl)benzonitrile **148** (106 mg, 0.61 mmol), acetonitrile (320 µl, 6.05 mmol), hydrazine hydrate (1.18 ml, 37.51 mmol) and nickel trifluoromethanesulfonate (112 mg, 0.31 mmol) were combined and sealed in a screw cap vial and stirred at 60°C for 24 h. Upon cooling to room temperature, a solution of sodium nitrite (835 mg, 12.1 mmol) in H_2O (5 mL) was added. The solution was acidified by dropwise addition of 1 *M* hydrochloric acid to pH 3. The magenta colored mixture was extracted with diethyl ether (3×20 ml), the organic phase was dried over $MgSO_4$ and evaporated under reduced pressure. Purification of the residue by flash column chromatography eluting with hexane-diethyl ether (80:20 v/v) afforded the desired product (60 mg, 41%) as a magenta crystalline solid.

R_f (System B): 0.38

MS-ESI$^+$ found 245.0 for $[M+H]^+$, $C_{12}H_{13}N_4O_2^+$ required 245.2.

δ_H ($CDCl_3$): 3.12 (3 H, s), 4.08-4.15 (2 H, m), 4.16-4.22 (2 H, m), 5.95 (1 H, s), 7.63 (1 H, dd, *J* = 7.7, 7,8), 7.75 (1 H, d, *J* = 7.6), 8.61(1 H, d, *J* = 7.6), 8.75 (1 H, s).

δ_C ($CDCl_3$): 21.2, 65.5 (2 C), 103.3, 126.2, 128.7, 129.4, 130.7, 131.9, 139.4, 163.9, 167.4.

3-(6-Methyl-1,2,4,5-tetrazin-3-yl)benzaldehyde 150

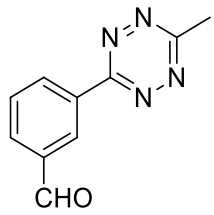

3-(3-(1,3-Dioxolan-2-yl)phenyl)-6-methyl-1,2,4,5-tetrazine **149** (25 mg, 0.102 mmol) and *para*-toluenesulfonic acid monohydrate (20 mg, 0.102 mmol) were mixed and stirred in a mixture of methanol (5 ml) and water (1 ml) overnight. The reaction was quenched by the addition of saturated aqueous sodium bicarbonate solution (10 ml) and the aqueous phase was extracted with dichloromethane (3×15 ml). The combined organic extracts were dried with $MgSO_4$ and concentrated under reduced pressure. The residue was purified by flash column chromatography on silica gel. Evaporation of the appropriate fractions, which were eluted with hexane-diethyl ether (70:30 v/v), gave the desired product as a magenta crystalline solid (20 mg, 98%).

R_f (System B): 0.53

δ_H ($CDCl_3$): 3.16 (3 H, s), 7.81 (1 H, t, J = 7.7), 8.18 (1 H, d, J = 7.6), 8.89 (1 H, d, J = 7.6), 9.13 (1 H, s).

δ_C ($CDCl_3$): 22.7, 125.5, 129.8, 130.1, 132.5, 133.3, 137.3, 163.3, 167.9, 191.4.

5,5-Difluoro-1,3,7,9-tetramethyl-10-(3-(6-methyl-1,2,4,5-tetrazin-3-yl)phenyl)-5*H*-dipyrrolo[1,2-*c*:2',1'-*f*][1,3,2]diazaborinin-4-ium-5-uide 89

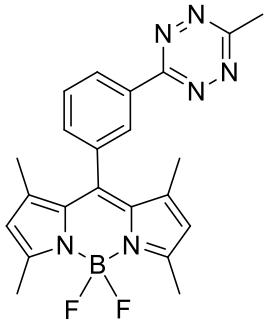

To a solution of 3-(6-methyl-1,2,4,5-tetrazin-3-yl)benzaldehyde **150** (20 mg, 0.099 mmol) and 2,4-dimethylpyrrole **145** (22 µl, 0.22 mmol) in dry dichloromethane (3 ml) under a nitrogen atmosphere was added trifluoroacetic acid (5 µl, 0.065 mmol). After the reaction mixture was stirred at room temperature for 30 min, a solution of 2,3-dichloro-5,6-dicyanobenzoquinone (DDQ, 23 mg, 0.099 mmol) in dry dichloromethane (3 ml), followed by *N*,*N*-diisopropylethylamine (203 µl, 1.17 mmol) and BF_3•OEt_2 (179 µl, 1.94 mmol, ~45% BF_3 content) were added. The reaction mixture was stirred overnight after which water (5 ml) was added and the aqueous phase was extracted with dichloromethane (3×15 ml). The combined organic extracts were dried with $MgSO_4$ and concentrated under reduced pressure. The crude mixture was purified using column chromatography (hexane-diethyl ether 70:30 v/v) to give the *title compound* (14 mg, 33%) as a red solid.

R_f (System A): 0.58

No clear ^{1}H NMR and ^{13}C NMR spectra were obtained for this compound

δ_B (DMSO-d_6): 0.39 (t, J = 33.3).

δ_F(DMSO-d_6): -146.09 (q, J = 33.0).

DNA synthesis

AB_0 and 5'-FAM were synthesized by Alpha DNA's lab using standard ABI 1.0 μmol cycle. The rest of the sequences AB_1, $AB_{1\text{-}1}$, $AB_{1\text{-}2}$, AB_2, $AB_{2\text{-}1}$, $AB_{2\text{-}2}$, AB_3 and AB_4 were synthesized by Dr. Richard Pon's DNA lab using standard ABI 0.2 μmol cycle with the following modifications:

- 10 min coupling at cAB position.
- 5 min coupling at the base immediately after cAB.

After solid phase synthesis was complete, the products were cleaved from solid support and deprotected by incubation with an equal volume of ammonium hydroxide/methylamine (AMA) at 65℃ for 5 min. After lyophilization, the products were purified by polyacrylamide gel electrophoresis.

References

1. Bloomfield, V. A.; Crothers, D. M.; Ignacio Tinoco, J., *Nucleic Acids Structures Properties and Functions*. University Science Books: Sausalito, CA, 2000.
2. Khudyakov, Y. E.; Fields, H. A., Artificial DNA Methods and Applications. CRC Press LLC: USA, 2003; pp 1-3.
3. Sinden, R. R., *DNA Structure and Function*. Academic Press, Inc.: San Diego, CA, 1994.
4. Neidle, S., *Nucleic Acid Structure and Recognition*. Oxford University Press: New York, 2002.
5. Berg, J.; Tymoczko, J.; Stryer, L., *Biochemistry*. 6th ed.; Sara Tenney: USA, 2006.
6. Heckel, A., *Angew. Chem. Int. Ed.* **2005,** *44*, 471-473.
7. Moss, T.; Leblanc, B., *DNA-Protein Interactions*. 3rd ed.; Humana Press: 2009; p 475-502.
8. Braasch, D. A.; Corey, D. R., *Biochemistry* **2002,** *41*, 4503-4510.
9. Mayer, G.; Heckel, A., *Angew. Chem. Int. Ed.* **2006,** *45*, 4900-4921.
10. Asanuma, H.; Liang, X.; Nishioka, H.; Matsunaga, D.; Liu, M.; Komiyama, M., *Nat. Protoc.* **2007,** *2*, 203-212.
11. Deiters, A., *ChemBioChem* **2010,** *11*, 47-53.
12. Szymański, W.; Beierle, J. M.; Kistemaker, H. A. V.; Velema, W. A.; Feringa, B. A., *Chem. Rev.* **2013,** *113*, 6114-6178.
13. Garcia-Amoros, J.; Velasco, D., *Beilstein J. Org. Chem* **2012,** *8*, 1003-1017.
14. Kloppstech, K., . *Physiol. Plant.* **1997,** *100*, 739-747.
15. Harper, M. S.; Neil, L. C.; Gardner, K. H., *Science* **2003,** *301*, 1541-1544.
16. Kao, J. P., *Current Protocols in Neuroscience* **2006,** *37*, 6.20:6.20.1–6.20.21.
17. Ellis-Davies, G. C. R., *Nat. Methods* **2007,** *4*, 619-628.

18. Klán, P.; Šolomek, T.; Bochet, C. G.; Blanc, A.; Givens, R.; Rubina, V.; Kostikov, A.; Wirz, J., *Chem. Rev.* **2013,** *113*, 119-191.
19. Martinek, K.; Varfolomeyev, S. D.; Berezin, L. V., *Eur. J. Biochem* **1971,** *19*, 242-249.
20. Kaplan, J. H.; Forbush III, B.; Hoffman, F. J., *Biochemistry* **1978,** *17*, 1929-1935.
21. Kaplan, J. H.; Ellis-Davies, G. C. R., *Proc. Natl. Acad. Sci.* **1988,** *85*, 6571-6575.
22. Pillai, V. N. R., *Synthesis* **1980,** *1*, 1-26.
23. Walbert, S.; Pfleiderer, W.; Steiner, U. E., *Helv. Chim. Acta* **2001,** *84*, 1601-1611.
24. Momotake, A.; Lindegger, N.; Niggli, E.; Barsotti, R. J.; Ellis-Davies, G. C. R., *Nat. Methods* **2006,** *3*, 35-40.
25. Hagen, V.; Frings, S.; Wiesner, B.; Helm, S.; Kaupp, U. B.; Bendig, J., *ChemBioChem* , **2003,** *4*, 434-442.
26. Fedoryak, O. D.; Dore, T. M., *Org. Lett.* **2000,** *4*, 3419-3422.
27. Lukeman, M.; Scaiano, J. C., *J. Am. Chem. Soc.* **2005,** *127*, 7698-7699.
28. Okamoto, A.; Tanabe, K.; Inasaki, T.; Saito, I., *Angew. Chem. Int. Ed.* **2003,** *42*, 2502-2504.
29. Ghosn, B.; Haselton, F. R.; Gee, K. R.; Monroe, W. T., *Photochem. Photobiol.* **2005,** *81*, 953-959.
30. Monroe, W. T.; McQuain, M. M.; Chang, M. S.; Alexander, J. S.; Haselton, F. R., *J. Biol. Chem.* **1999,** *274*, 20895-20900.
31. Ando, H.; Furuta, T.; Tsien, R. Y.; Okamoto, H., *Nat. Gene.* **2001,** *28*, 317-325.
32. Young, D. D.; Deiters, A., *Org. Biomol. Chem.* **2007,** *5*, 999-1005.
33. Tang, X.; Zhang, J.; Sun, J.; Wang, Y.; Wu, J.; Zhang, L., *Org. Biomol. Chem.* **2013,** *11*, 7814-7824.
34. Tang, X.; Dmochowski, I. J., *Mol. BioSyst.* **2007,** *3*, 100-110.

35. Wenter, P.; Furtig, B.; Hainard, A.; Schwalbe, H.; Pitsch, S., *Angew. Chem. Int. Ed.* **2005,** *44*, 2600-2603.

36. Hobartner, C.; Silverman, S. K., *Angew. Chem. Int. Ed.* **2005,** *44*, 7305-7309.

37. Dieters, A.; Garne, R. A.; Lusic, H.; Govan, J. M.; Dush, M.; Nascone-Yoder, N. M.; Yoder, J. A., *J. Am. Chem. Soc.* **2010,** *132*, 15644-15650.

38. Beharry, A. A.; Sadovski, O.; Woolley, G. A., *J. Am. Chem. Soc.* **2011,** *133*, 19684-19687.

39. Beharry, A. A.; Woolley, G. A., *Chem. Soc. Rev.* **2011,** *40*, 4422-4437.

40. Waldeck, D. H., *Chem. Rev.* **1991,** *91*, 415-436.

41. Letsinger, R.; Wu, T., *J. Am. Chem. Soc.* **1995,** *117*, 7323-7328.

42. Cammenga, H. K.; Emel'yanenko, V. N.; Verevkin, S. P., *Ind. Eng. Chem. Res.* **2009,** *48*, 10120-10128.

43. Berkovic, G.; Krongauz, V.; Weiss, V., *Chem. Rev.* **2000,** *100*, 1741-1753.

44. Lukyanov, B. S.; Lukyanova, M. B., *Chem. Heterocycl. Compd.* **2005,** *41*, 281-311.

45. Beyer, C.; Wagenknecht, H., *Synlett* **2010,** *9*, 1371-1376.

46. Kellogg, R. M.; Groen, M. B.; Wynberg, H., *J. Org. Chem.* **1967,** *32*, 3093-3100.

47. Nakamura, S.; Irie, M., *J. Org. Chem.* **1988,** *53*, 6136-6138.

48. Irie, M., *Chem. Rev.* **2000,** *100*, 1685-1716.

49. Cahova, H., *Angew. Chem. Int. Ed.* **2013,** *52*, 3186 –3190.

50. Hamon, F.; Djedaini-Pilard, F.; Barbot, F.; Len, C., *Tetrahedron* **2010,** *66*, 2538-2538.

51. Hamon, F.; Djedaini-Pilard, F.; Barbot, F.; Len, C., *Tetrahedron* **2009,** *65*, 10105-10123.

52. Sudesh kumar, G.; Neckers, C. D., *Chem. Rev.* **1989,** *89* 1915-1925.

53. Paudler, W. W.; Zeiler, A. G., *J. Org. Chem.* **1969,** *34*, 3237-3239.

54. Cattaneo, P.; Persico, M., *Phys. Chem. Chem. Phys.* **1999,** *1*, 4739-4743.

55. Joshi, K. D.; Mitchell, J. M.; Bruce, D.; Lough, J. A.; Yan, H., *Tetrahedron* **2012,** *68*, 8670-8676.

56. Kashida, H.; Liang, X.; Asanuma, H., *Curr. Org. Chem.* **2009,** *13*, 1065-1084.

57. Merino, E.; Ribagorda, M., *Beilstein J. Org. Chem.* **2012,** *8*, 1071-1090.

58. Renner, C.; Moroder, L., *ChemBioChem* **2006,** *7*, 869-878.

59. Asanuma, H.; Matsunaga, D.; Komiyama, M., *Nucleic Acids Symp. Ser. (Oxf)* **2005,** *49*, 35-36.

60. Liu, M.; Asanuma, H.; Komiyama, M., *J. Am. Chem. Soc.* **2006,** *128*, 1009-1015.

61. Harbour, J. R.; Hair, M. L., *J. Phys. Chem.* **1979,** *83*, 648-652.

62. Duval, H., *Bull. Soc. Chim. Fr.* **1910,** *7*, 727-732.

63. Siewertsen, R.; Neumann, H.; Buchheim-Stehn, B.; Herges, R.; Nather, C.; Renth, F.; Temps, F., *J. Am. Chem. Soc.* **2009,** *131*, 15594-15595.

64. Rau, H.; Greiner, G.; Gauglitz, G.; Meier, H., *J. Phys. Chem.* **1990,** *94*, 6523-6524.

65. Foster, R. A. A.; Willis, M. C., *Chem. Soc. Rev.* **2013,** *42*, 63-76.

66. Knall, A.; Slugovc, C., *Chem. Soc. Rev.* **2013,** *42*, 5131-5142.

67. Sauer, J.; Sustmann, R., *Angew. Chem., Int. Ed.* **1980,** *19*, 779-807.

68. Dang, A.; Miller, D. O.; Dawe, L. N.; Bodwell, G. J., *Org. Lett.*, **2008,** *10*, 233-236.

69. Rostovtsev, V. V.; Green, L. G.; Fokin, V. V.; Sharpless, K. B., *Angew. Chem., Int. Ed.* **2002,** *41*, 2596-2599.

70. Baskin, J. M.; Prescher, J. A.; Laughlin, S. T.; Agard, N. J.; Chang, P. V.; Miller, I. A.; Lo, A.; Codelli, J. A.; Bertozzi, C. R., *Proc. Natl. Acad. Sci. U.S.A.* **2007,** *104*, 16793-16797.

71. Codelli, J. A.; Baskin, J. M.; Agard, N. J.; Bertozzi, C. R., *J. Am. Chem. Soc.* **2008,** *130*, 11486-11493.

72. Laughlin, S. T.; Baskin, J. M.; Amacher, S. L.; Bertozzi, C. R., *Science* **2008,** *320*, 664-667.

73. Devaraj, N. K.; Weissleder, R.; A., H. S., *Bioconjugate Chem.* **2008,** *19*, 2297–2299.

74. Chen, W.; Wang, D.; Dai, C.; Hamelberg, D.; Wang, B., *Chem. Commun.* **2012,** *48*, 1736-1738.

75. Carboni, R. A.; Lindsey, R. V., *J. Am. Chem. Soc.* **1959,** *81*, 4342-4346.

76. Thalhammer, F.; Wallfahrer, U.; Sauer, J., *Tetrahedron Lett.* **1990,** *31*, 6851-6854.

77. Sauer, J.; Heldmann, D. K.; Hetzenegger, J.; Krauthan, J.; Sichert, H.; Schuster, J., *Eur. J. Org. Chem.* **1998**, 2885-2896.

78. Blackman, M. L.; Royzen, M.; Fox, J. M., *J. Am. Chem. Soc.* **2008,** *130*, 13518-13519.

79. Devaraj, N. K.; Weissleder, R., *Acc. Chem. Res.* **2011,** *44*, 816-827.

80. Lang, K.; Davis, L.; Torres-Kolbus, J.; Chou, C.; Deiters, A.; Chin, J. W., *Nat. Chem.* **2012,** *4*, 298-304.

81. Seitchik, J. L.; Peeler, J. C.; Taylor, M. T.; Blackman, M. L.; Rhoads, T. W.; Cooley, R. B.; Refakis, C.; Fox, J. M.; Mehl, R. A., *J. Am. Chem. Soc.* **2012,** *134*, 2898-2901.

82. Slettem, E. M.; Bertozzi, C. R., *Acc. Chem. Res.* **2011,** *44*, 666-676.

83. Schoch, J.; Staudt, M.; Samanta, A.; Wiessler, M.; Jaschke, A., *Bioconjugate Chem.* **2012,** *23*, 1382-1388.

84. Yang, J.; Seckute, J.; Cole, C. M.; Devaraj, N. K., *Angew. Chem.* **2012,** *124*, 7594-7597.

85. Kamber, D. N.; Liang, Y.; Blizzard, R. J.; Liu, F.; Mehl, R. A.; Houk, K. N.; Prescher, J. A., *J. Am. Chem. Soc.* **2015,** *137*, 8388-8391.

86. Devaraj, N. K.; Upadhyay, R.; Haun, J. B.; Hilderbrand, S.; Weissleder, R., *Angew. Chem., Int. Ed.* **2009,** *48*, 7013-7016.

87. Karver, M. R.; Weissleder, R.; Hilderbrand, S. A., *Angew. Chem., Int. Ed.* **2012,** *51*, 920-922.

88. Beal, D. M.; Jones, L. H., *Angew. Chem., Int. Ed.* **2012,** *51*, 6320-6326.

89. Kempe, K.; Krieg, A.; Remzi Becer, C.; Schubert, U. S., *Chem. Soc. Rev.* **2012,** *41*, 176-191.

90. Lang, K.; Chin, J. W., *Chem. Rev.* **2014,** *114*, 4764-4806.

91. Clavier, G.; Audebert, P., *Chem. Rev.* **2010,** *110*, 3299-3314.

92. Yang, J.; Karver, M. R.; Li, W.; Sahu, S.; Devaraj, N. K., *Angew. Chem., Int. Ed.* **2012,** *51*, 5222-5225.

93. Coburn, M. D.; Buntain, G. A.; Harris, B. W.; Hiskey, M. A.; Lee, K. Y.; Ott, D. G., *J. Heterocycl. Chem.* **1991,** *28*, 2049-2050.

94. Chavez, D. E.; Hiskey, M. A., *J. Heterocycl. Chem.* **1998,** *35*, 1329-1332.

95. Gong, Y. H.; Miomandre, F.; Meallet-Renault, R.; Badre, S.; Galmiche, L.; Tang, J.; Audebert, P.; Clavier, G., *Eur. J. Org. Chem.* **2009,** *35*, 6121-6128.

96. Wieczorek, A.; Buckup, T.; Wombacher, R., *Org. Biomol. Chem.* **2014,** *12*, 4177-4185.

97. Dumas-Verdes, C. M., F.; Lepicier, E.; Galangau, O.; Vu, T. T.; Clavier, G.; Meallet-Renault, R.; Audebert, P., *Eur. J. Org. Chem.* **2010,** *13*, 2525-2535.

98. Devaraj, N. K.; Hilderbrand, S.; Upadhyay, R.; Mazitschek, R.; Weissleder, R., *Angew. Chem., Int. Ed.* **2010,** *49*, 2869-2872.

99. Karver, M. R.; Weissleder, R.; Hilderbrand, S. A., *Bioconjugate Chem.* **2011,** *22*, 2263-2270; Chen, W.; Wang, D.; Dai, C.; Hamelberg, D.; Wang, B., *Chem. Commun.* **2012,** *48*, 1736–1738.

100. Taylor, M. T.; Blackman, M. L.; Dmitrenko, O.; Fox, J. M., *J. Am. Chem. Soc.* **2011,** *133*, 9646-9649.

101. Jiao, G. S.; Thoresen, L. H.; Burgess, K., *J. Am. Chem. Soc.* **2003,** *125*, 14668-14669.

102. Kowalczyk, T.; Lin, Z.; Voorhis, T. V., *J. Phys. Chem. A.* **2010,** *114*, 10427-10434.

103. Shieh, R.; Bertozzi, C. R., *Org. Biomol. Chem.* **2014,** *12*, 9307-9320.

104. Carlson, J. C. T.; Meimetis, L. G.; Hilderbrand, S. A.; Weissleder, R., *Angew. Chem., Int. Ed.* **2013,** *52*, 6917-6920.

105. Meimetis, L. G.; Carlson, C. T.; Giedt, R. J.; Kohler, R. H.; Weissleder, R., *Angew. Chem., Int. Ed.* **2014,** *53*, 7531-7534.

106. Schoch, J.; Wiessler, M.; Jäschke, A., *J. Am. Chem. Soc.* **2010,** *132*, 8846-8847.

107. Schoch, J.; Ametaz, S.; Jäschke, A., *Chem. Commun.* **2011,** *47*, 12536-12537.

108. Pitulle, C.; Kleineidam, R. G.; Sproat, B.; Krupp, G., *Gene* **1992,** *112*, 101-105.

109. Milligan, J. F.; Groebe, D. R.; Witherell, G. W.; Uhlenbeck, O. C., *Nucleic Acids Res.* **1987,** *15*, 8783-8798.

110. Asare-Okai, P. N.; Agustin, E.; Fabris, D.; Royzen, M., *Chem. Commun.* **2014,** *50*, 7844-7847.

111. Jarchow-Choy, S. K.; Sjuvarsson, E.; Sintim, H. O.; Eriksson, S.; Kool, E. T., *J. Am. Chem. Soc.* **2009,** *131*, 5488-5494.

112. Joshi, D. K. Synthesis of Cyclic Azobenzene Analogues for Incorporation into Oligonucleotides, Peptides and Polymers. MSc thesis, Brock University, St. Catharines, ON, 2013.

113. Blackburn, G. M.; Gait, M. J.; Loakes, D.; Williams, D. M., *Nucleic Acids in Chemistry and Biology*. 3th ed.; The Royal Society of Chemistry: UK, 2006.

114. Sinha, N. D.; Davis, P.; Usman, N.; Perez, J.; Hodge, R.; Kremsky, J.; Casale, R., *Biochimie* **1993,** *75*, 13-23.

115. Schulhof, J. C.; Molko, D.; Teoule, R., *Tetrahedron Lett.* **1987,** *28*, 51-54.

116. Pon, R. T.; Yu, S., *Tetrahedron Lett.* **1997,** *38*, 3327-3330.

117. Meier, H.; Mayer, W.; Kolshorn, H., *Chem. Ber.* **1987,** *120*, 685-689.

118.Royzen, M.; Yap, G. P. A.; Fox, G. M., *J. Am. Chem. Soc.* **2008,** *130*, 3760-3761.